Tampere University

Jani Viljakka

SYNTHESIS AND CHARACTERIZATION OF INDIGO PHOTOSWITHES

Master of Science thesis
Faculty of Engineering and
Natural Sciences
[Examiner:] Prof. Arri Priimägi
[Examiner:] MSc Kim Kuntze
August 2021

ABSTRACT

Jani Viljakka: Synthesis and characterization of indigo photoswitches
Master of Science thesis
Tampere University
Science and Engineering
August 2021

Controlling the function and properties of materials, pharmaceuticals and catalysts after manufacturing is essential for contemporary chemists. Such control can be achieved via use of molecular switches, which change their chemical and/or physical properties in response to external stimuli. Light is a particularly attractive stimulus because of its high degree of controllability without physical contact, and clean nature. Therefore, organic light-responsive molecules – photoswitches – are studied for such purposes. The synthesis of new photoswitches with different photochemical properties is needed for various applications. In the molecular design of such photoswitches, compatibility with different matrices such as polymers or elastomers, is necessary to be taken into account.

In this thesis, three different previously unreported indigo photoswitches were designed and synthesized and their photochemical properties characterized in different environments. Photoswitches with similar indigo-core had been previously syntheized and characterized in solution, so the focus was to enable implementation to liquid crystalline and polymer matrices and study the photochemical properties in these environments, with a particular aim of obtaining indigo photoswitching in the solid state.

The photochemical properties of the indigo photoswitches were first studied in solution, after which they were incorporated as dopants in liquid crystals and in polymer films. Photoisomerization efficiency, molar absorption coefficient, thermal stability of the metastable *Z*-isomer and fatigue resistance were determined. All studied molecules showed similar properties to reference molecules in solution: reversible and efficient photoswitching with moderate thermal lifetimes and high fatigue resistance. Photoswitching was less efficient in liquid crystals than in solutions, probably due to shorter *Z*-lifetimes dominating the photostationary states. All compounds showed fatigue resistance of over 50 cycles in liquid crystals. In a polymer film the photoswitching efficiency was higher than in liquid crystals but lower than in solution. Thermal lifetimes were multiple times longer than in a solution, and all photoswitches could be switched to both direction with 660 nm and 525 nm light.

Indigo photoswitches studied in this work were compatible with liquid crystals and polymer films. Photoswitching was observed in all studied environments with moderate *E* to *Z* conversion with low-energy irradiation. Regarding the synthetic routes, more studies for optimization of the reactions is required. The synthesized indigo photoswitches are ready for further studying as crosslinkers in liquid crystal elastomers or polymer networks.

Keywords: Photoswitching, Indigo, synthesis

TIIVISTELMÄ

Jani Viljakka: Indigo valokytkimien synteesi ja valokemiallinen karakterisointi
Diplomityö
Tampereen yliopisto
Teknis-luonnontieteellinen diplomi-insinöörin tutkinto-ohjelma
Elokuu 2021

Uuden sukupolven materiaalien, lääkeaineiden ja katalyyttien ominaisuuksien ja toiminnallisuuden kontrollointi valmistuksen jälkeen on välttämätöntä nykykemisteille. Tämä on mahdollista molekyylikytkimien eli ulkopuolisiin ärsykkeisiin reagoivien yhdisteiden avulla. Valo on suotuisa ärsyke, koska se on hyvin kontrolloitavissa ja luonteeltaan puhdas Siksi orgaanisia valoon reagoivia molekyylejä – valokytkimiä – tutkitaan kyseisiin tarkoituksiin. Uusien valokytkimien, joilla on erilaiset valokemialliset ominaisuudet, synteesiä tarvitaan erilaisiin sovelluksiin. Tällaisten valokytkimien suunnittelussa soveltuvuus erilaisiin ympäristöihin, kuten usein käytettyihin nestekide-elastomeereihin, pitää ottaa huomioon.

Tässä työssä kolme ennen julkaisematonta indigovalokytkintä suunniteltiin ja syntetisoitiin, ja niiden valokemiallisia ominaisuuksia tutkittiin eri ympäristöissä. Valokytkimiä, joissa on vastaava indigokeskus, on aiemmin syntetisoitu ja tutkittu liuoksessa, joten tarkoituksena oli mahdollistaa valokytkimien käyttö nestekiteessä ja polymeerissä ja tutkia valokemiallisia ominaisuuksia kiinteässä olomuodossa.

Indigovalokytkimen valokemiallisia ominaisuuksia tutkittiin liuoksessa ja lisäaineena sekä nestekiteessä että polymeerikalvossa. Valoisomerisaation tehokkuus, molaariset absorptiokertoimet, epävakaamman isomeerin terminen stabiilisuus ja väsymiskestävyys määritettiin. Kaikilla tutkituilla molekyyleillä oli liuoksessa vastaavat ominaisuudet kuin aiemmin julkaistuilla vastaavilla molekyyleillä: reversiibeli ja tehokas valoisomerisaatio sekä keskipitkät termiset elinajat. Valoisomerisaatio ei ollut aivan yhtä tehokasta nestekiteessä, johtuen mahdollisesti lyhyiden elinaikojen hallitsemasta tasapainotilasta. Kaikki yhdisteet kestivät isomerisaatiota yli 50 sykliä. Polymeerikalvossa isomerisaatiotehokkuus oli nestekideympäristön ja liuoksen väliltä. Termiset elinajat olivat moninkertaisia liuokseen verrattuna, ja kaikkia valokytkimiä pystyttiin isomeroimaan kumpaankin suuntaan 660 nm ja 525 nm valon avulla.

Tässä työssä tutkitut indigovalokytkimet olivat yhteensopivia nestekide- ja polymeeriympäristöjen kanssa. Valoisomerisaatiota havaittiin kaikissa tutkituissa ympäristöissä matalaenergisellä säteilytyksellä. Lisätutkimusta tarvitaan synteesireittien reaktio-olosuhteiden optimointiin. Syntetisoidut indigovalokytkimet ovat valmiita jatkotutkimuksiin ristisilloittimina nestekide-elastomeereissa tai polymeeriverkostossa.

Avainsanat: Indigo, valokytkin, synteesi

PREFACE

This Master of Science thesis was done in the Smart Photonic Materials group at the Faculty of Engineering and Natural Sciences of Tampere University. All experimental work was carried out at the Red Labs Research Environment at Tampere University. The work was funded by European Research Council (Starting Grant project PHOTOTUNE, Decision Number 679646)

I thank my supervisor prof. Arri Priimägi for enabling this challenging and interesting work, and for the support and guidance during the process. I'm grateful for the invaluable help from Mr. Kim Kuntze who supervised and guided my whole thesis project from the synthesis of the molecules to the writing of this thesis. Thanks to Dr. Matti Virkki for the help with preparation and characterization of polymer films. All co-workers in the Red Labs, Rakesh, Suvi H, Anastasia, Suvi L, Matias, Sami and others, thanks for making the working days nice. Also, thanks to the whole SPM gang, it has been a pleasure to work with you all.

Final thanks for my family and friends for the support during the work. Helmiina, thanks for the supportiveness and encouragement, every day.

Tampere, 2.8.2021

Jani Viljakka

CONTENTS

LIST OF SYMBOLS AND ABBREVIATIONS

τ	thermal lifetime
ε	molar extinction coefficient
λ	wavelength
δ	chemical shift
Al-	alkyl
Ar-	aryl
Bu-	butyl
bp	boiling point
Cy-	cyclohexyl
DAE	diarylethene
dba	dibenzylideneacetone
DCB	1,2-dichlorobenzene
DCM	dichloromethane
DFT	density functional theory
DMAP	4-dimethylaminopyridine
DMF	*N,N'*-dimethylformamide
EDG	electron donating group
Et-	ethyl
EtOAc	ethyl acetate
EWG	electron withdrawing group
IR	infra-red
ITO	indium tin oxide
LC	liquid crystal
LCE	liquid crystal elastomer
Me-	methyl
MeCN	acetonitrile
NMR	nuclear magnetic resonance
PE	polyethylene
Ph-	phenyl
PSS	photostationary state
PTFE	polytetrafluoroethylene
P4VP	poly-4-vinylpyridine
RT	room temperature
t	*tert*
TBAF	tetrabutylammonium fluoride
TBS	*tert*-butyldimethylsilyl
TEA	triethylamine
THF	tetrahydrofuran
TLC	thin-layer chromatography
UV	ultraviolet
vis	visible

1. INTRODUCTION

Conventional materials, catalysts and pharmaceuticals all share one property; they are static in their nature. Once created, their functionalities cannot be controlled. During last decades countless advances have been made in conventional materials, for example, using nanotechnology in sensors [1] or nanomedicine [2], [3] and stem-cell-based treatments. [4] But scientists have also focused on new types of materials that can be considered “smart” and in which the properties could be controlled after manufacturing with external stimuli.

Control over materials properties can be achieved with molecular switches – molecules that respond to external stimuli such as electric field [5], magnetic field [6], pH [6] or light [7]. Light is a highly interesting stimulus due to its nature, being non-invasive, clean, and highly controllable with good spatial and temporal resolution. Photochromic molecular switches (*photoswitches*) by definition undergo a *reversible* change in their absorption spectrum upon isomerization from thermodynamically stable to more energetic, or metastable, form when irradiated with light. [7] The change between the two forms also alters the chemical and physical properties of the photoswitch, such as geometry, dipole moment, conductivity and coordination [8].

The changes in molecular properties can be exploited in multiple fields. Photoinduced changes can be used in catalysis to externally control chemical reactions. This generates possibilities for one-pot multi-step reactions unattainable with conventional catalysts. [9], [10] From biomaterials to photopharmacology, photoswitches can be used for a variety of functions from controlling peptide chain folding and enzyme activity to light-controlled antibacterials and targetable and controllable drugs. [11]–[15] Photoswitches can also be integrated to different materials such as polymers [16] or liquid crystal elastomers (LCEs) [17], or attached to their surface to control properties such as wettability [18]. This enables a wide range of light-controlled applications from optical memories [19] and biomimicking smart systems [20] to molecular motors [21] and self-healing materials [22].

There are multiple different families of photoswitches, azobenzenes, diarylethenes, spiropyrans, fulgides, chromenes and indigoids to name a few. [7], [23] Different pho-

toswitch families have different properties, but properties inside a given photoswitch family can also be tuned by functionalizing the molecules. Each photoswitch family has their advantages and disadvantages, hence suiting for different kinds of applications. Azobenzenes undergo a large geometrical change with fast isomerization and are relatively fatigue resistant. However, azobenzenes are often isomerized in the UV-region or short-wavelength visible light. [24] Diarylethenes' ring-closing isomerization induces only small geometrical changes, but their optical and electronic properties change significantly. They are often bistable and have superior fatigue resistance compared to other photoswitches. [25] Spiropyran molecules exhibit a large change in the dipole moment as well as geometry between open- and closed-ring isomers. The open-ring form can also exist in a charge-bearing zwitterionic form. [26]

Indigo has been known and used as a dye for centuries. It is blue, which is a unique feature for natural dyes. Indigo is known in the field of organic electronics because of its remarkable stability and great charge transport properties. [27], [28] In the field of photoswitches it is a new emerging molecule with little research done on it. [29] The absorption spectrum of indigo is naturally red-shifted compared to other conventional photoswitches, which makes it potent for many applications especially in biology and photopharmacy. In addition, the isomerization of indigo stimulates an even bigger geometrical change than azobenzene molecules, yielding it potentially attractive for light-controllable functional materials such as photoactuators. [30]–[32]

To give context for the indigo studies, the three most widespread photoswitches – azobenzenes, diarylethenes and spiropyrans – are introduced in the theoretical part of this work. The basic chemical structures, common synthetic pathways and spectral properties are covered in Chapter 2. A short history of indigo, its synthetic preparation and photochemical properties are presented in Chapter 3. In the experimental part of the work (Chapter 4), three new indigo photoswitches with different lifetimes are synthetized and studied in solution, as dopant in liquid crystals and in polymer films. To authors knowledge properties of indigo photoswitches haven't been studied before in solid state.

2. INTRODUCTION TO MOLECULAR PHOTOSWITCHES

Photochromic molecules (photoswitches) by definition undergo a reversible transformation between two forms, which have different absorption spectra, by absorption of electromagnetic radiation. The thermodynamically stable form *A* is transformed into less stable form *B*, which relaxes back to form *A* either thermally (T-type photochromism) or photochemically (P-type photochromism). Many photochromic molecules have pale or colourless form *A* and coloured form *B*, which is referred to as *positive photochromism*. When $\lambda_{max}(A) > \lambda_{max}(B)$, photochromism is *negative*. [7]

There are dozens of different photoswitch families. In this chapter three most widespread ones, azobenzenes, diarylethenes and spiropyrans are introduced. [8], [33] Other photoswitch families are for example chromenes, fulgides, spirooxazines, stillbenes and indigoids. Diarylethenes and spiropyrans have thermally stable closed-ring form which opens during photoexcitation. Azobenzene undergoes *E* → *Z* isomerization during photoexcitation and relaxes back to the more stable *E* isomer thermally or via photoexcitation with different wavelength. These photoswitches have applications in multiple fields, such as catalysis, photopharmacology and advanced materials, which are shortly described below.

2.1 Azobenzenes

Azobenzenes are a vast family of photocontrollable molecules. Parent azobenzene molecule **1** constitutes of two benzene rings linked with an azo bond.

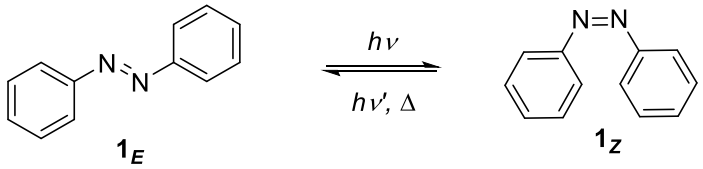

Figure 1 *Azobenzene **1** in its E and Z isomers.*

It is possible to substitute hydrogens on the benzene rings of **1** in symmetric or asymmetric way in *ortho-*, *para-* or *meta-positions* with different atoms or groups, creating an almost infinite number of possible structures for chemists. Substitution has a huge impact

on the properties of azobenzene molecules, including absorption spectrum of both isomers, thermal lifetime of the *Z* isomer, isomerization quantum yields and molecular shape and size.

A vast library of different synthetic methods exists for the preparation of different azobenzenes. Oxidizing anilines, azo coupling and Mills reaction are some of the most common methods. Other methods include for example Wallach reaction, reduction of azoxybenzenes, triazene rearrangement, thermolysis of azides and opening of benzotriazoles. [34]

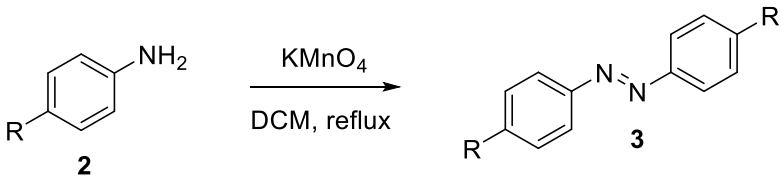

Scheme 1 *Oxidizing aniline* ***2*** *(R = H) or substituted aniline yields symmetric azobenzene* ***3.***

Oxidation of anilines is a simple way to create symmetrical azobenzenes. It uses oxidizing agents in non-polar solvents, for example $KMnO_4$ supported on iron (II) sulfate in dichloromethane (DCM) (Scheme 1). Many other oxidizing agents and different non-polar solvents can also be used. Reaction is not limited to only 4-substituted (R in Scheme 1) anilines, but also, e.g., 2,5-dihalogenated anilines can be used. A drawback of the reaction is its low yield for highly functionalized molecules, ranging from 15% to 80% for simple *para*-functionalized molecules. [34]–[36]

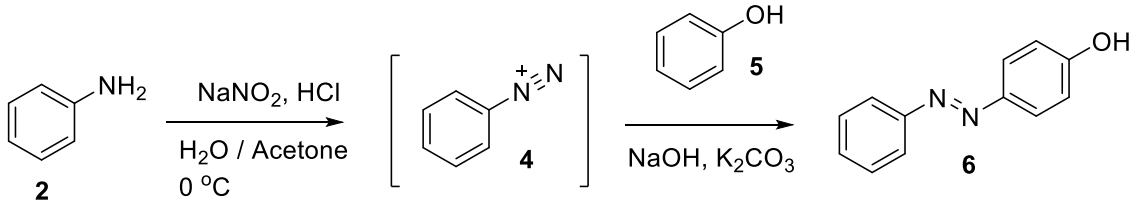

Scheme 2 *Azo coupling reaction.*

The azo coupling reaction is the oldest known method to synthetize azobenzenes. It starts by reacting **2** (R = H) with sodium nitrite in acidic conditions to form a reactive diazonium compound **4**, which is then reacted with phenol **5** to form 4-hydroxyazobenzene **6**. Acidic conditions for the first step serve to liberate nitrous acid *in situ* from sodium nitrite. Diazonium compounds might be explosive, so the reaction temperature must be kept low. [34] Unlike the oxidation of anilines, azo coupling reactions usually have very

good yields, but the reaction requires an electron-rich aromatic nucleophile for the second step, so it is not suitable for all azobenzenes.

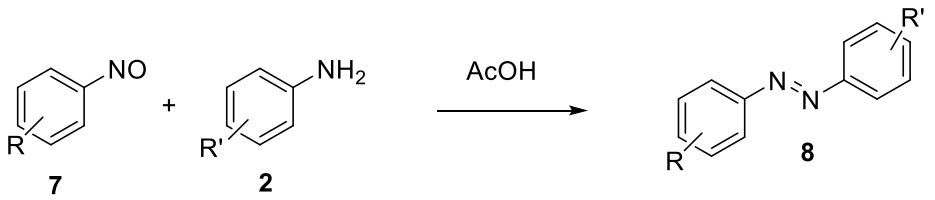

Scheme 3 *Mills reaction.*

Asymmetric azobenzenes **8** (R ≠ R') can also be made with Mills reaction (Scheme 3) by reacting an aromatic nitroso derivative **7** with the aniline **2** in glacial acetic acid. Some nitroso derivatives are available commercially, but they can also be prepared by oxidating the corresponding aniline.

Azobenzene has two major absorbance peaks, corresponding to the π → π* transition (peak in the UV region for azobenzene, red-shifted for NHA and DR1 in Figure 2) and the n → π* transition (peak at > 400 nm for azobenzene). For unsubstituted azobenzene these peaks are separated from each other (black line in Figure 2) but overlap for different isomers.

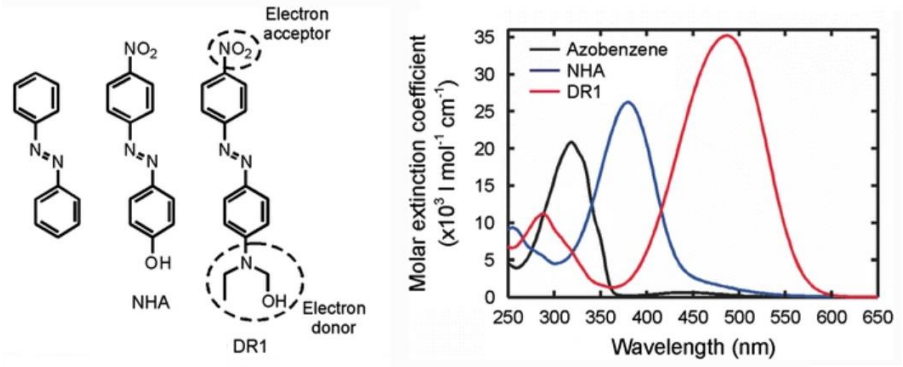

Figure 2 *Absorption spectra of azobenzene, weak push-pull 4-nitro-4'-hydroxyazobenzene (NHA) and disperse red 1 (DR1) in THF solutions, reproduced from* [37].

As seen in Figure 2, substituents have a huge impact on the location of these absorption peaks. Including an electron donating group (EDG) like an amino group or an electron withdrawing group (EWG) like a nitro- or hydroxy group in *para*-position redshifts the π → π* transition absorption peak by ca. 50 nm. Push-pull type azobenzenes, which have one EWG and one EDG in *para*-positions, are red-shifted even more (Figure 2), but have very short, highly solvent-dependent *Z*-lifetimes down to 100 fs in protic solvents. [38]–[41] Further red-shift can be achieved via protonation of the azo-bond to an azonium-ion. The group of Woolley optimized the molecular structure of these and achieved near-IR

functioning (λ_{max} = 597 nm, λ_{irrad} =720 nm) molecules with a *Z*-lifetime in scale of seconds. [42]

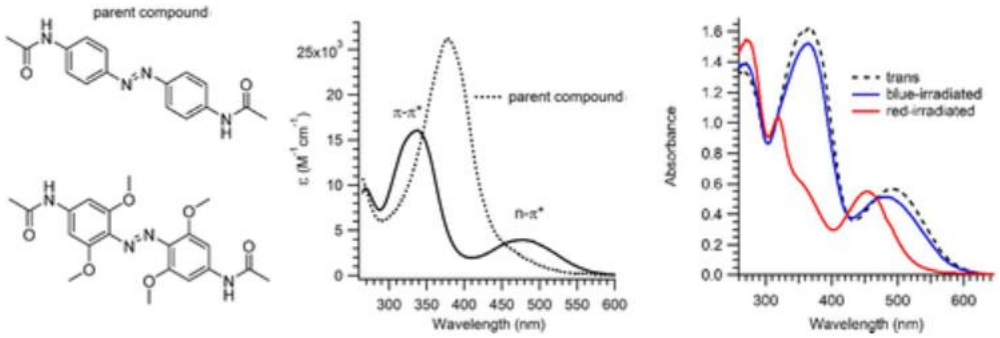

Figure 3 Ortho-*substitution can separate the n → π* and π → π* transitions compared to parent compound (middle) and enable two-way switching with different wavelengths (right), reproduced from* [40]*.*

Different *ortho*-substitution patterns can separate n → π* transition peak from π → π* transition (Figure 3, middle). Some *ortho*-substitutes also separate the n → π* transition of *E* and *Z* isomers making it possible to address this band for the two isomers separately and to efficiently switch in both directions *E* → *Z* and *Z* → *E* with visible-light irradiation (Figure 3, right). [43] EWGs, such as chlorine, fluorine or methoxy-group, in *ortho*-position also stabilizes the *Z*-isomer, resulting at best in over 20-fold lifetimes compared to **1**. Combining these properties can lead to photoswitches with long thermal lifetime and high visible light absorbance. [36]

Three different mechanisms have been proposed for *E* → *Z* isomerization: rotation, inversion and rotation-assisted inversion. Many studies done on this field conclude that depending on the structure of azobenzene and conditions such as solvent (if liquid phase) and temperature, all of them are possible. [24] In the case of photoisomerization, also the energy of excitation might affect the mechanism, n → π* excitation (corresponds to $S_0 \rightarrow S_1$ electronic transition) isomerizing the azobenzene through inversion, while π → π* ($S_0 \rightarrow S_2$) through rotation mechanism. [44]

Different substitutions have been vastly studied for various applications, to fine-tune the wanted properties. For many applications, for example in biological use, red-shifting the absorption spectra while maintaining long *Z*-lifetime (ultimately, targeting bistable compounds), photostability and good quantum yields would be essential. For some other applications, on-off switches with very short lifetimes are preferred. [36], [40], [43]–[49]

2.2 Diarylethenes

Compared to azobenzenes, diarylethenes are fairly new class of photoswitches; first articles in the field were published in late 1980s by group of Irie [50], [51]. It was known that in addition to *E* → *Z* isomerization between $\mathbf{9}_E$ and $\mathbf{9}_Z$, *Z*-stilbene $\mathbf{9}_Z$ can undergo a reversible cyclization reaction to 9_c under UV-irradiation (Figure 4). $\mathbf{9}_c$ can be dehydrogenated to form phenanthrene, which can be prevented via methylation to $\mathbf{10}_c$.

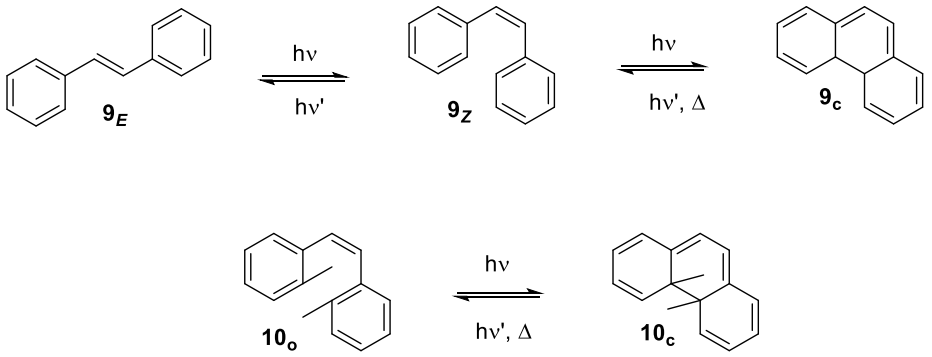

Figure 4 *Stillbene **9** in E and Z isomers and ring-closed form $\mathbf{9}_c$, ring closing also worked for ortho-methylene substituted stilbene **10**.*

However, both *E* → *Z* isomerization and cyclization were thermally reversible and the aim of the study was to create thermally stable molecules. From a previous study [52] it was known that furyl- and thienylethenes have longer ring-closed lifetimes. Also substituting the ethylene part of the molecule not only red-shifts the absorption but also slows down or even prohibits *Z* → *E* isomerization.

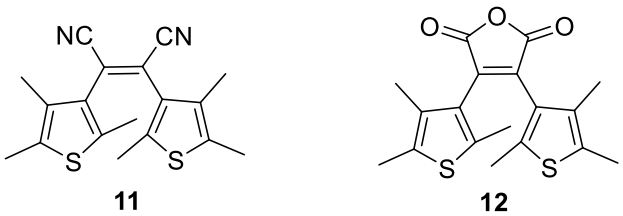

11 **12**

Figure 5 *The first thermally stable diarylethene photoswitches* [50].

Compounds **11** and **12** were thermally stable at high temperatures and had fatigue resistance for multiple cycles. Soon after it was discovered that instead of ethylene moiety, perfluorinated cyclopentene leads to the most stable molecules. These are arguably the most common subtype of diarylethenes, bisthienylcyclopentenes **15**. Many other alternatives for the ethylene bridge also exists, providing several routes for thermally stable diarylethene derivatives with good fatigue resistance. [19], [25], [53]

There are many synthetic ways to produce diarylethenes. Substitution of octafluorocyclopentene **14** with thiophene derivatives **13**, Suzuki-Miyaura coupling and intramolecular McMurry reaction being the most common ones. [53]

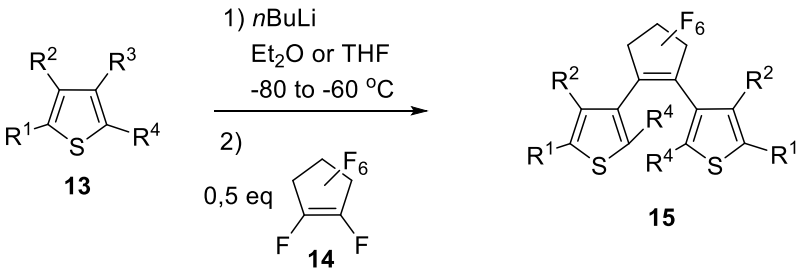

Scheme 4 *General reaction conditions for substitution of* ***14****, reproduced from* [53].

In the substitution reaction a halogen in the thiophene unit **13** (usually, and in Scheme 4 R^3) is first lithiated with *n*BuLi and then reacted with **14**. A wide range of other substituents may be used in **13**. R^1 can be halogen, alkyl, aryl, S-alkyl or heteroaryl group and **15** can often be further functionalized through it. R^2 can be H, halogens, alkyl or O-alkyl and R^4 can be H, halogen, alkyl, aryl or heteroaryl. This reaction also supports asymmetric substitution; when excess of **14** is used on step 2, only one fluorine will be substituted and can be further reacted in similar fashion with differently substituted **13**. The drawback of this reaction is the low boiling point (bp.) of **14** (26–28°C) which might create some practical difficulties. Depending on substituents, yields range from low to excellent.

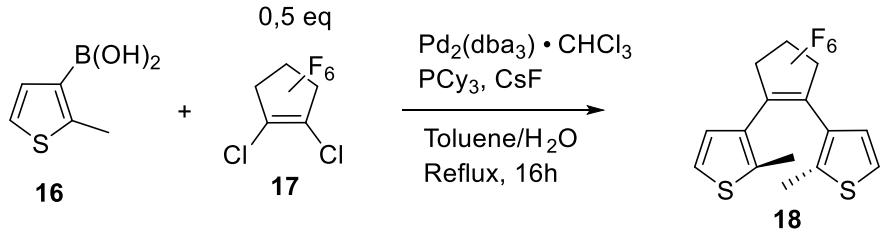

Scheme 5 *Suzuki-Miyaura coupling with optimized conditions* [54].

Suzuki-Miyaura coupling uses aryl boronic acids such as 2-methyl-3-thienylboronic acid **16** or a respective boronic ester to couple with less volatile (bp. 90 °C) 1,2-dichlorohexafluoropentene **17**.

In optimized conditions the coupling reaction has an excellent yield, 86% in Scheme 5. Boronic acid or ester compounds are storable unlike lithiated compounds and they do not require cryogenic conditions. Also substituents like carbonyl- or cyano groups can be included in the precursor **16**, unlike in Scheme 4 type reaction. [54]

The open-ring form of diarylethene is pale and colourless and the closed-ring form coloured. Substituents affect the spectrum of closed ring form, reported λ_{max} varying from 426 nm to near-IR region at 828 nm in Ref. [19].

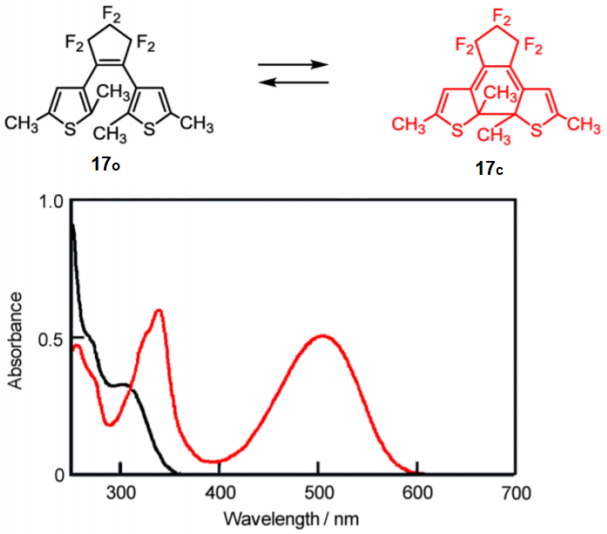

Figure 6 *Absorption spectra for 4,4'-dimethylbisthienylcyclopentene* ***17****, reproduced from* [25].

Compared to other photoswitches, diarylethenes are superior in thermal stability of both isomers and fatigue resistance. With good molecular design, thermal half-life is reported to be over 400,000 years and fatigue resistance over 10,000 cycles. [19], [25] These are necessary properties for applications such as optical memories. Other important properties are high, close-to-unity quantum yields of cyclization, fast cyclization reaction (picosecond scale) and efficient photoswitching also in single crystal state.

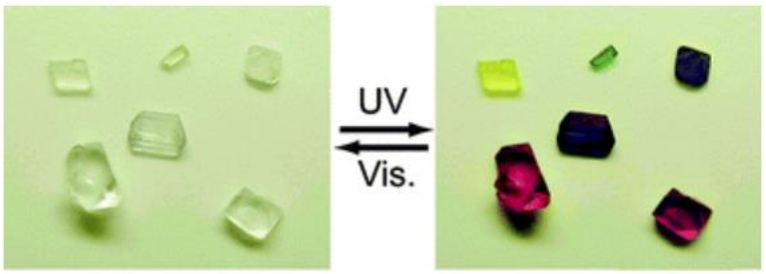

Figure 7 *Diarylethene photoswitching in single crystal state, reproduced from* [55].

2.3 Spiropyrans

Spiropyrans have been known since the beginning of 20th century [56]. Interest in them started when their reversible thermochromic properties were discovered [57], [58] and the interest was further increased when their photochromic properties were found. [59], [60] In addition to temperature and light, spiropyrans are known to respond to multiple other stimuli such as different solvents, redox potential, mechanical stress and metal ions. [61] The spiropyran structure in its ring-closed (spiro) and open chain (merocyanine) form is presented in Figure 8.

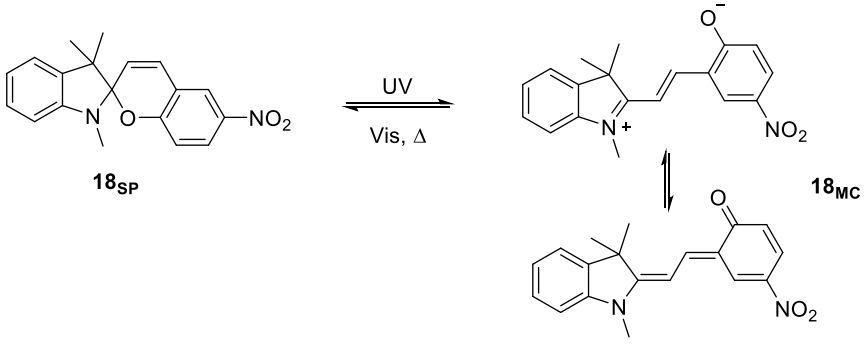

Figure 8 *Spiropyran in its ring-closed- (**18_{SP}**) and merocyanine (**18_{MC}**) forms with zwitterionic (top) and quinoidal (bottom) structure.*

The general synthesis of spiropyrans was introduced by Wizinger in 1940, and it still remains practically unchanged. In this procedure an indolino compound **19** and *ortho*-hydroxy aldehyde **20** are boiled in solvent (usually alcohol) to condensate the desired spiropyran **21** (Scheme 6). In the reaction multiple side products are formed as well. The amount of these can be reduced by using an indolenylium salt of **19** and an equimolar amount of organic base such as piperidine. [26]

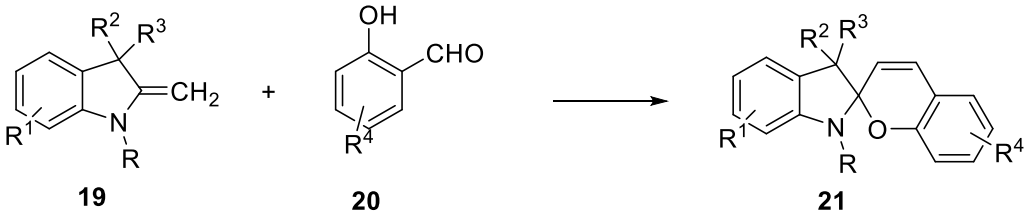

Scheme 6 *General synthesis method for spiropyrans.*

The spiro form is colourless and the merocyanine form is coloured. The absorption spectrum of the coloured form can be tuned, for example, via substitution in the chromene part of the molecule. It has been established that π-accepting substituents red-shift the merocyanine absorption spectrum. [26], [61]

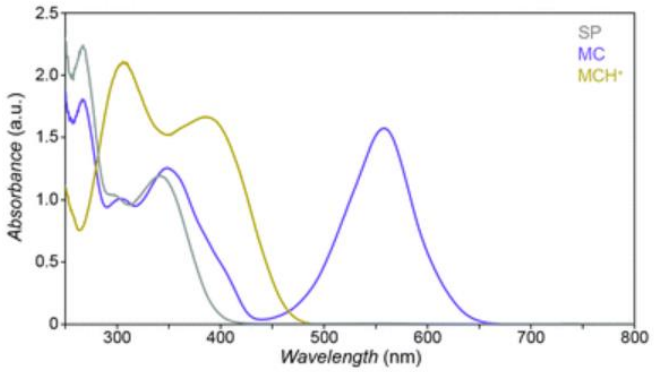

Figure 9 *Absorption spectra of spiropyran in spiro (SP), merocyanine (MC) and protonated merocyanine (MCH^+) forms, reproduced from* [61].

2.4 Applications for photoswitches

Photoswitchable molecules undergo structural or conformational changes upon irradiation, changing their properties significantly. Azobenzenes, for instance, have a huge change in molecular shape and therefore length of the molecule and geometrical position of its substitutes. Diarylethenes do not change much in shape, but the molecule becomes much more rigid in the closed-ring form. Also its electronic properties are markedly different in the open- and closed-ring forms. These properties are examples of what scientists have used in development of light-controllable materials [10], [12], [14], [15], [46], [62], [63]. When incorporated into materials, the molecular-level changes can be harnessed to induce changes in materials properties at the macroscopic level.

2.4.1 Catalysis and photopharmacology

Usual catalysts have their activity set when they are introduced to, for example, a reaction mixture. Their catalytic activity cannot be controlled without removing or poisoning the catalyst. Photoswitchable catalysts could be turned on and off with simple light irradiation (Figure 10).

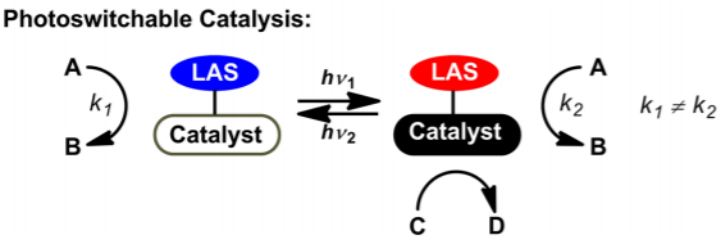

Figure 10 *Principle of photoswitchable catalysis, LAS = light absorbing species, k_1 and k_2 are reaction rates, reproduced from* [10].

Efficiency of photoswitching in catalysis can be described with reaction rates. For a well-controlled system, the reaction rate k_1 with an unactivated catalyst (white in Figure 10) is small or negligible, and when the catalyst is activated, $k_2 \gg k_1$.

In the field of heterogenous catalysis, photoswitches are usually mounted on surface. For example, Niazov *et al.* made a monolayer of spiropyran molecules on an indium tin oxide (ITO) surface. In the spiro form the molecules are electrochemically passive, but when switched to MC form with UV light they bear charge (see Figure 9) and become active. In their active state they bind Pt-nanoparticles which catalyze H_2O_2 reduction. By irradiating with 460 nm light the spiro form is reformed and catalytic activity lost. [64]

As homogenous catalysts there are many examples of molecules with an azobenzene core as photoswitching unit. Two main pathways for azobenzene-mediated control over catalysis are blocking the catalyzing site of molecule as in Figure 11, or creating an active site upon irradiation as in Figure 12.

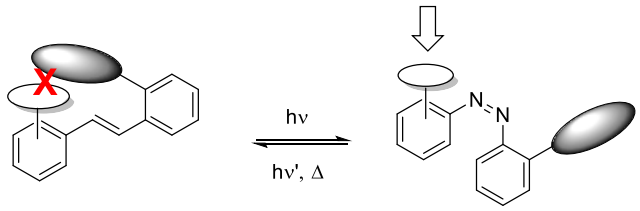

Figure 11 *Schematic picture of light activated catalyst with azobenzene core*

With careful molecular design it is possible to create systems which can be activated and blocked by light. Peters *et al*. [65] synthesized a molecule which had a piperidine lone electron pair acting as a catalytic base, blocked by bulky *tert*-butyl (*t*-Bu) groups on the other azobenzene ring. The best molecule described had k_1/k_2 >35, a lifetime of over 450 h and $E \rightarrow Z$ conversion of over 90% to both directions, making it an efficiently controllable bistable system.

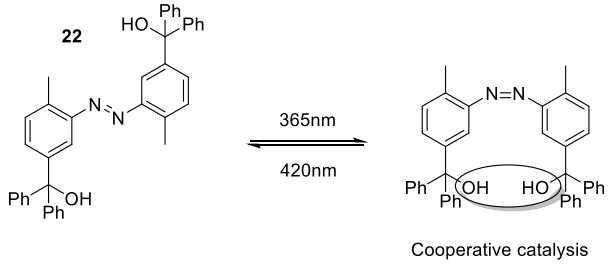

Figure 12 *Creating a catalytic site by irradiating* ***22****, reproduced from* [10].

Imahori *et al.* synthesized an azobenzene-tethered bis(trityl alcohol) **22**, which has two hydroxy groups. When irradiated with UV light, hydroxy groups form intramolecular hydrogen bond which increases acidity, and catalyzes Morita-Baylis-Hillman reaction. This increased the reaction rate by 25% compared to $\mathbf{22_E}$. [66]

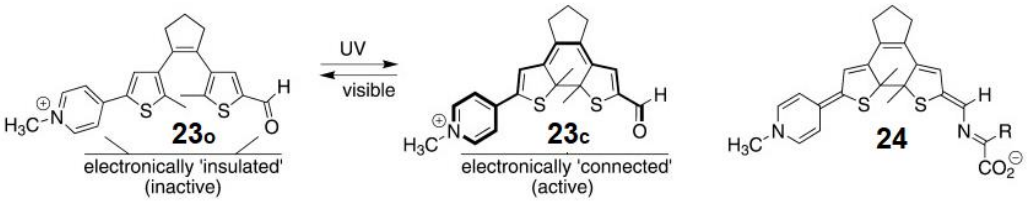

Figure 13 *Photoactivated catalysis based on different electronical properties of diarylethene* ***23*** *isomers, reproduced from* [67].

Also other photoinduced properties can be used in catalytic systems, for example, diarylethenes' electronical properties (Figure 13). This system by Wilson and Branda mimics a biologically active form of B_6-vitamin. Upon irradiation with UV-light, the diarylethene ring closes and pyridinium and aldehyde groups are electronically connected. This fully conjugated system stabilized the quinoid structure **24**, formed upon condensation with an amino acid and subsequent deprotonation of the aldamide α-hydrogen. Racemization of the amino acid can be observed in closed form $\mathbf{23_c}$ but under visible light the ring structure opens ($\mathbf{23_o}$) and racemization doesn't happen. [67]

Pharmacotherapy means the curing of diseases by using drugs. Conventional drugs usually have several problems such as poor selectivity which can lead into side-effects, uncontrollable activity and dosage problems emerging from poor selectivity and toxicity. Antibiotic-resistant bacteria are one of the major concerns, which emerges from uncontrollability of conventional drugs, as they are active also after exiting the body.

Light would offer a superior way to regulate biological systems. Excluding low-wavelength UV region, it is harmless, non-toxic, non-invasive, easily regulated and extremely precise compared to, for example, drug-activating chemicals. Photodynamic therapy is sometimes used for cancer treatment. It relies on locally irreversibly photoactivated singlet-oxygen-generating molecules. $^1O_2$, however, unselectively destroys cells on the targeted area. Photopharmacology uses synthetic photoswitches incorporated to molecules with biological effect in order to make reversibly activated/deactivated drugs with highly selective activity. Photoswitches can be bound to, for example, enzymes, ion-channels, transporters, pumps, proteins, metabotropic receptors and lipids. [11]–[15], [68]–[70]

There are multiple key elements for photoswitches to fulfill in order to succeed in photopharmacology. They must undergo a significant change in their properties upon irradiation, so that one form is inactive and the other active. Isomerization must be efficient to both directions; good quantum yields and PSSs containing mostly one isomer. For this both T- and P-type photoswitches could work, depending on the design. Of course, they have to work under physiological conditions, and be non-toxic. Also absorption in the "biological window", at 650–900 nm, would be beneficial because of lower energy (less chance for side reactions) and superior tissue penetration. [69]–[73] Indigo would offer an easy way for operating at optimal wavelength due to its naturally red-shifted absorption spectrum.

Photopharmacology is not yet at clinical state, but there are multiple working proofs of concept on the field. Mostly the azobenzene core is used for superior change in molecular length (~3 Å) and shape, but because of very precise working shape of enzymes, even the minor structural change (~0,1 Å) of diarylethene has been utilized. [11] Ion channels have been blocked/deblocked efficiently with azobenzene units [15], [68], [74], and incorporated to insulin release. [75] Azobenzene units have also been incorporated to DNA and peptide chains to control folding. [76], [77] Efficiently photocontrolled antibacterial molecules have been developed [14] and there's even a recent patent on the field. [78]

2.4.2 Materials

Materials that react to external stimuli are often denoted as smart materials. Common for this kind of materials is the need for molecular switches that react to such stimuli. For the scope of this work, focus is put on photoresponsive materials. Photoswitches undergo a change in their physical (and/or chemical) properties which can be transferred and amplified into macroscopic change in materials.

Photoswitchable molecules have been incorporated into multiple different materials such as liquid crystals (LCs), liquid crystal elastomers (LCEs), amorphous polymer matrices, gels, nanoparticles and metal-organic frameworks. [77] Liquid crystals are mostly organic molecules which combine the properties of fluids and the molecular order of crystals in their liquid crystalline state, located between crystalline and isotropic phases on a temperature scale. Depending on the orientation of molecules, there are multiple different liquid crystalline phases such as nematic or smectic. Heating a liquid crystalline phase leads to an isotropic liquid phase in which the molecular orientation is lost. Liquid crystal elastomers are polymeric materials in which liquid crystalline molecules, often

rod-like calamitic LCs, are used as monomers or crosslinks within the polymer network. [79]–[81]

Photoswitches can be either covalently bonded to the material network, used as a dopant inside the material or bound to the surface of the material. A number of ways can be utilized for covalent bonding of photoswitches. The most common way is using a vinyl-function containing group like acrylate or methacrylate in the end of the photoswitch, enabling linkage via polymerization. Numerous applications of photoresponsive materials have emerged, ranging from optical data storages to molecular motors and biomimicking systems. [10], [20], [82]–[85], [21], [26], [30], [31], [46], [47], [77], [81]

The photochemical characterization of photoswitches is typically carried out in solution. However, a solid environment might interfere with the switches, changing the observed properties. Azobenzenes' photochemical and photomechanical properties have been studied in amorphous polymers, and in a recent review [86] it is concluded that higher rigidity and degree of crystallinity of the polymer matrix results in less photomechanical bending of the polymer strips. Strips with covalently bonded photoswitches returned to non-bent state faster than strips where azobenzene was used as a dopant.

In the field of photoactuators, azobenzenes are mostly used due to their superior change in molecular length and shape, easily transferred into macroscopic motion of the material. LCEs are often used for photoactuators because of the soft and highly ordered molecular network. [8], [31]–[33] An example from field of photoactuators is a completely optically driven motor (Figure 14).

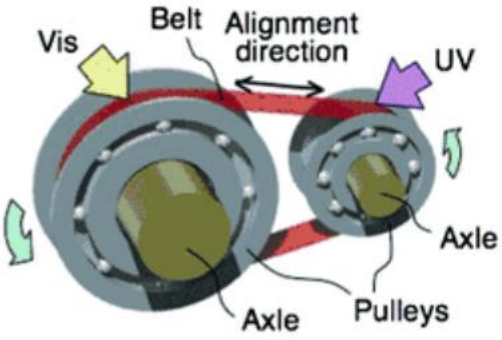

Figure 14 *Light-driven plastic motor, belt consists of azobenzene containing LCE laminated on a PE film. Direction of rotation can be swapped easily by changing UV and Vis irradiations with each other. Reproduced from* [87].

In LCEs photoswitches can translate molecular changes to macroscopic scale via either photothermal or photochemical effect. Photothermal effect is based on heat released by the photoswitch, thus inducing an LC-to-isotropic phase transition, which then deforms

the material provided that proper molecular orientation inside the material is found (Figure 15). This effect is present in LCEs containing photoswitches or just dyes and does not require covalent linkage of the photoswitch to the material. The effect can be exploited in, for example, self-oscillating LCE strips. [88] The photothermal effect is usually fast and the material returns to its original state shortly after the irradiation is ceased. Photochemical effect, on the other hand, is based on photoswitching, and covalent bonding to the material is required. Deformation of material is based on the shape change of the photoswitch molecules, amplified into macroscopic change by the molecular alignment of the LC material. [89] Photochemical effect has also been used to pattern reconfigurable LCE actuators, in synergy with photothermal effect to cause deforming. [90]

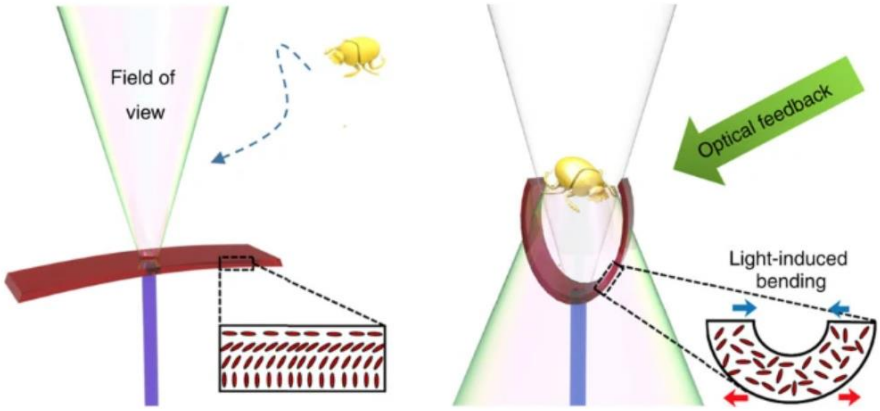

Figure 15 *Artificial flytrap mimicking venus flytrap -plant by Priimägis group. Reflected light from the target induces photothermal effect, which bends LCE film and traps the target. Reproduced from* [20].

Photoswitches can also be used in sensor applications. Different features of photoisomerization are dependent on environmental factors such as humidity or the presence of ions. For some azobenzenes the thermal relaxation rate depends on relative humidity. [91] Huber *et.al.,* on the other hand, showed that some *N*-monoarylated indigo molecules were sensitive for water present in the solvent. Thermal relaxation of these molecules was accelerated by water, and theoretical sensitivity up to 1ppm water content was calculated. [92] Zhuge *et.al.* presented a diarylethene molecule with selective sensitivity towards cyanide ions. In their work no sensitivity towards a wide range of other ions was seen, and when mounted on paper colorimetric recognition of CN^- in water was realized. [93]

3. INDIGO PHOTOSWITCHES

Earliest uses of indigo as a dye date back to ancient times [94], [95], and it has been one of the most used dyes in latest centuries. The absorption spectrum of indigo is the most redshifted among common photochromic molecules, making it interesting for many applications, especially in photopharmacology. Indigo and its derivatives can be isomerized around the central double bond with light, switching between the *E* and *Z* isomers. However, the photoswitching of indigo has been rarely studied [29]. Due to fast intramolecular proton transfer in excited state, the parent indigo does not isomerize. [82] It is also poorly soluble because of intramolecular hydrogen bonding, and there are only scattered reports of *N,N'*-disubstituted indigos [96]. A recent study showed synthetic pathways to *N,N'*-disubstituted indigos with thermally stable *Z* isomers and red-light-induced switching from *E* to *Z* isomer. [29]

3.1 Introduction to indigo

Indigo, or indigotin, has been used for thousands of years in different cultures as a dye. The blue colour of indigo is uncommon in nature. In fact, indigo (and tyrian purple, a derivative of indigo found in some animals) was throughout history the only available dye with blue colour for textile colouring. In ancient times this made indigo extremely valuable, and indigo-coloured garments were symbols of wealth and power. [97], [98]

Indican, the precursor for indigo, has originally been extracted from *Indigofera* family plants such as *Indigofera tinctora* which grows naturally mostly in India. An European plant *Isatis tinctoria* (a.k.a. Dyers' Woad) contains indican as well – however, 30 times less than the Indian one. Production of indigo from this percursor was done by fermenting indican-containing plants.

Natural indigo was imported to Europe for centuries, mostly between 1600 and 1900. Many historical events have hindered and re-started the woad-derived indigo production in Europe. Imported indigo was produced in, for example, India and described as "better quality". To the death of natural indigo production, industrial scale production of synthetic indigo grew in the beginning of the 20th century. Adolf von Baeyer showed the first synthetical route to make "artificial indigo" in 1882. Later in 1905 he received the Nobel prize in chemistry "*in recognition of his services in the advancement of organic chemistry and the chemical industry, through his work on organic dyes and hydroaromatic compounds*". [99] His synthetic route was not yet economically viable because of its low yield, but the

procedure of K. Heumann (and improved by J. Pfleger 1901) from 1897 was the start for the industrial synthesis of indigo. [28], [94], [97]

Today, indigo is the most produced synthetic dye worldwide, industry producing 50,000 tons of synthetic indigo annually. These processes use many hazardous chemicals such as inorganic catalysts, reducing agents and petrochemical derivatives. For example, Heumann's process uses a mercury-based catalyst, and the synthetic route from 1897 includes aniline, hydrogen cyanide, strong bases, excess of sodium azanide and formaldehyde. [100]–[102] Industrial-scale synthesis and textile dyeing are estimated to be among the most polluting industries in the world, and research is carried out for cleaner processes. [103], [104]

Indigo in its stable form is highly insoluble. Hence it will not penetrate fibres and cannot be used for dyeing as such. When reduced to its *leuco*-form, indigo turns pale yellow and is soluble in water. In alkaline solutions *leuco*-indigo further deprotonates, increasing solubility. Now the anionic dye penetrates into fabric, and when fabric is removed from the alkaline solution *leuco*-indigo rapidly oxidises back into blue indigo which remains trapped inside the fabric. This vat dyeing process is most commonly used for blue denim, which consumes around 95% of yearly produced indigo. [28], [97]

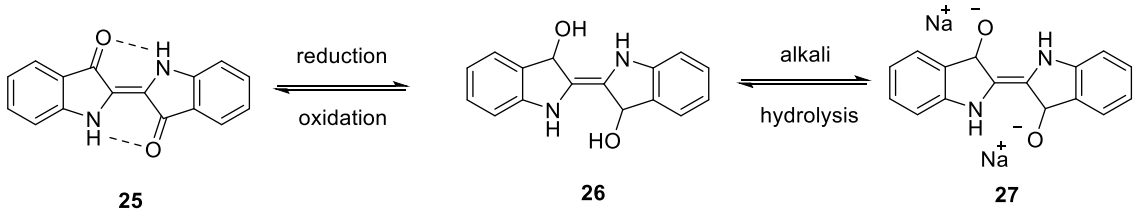

Figure 16 *Keto (**25**) and leuco-forms (**26**) of indigo. Leuco-indigo is deprotonated (**27**) in an alkaline solution and stabilized with cations, for example sodium.*

Many properties such as insolubility, high stability, absorption spectra and high melting point of indigo can be explained with double intramolecular hydrogen bonds (dashed lines in Figure 16). Hydrogen bonding is also used to explain the absence of *Z* isomer of plain indigo. Functionalizing *N*-atoms in an indigo molecule removes intramolecular bonding and has a drastic effect on its properties [29], [81], [105]

3.2 Synthesis

The different synthetic routes to produce indigo are presented here. Some methods, despite being old, are still used because of their ease or suitable conditions such as solubility of reagents and starting materials. Natural syntheses include an enzymatic cleavage of D-glucose from indican (**28)** to form indoxyl (**29)**, which oxidizes in atmospheric conditions into indigo. (Scheme 7) [28], [81], [97], [98], [106]

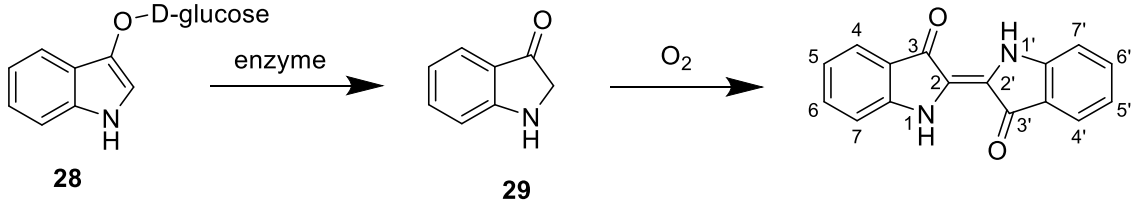

Scheme 7 *Natural synthesis of indigo and indigo atom numbering for later references.*

First proofs for the synthesis of indigo were made by Baeyer in 1878 by first making oxoindol (**33**) from phenylacetic acid (**31)**, which was then converted into isatin (**34**). Isatin was chlorinated with phosphorus trichloride and subsequently condensated, and then reduced with phosphorus to form indigo.

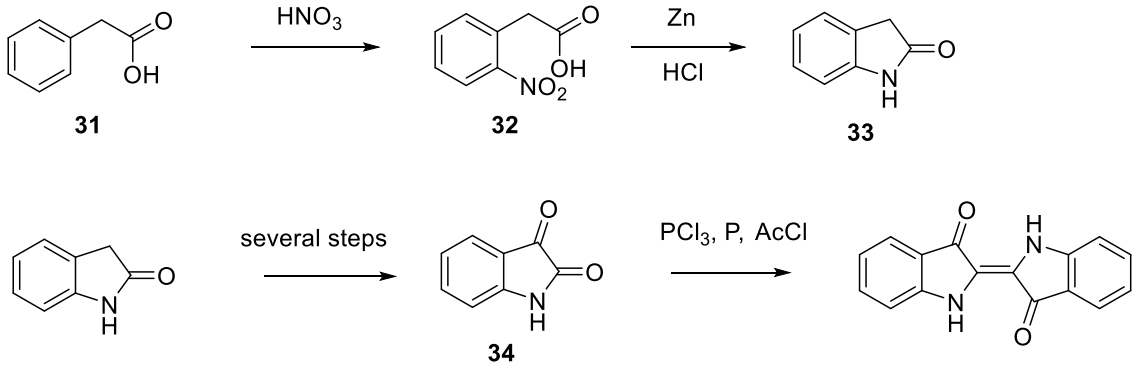

Scheme 8 *Indigo synthesis by Baeyer in 1878, reproduced from* [28], [107].

This method, with some modifications to reducing reagents, is still used in making some derivatives of indigo, because it works even with substituents in the aromatic ring of isatin. [81] Baeyer also published two synthetic routes for indigo in 1882 (Scheme 9).

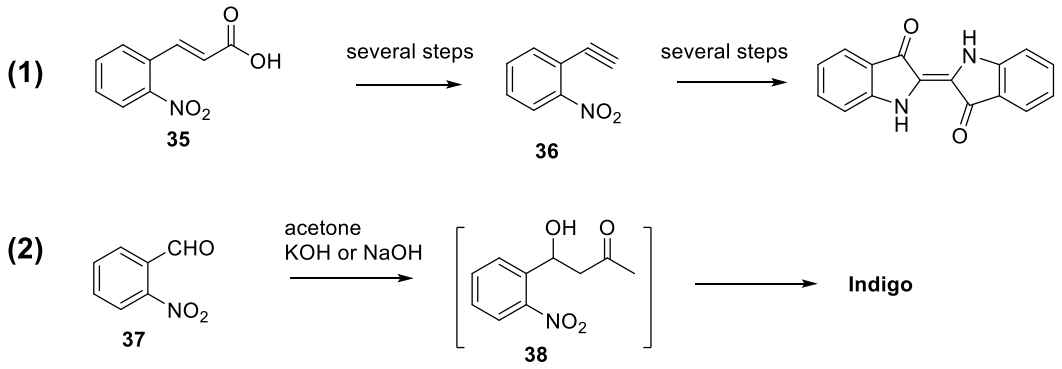

Scheme 9 *Baeyer indigo synthesis from o-nitro cinnamic acid (**35**) (1) and Baeyer-Drewsen one-pot synthesis from o-nitro benzaldehyde (**37**) (2), reproduced from* [28], [107], [108].

The Baeyer-Drewsen method (2 in Scheme 9) is still one of the easiest procedures of producing indigo and its substituted derivatives. For example 6,6'-dibromo indigo can be produced with this method from 2-nitro-4-bromobenzaldehyde. [97], [109] For industrial production first Heumanns (1 in Scheme 10) and later Heumann-Pfleger (2 in Scheme 10) synthetic route are used.

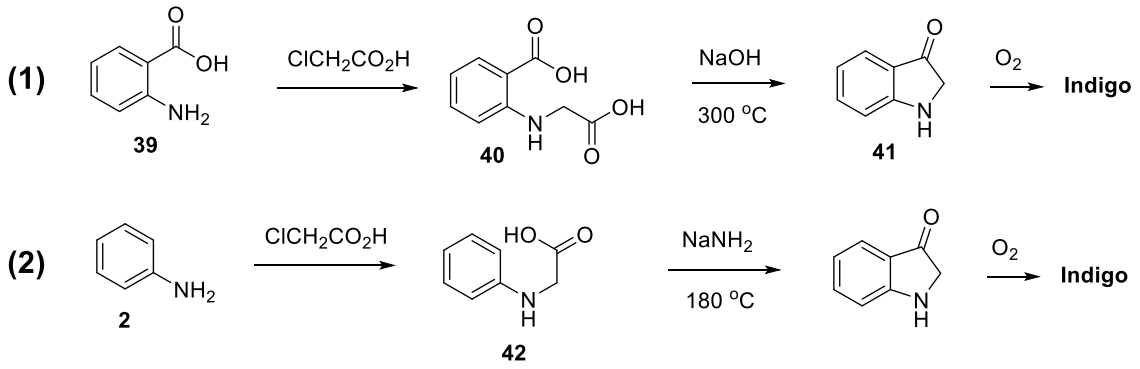

Scheme 10 *Industrial reactions to produce indigo.*

From the many different routes to synthetize indigo, the Heumann-Pfleger route proved most commercially successful and is still used. [110], [111] Recently, indigo and many of its derivatives have been studied in organic electronics, but synthesis in these is based on methods described herein or slightly modified ones [27], [28], [97], [109], [112]–[114]

As a photoswitch indigo has not been studied much. To undergo *E* → *Z* isomerization, hydrogens on nitrogen atoms of indigo must be substituted. This removes the intramolecular proton transfer on the excited state indigo, allowing excited state to relax via isomerization. [82] Up to the last decade, procedures for substitution were few and usually contained harsh conditions and huge excesses of reagents. [81], [96] Two more recent procedures have been established by Huang *et al.* [29] and Tanaka *et al.* [115].

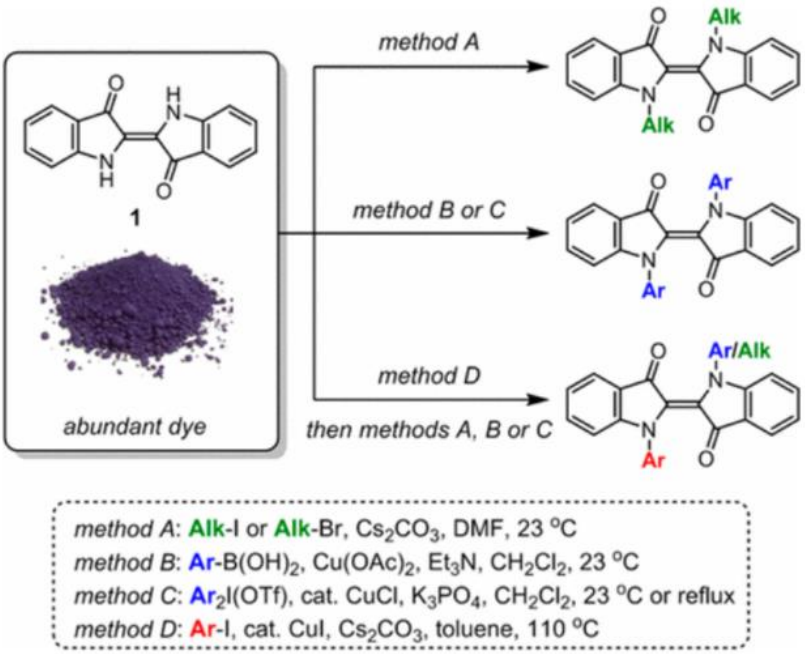

Scheme 11 *Procedure for N-substitution and N,N'-disubstitution of indigo molecules described by Huang* et al*. Reproduced from* [29].

In their work Huang *et.al.* found that with weak bases and activated electrophiles, *N,N'*-dialkylated indigos could be easily produced (method A in Scheme 11). To install electron-rich or -neutral aryl substituents, Chan-Lam coupling was found to be the most suitable (method B), while Cu-catalyzed cross-coupling reaction with aryliodonium salts (method C) worked for electron-deficient aryl groups. Both of these were selective towards double-*N,N'*-arylation. To gain access to asymmetric substitution Goldberg-Ullman reaction (method D) proved to be useful for mono-N-arylated indigos. Yields for all methods were moderate or low, mostly between 10% and 30%. [29] Method by Tanaka *et al.* also used Goldberg-Ullman type reaction (Scheme 12) with aryl halides **43** (X = Br or I).

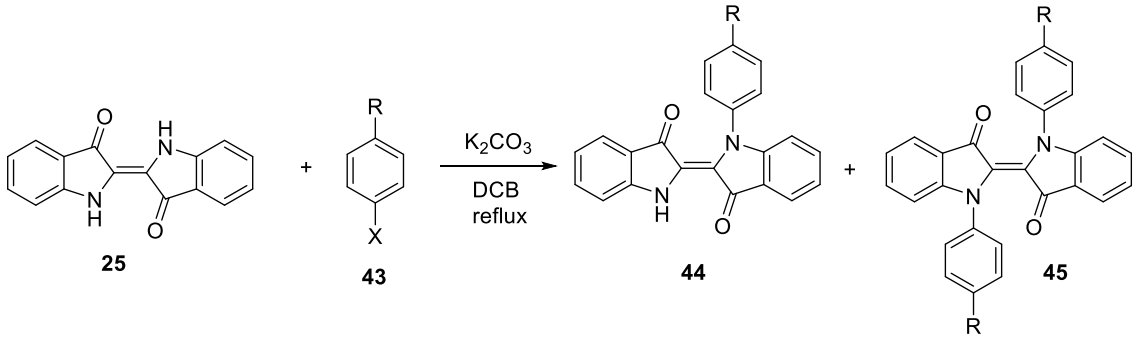

Scheme 12 *Goldberg-Ullman type coupling reaction for N(N')-(di)arylindigos.*

This method was also utilized by Huber *et al*. [92] with yields between 6% and 37% for different R-groups. Choosing between mono-N-arylated indigo **44** and *N,N'*-diarylindigo

45 product was easily controllable by using different (1.1 and 2.1, respectively) molar equivalents of **43**.

3.3 Photochemical properties

The absorption spectra of indigos are found to depend slightly on the solvent. [45], [105], [116] Substitution on *N,N'*-positions shifts the absorption maximum, but it still remains on longer wavelengths of visible light.

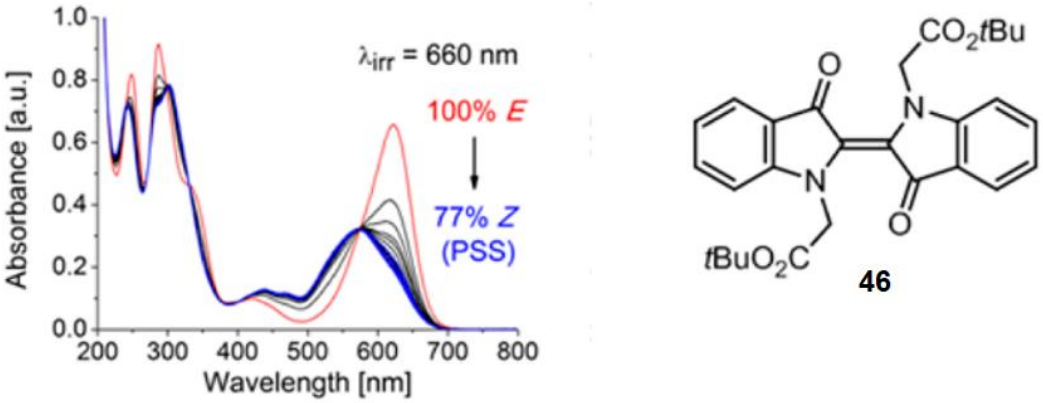

Figure 17 *Absorption spectra of N,N'-di(*tert*-butyloxycarbonylmethyl) indigo* ***46****, reproduced from* [29].

Attaching an electron-withdrawing alkyl group blue-shifts the absorption slightly (for **46** λ_{max} 622nm) compared to methyl group (λ_{max} 635nm). It, however, increases the thermal lifetime of the *Z* isomer significantly, and separates the absorption of *E* and *Z* isomers ($\Delta\lambda_{max}$ 62nm) (Figure 17). In the asymmetric case with fixed aryl group, if *tert*-butyloxycarbonyl group is attached directly to indigo, a significant blue-shift is observed (λ_{max} 584nm) with 50-fold increase in thermal lifetime compared to CH_2CO_2tBu as aryl chain. [29]

In the case of *N,N'*-diaryl indigos **45**, absorption maxima for all molecules functionalized with electron-withdrawing or electron-donating R-groups in the *para*-position remain around 630 nm. However, thermal relaxation displays a 400-fold difference between the molecules bearing an electron donating methoxy (58 s) and an electron withdrawing nitro group (408 min). It was also found that all *N,N'*-diaryl indigos exist as mixtures of *E* and *Z* isomers, which implies that they exhibit rather comparable stabilities. Density functional theory (DFT) -calculations showed < 1kcal/mol difference in ground state energies for *E* and *Z* isomers, which is within the typical DFT error bar. This indicates nearly isoenergetic structures and explains bidirectional thermal isomerization in both directions at room temperature. [29]

4. RESULTS

In the experimental part of this thesis, three different indigo photoswitches were synthesized and characterized in different environments. The design of the synthesized molecules was based on the work of Huang *et al.* [29] and is presented in Chapter 4.1. Properties of these molecules were studied in acetonitrile solution, as a dopant in an E7 liquid crystal mixture and poly-4-vinylpyridine polymer films and are presented in Chapter 4.2.

4.1 Synthesis of indigo photoswitches

Initially, 3 different molecules (**47**–**49**) were designed to be synthesized (Figure 18). The alkyl indigo (**47**) was expected to have a relative short *Z*-lifetime, but largest separation of *E*- and *Z* absorption maxima ($\Delta\lambda_{max}$). The aryl indigo (**48**) was expected to have the longest *Z*-lifetime and properties of the asymmetric indigo (**49**) would lie in between of these two. Electron-withdrawing -CH_2CO_2R structure was chosen as alkyl group because of longer lifetime (minute scale) than plain alkyl chain (seconds for -CH_3) and still operational under wavelength of 660nm, unlike for directly attached -CO_2R structure. For aryl sidechain, an electron-withdrawing nitro group in the *para* position would have the longest *Z* lifetime but would leave no room for further modifications. Therefore, a -CO_2R structure was chosen, as it presumably has a long *Z* lifetime because of the electron-withdrawing nature of carbonyl group and can be further functionalized from the R group.

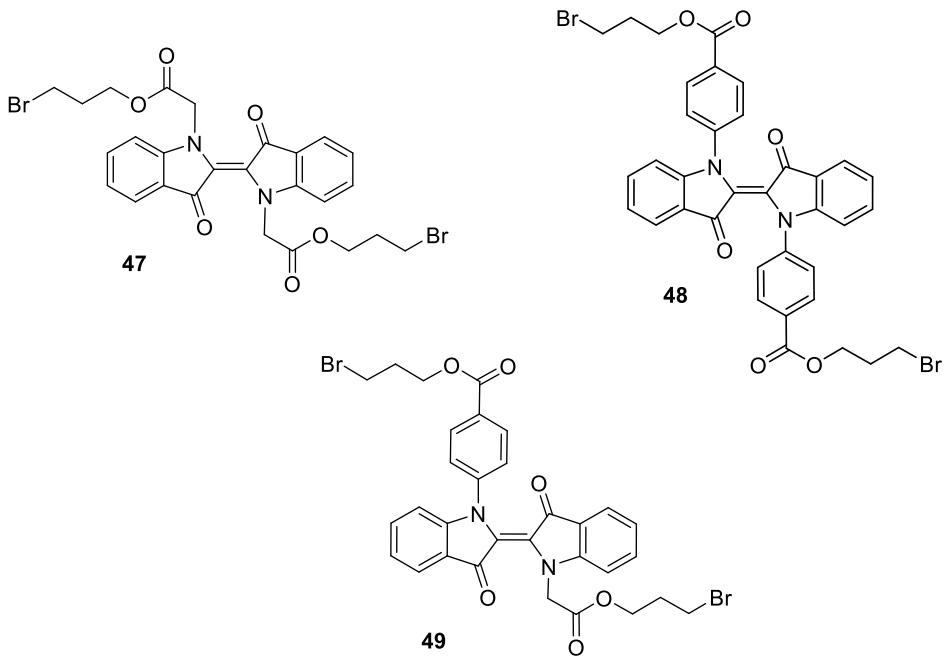

Figure 18 *Designed N,N'-disubstituted indigo compounds.*

Bromine atoms in the end of the sidechains would provide an easy way for further functionalization of the molecules, e.g., for the addition of polymerizable moieties. Ultimately, the goal was to have acrylate groups in the ends, but they were not necessary for this work, as the photochemical properties can be assumed to be same regardless of the end groups.

4.1.1 Symmetric *N,N'*-dialkyl indigo

N-functionalization of indigo with similar sidechain with moderate yield had been described before by Huang *et al.*; therefore, the same procedure was used. The side-chain was prepared by reacting 3-bromopropan-1-ol (**50**) with bromoacetyl bromide (**51**) to yield (**52**), which was coupled with indigo utilizing a synthetic route reported by Huang *et al.* [29].

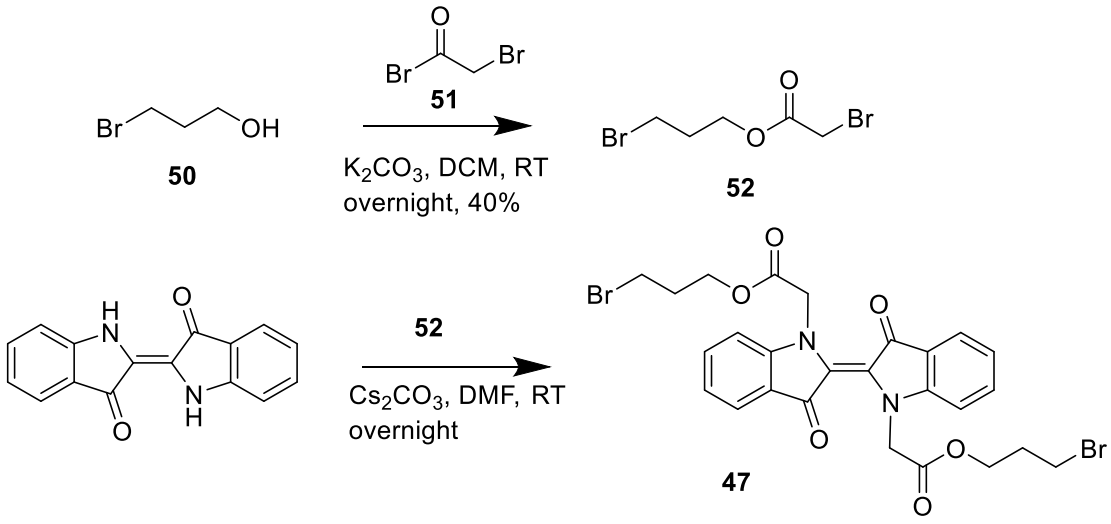

Scheme 13 *Synthetic route for symmetric N,N'-dialkylindigo.*

The yield for the coupling reaction was quite low, so the reaction was studied with different conditions by changing the molar amount of **52**, the concentration of the reaction mixture and reaction time (**Error! Reference source not found.**). Diluting the reaction increased the yield. Increasing the molar concentration of **52** yielded less side products and thus, a cleaner product.

Table 1 *Screening of N,N'-dialkyl coupling reaction.*

Entry	*sidechain (eq.)*	*DMF (ml)*	*Yield (%)*
A	4	1	12.7
B	4	3	26.1
C	8	1	11

However, NMR and TLC analyses of the product revealed that the formed **47** spontaneously decomposes, possibly due to ring formation between the indigo nitrogen and bromine. To avoid this problem, **47** was further reacted with acrylic acid (**53**) in an S_N2 reaction to yield **54** (Scheme 14).

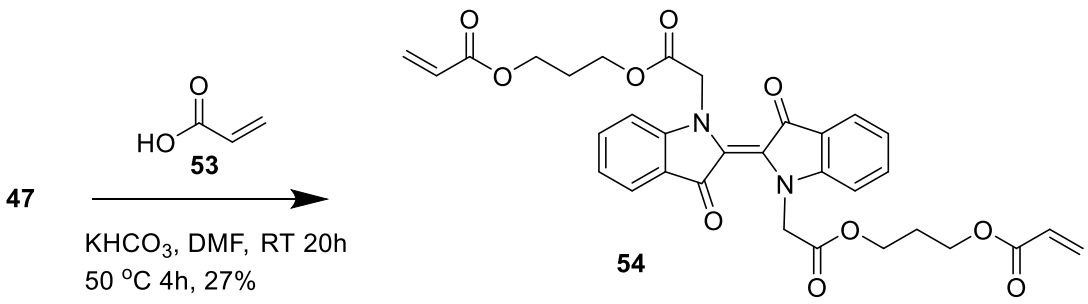

Scheme 14 *Acrylation of **47** into N,N'-dialkylacrylate (**54**).*

The acrylation reaction had a decent yield, and the product was stable according to NMR analysis. To have similar structures for later characterization, **48** and **49** were also acrylated as the last step.

4.1.2 Symmetric *N,N'*-diaryl indigo

An aryl sidechain was prepared via a simple acyl substitution reaction between 3-bromopropan-1-ol (**50**) and 4-iodobenzyl chloride (**55**) with good yield. The sidechain (**56**) was then coupled with indigo with in a copper catalyzed reaction described by Tanaka *et al.* [115]. *N,N'*-diaryl indigo **48** was then acrylated to yield final product **57** (Scheme 15).

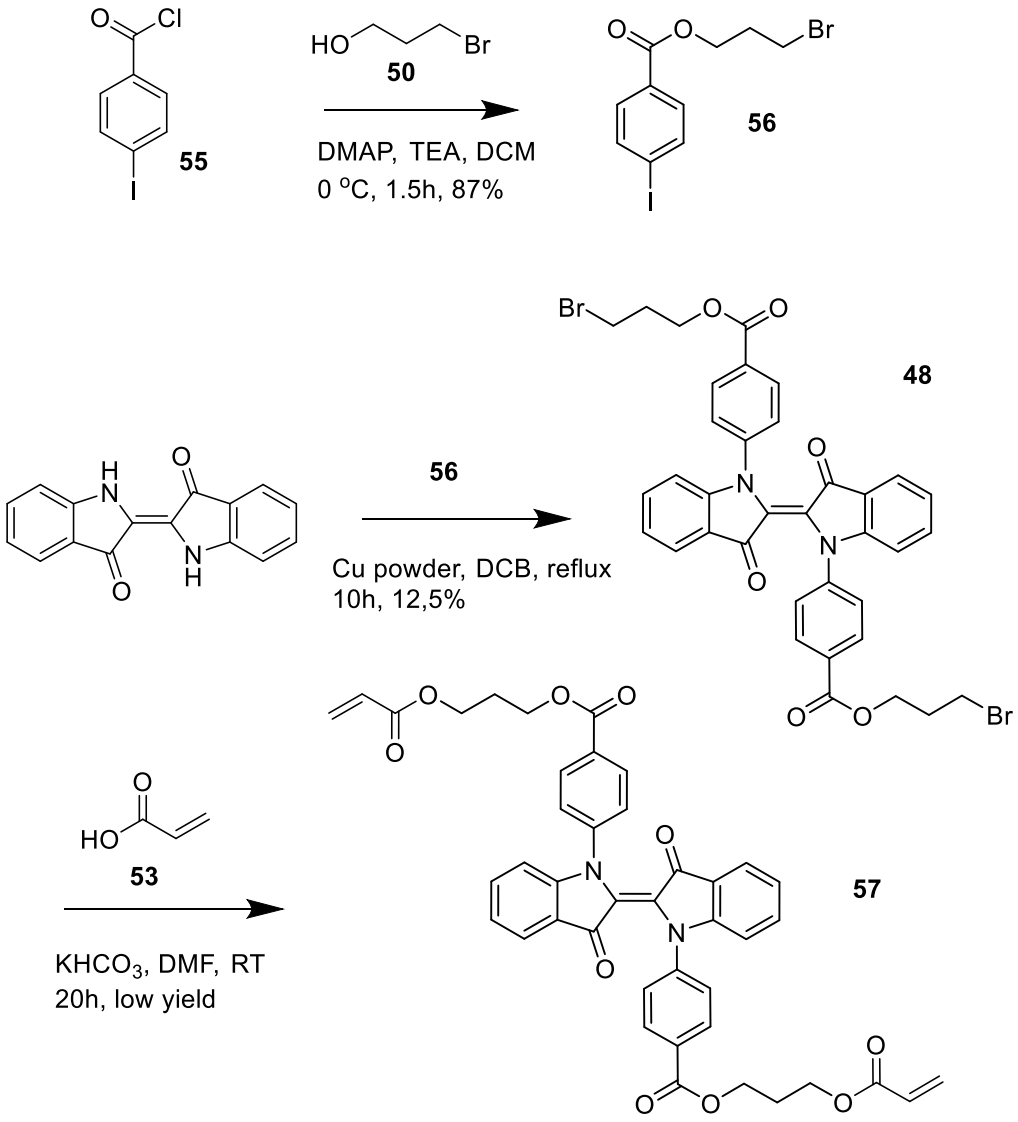

Scheme 15 *Synthetic route for N,N'-diarylindigo acrylate.*

The coupling reaction suffered from poor yield and a complex mixture of side products, and further acrylation yielded too little product for later characterization. Second approach for *N,N'*-diarylindigo was to eliminate the need for bromine in the side-chain by using a hydroxy functionality as an end group. Preliminary studies had revealed that a free hydroxy group hampers the coupling reaction, so the alcohol was first protected with a *tert*-butyldimethylsilyl (TBS) group, after which the coupling followed via the same method as before to afford **61** in a moderate yield as well as some mono-arylated indigo **62**. (Scheme 16)

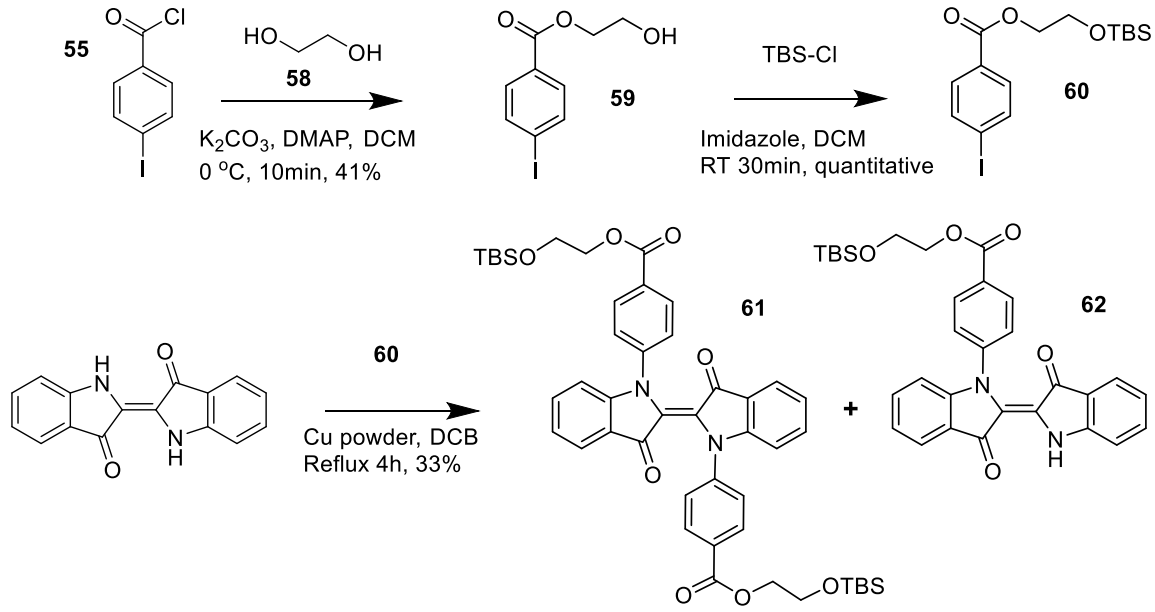

Scheme 16 *Second approach for N,N'-diarylindigo.*

The silyl protection was cleaved with tetrabutylammonium fluoride (TBAF). This required multiple tries due to the fast decomposition of **63** even at lowered temperatures. An optimized yield for the reaction was only 31%, accomplished at -30°C. The acquired product was then reacted with acryloyl chloride to yield the final target molecule **66**.

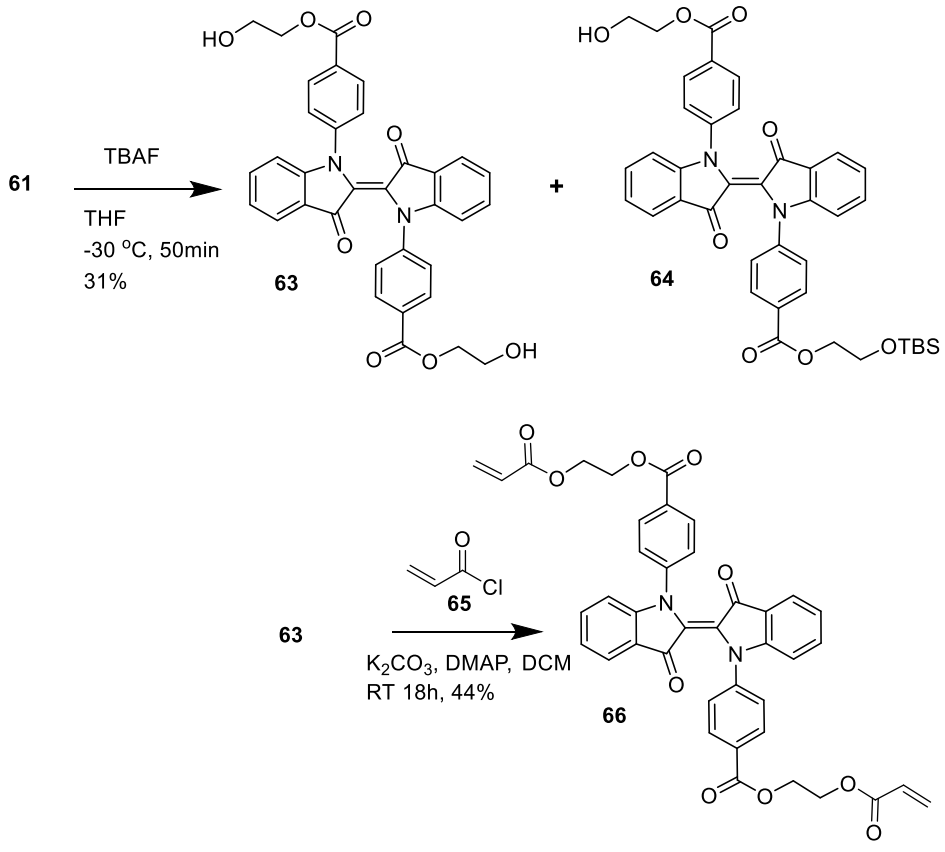

Scheme 17 *Deprotection of alcohol group and acrylation of N,N'-diarylindigo.*

The deprotection step yielded a mixture of fully protected starting material, mono-deprotected indigo (**64**) and fully deprotected indigo (**63**). The starting material and **64** can be further reacted with TBAF to increase the total the yield of the reaction.

4.1.3 Asymmetric indigo

The synthesis of the asymmetric *N,N'*-disubstituted indigo was carried out in two steps (Scheme 18). First, one nitrogen in the indigo core was functionalized with an aryl side-chain. This *N*-substituted indigo **67** was further reacted with the alkyl side-chain with almost quantitative yield. The *N,N'*-disubstituted indigo **49** was then acrylated to yield the target molecule **68** in a moderate yield.

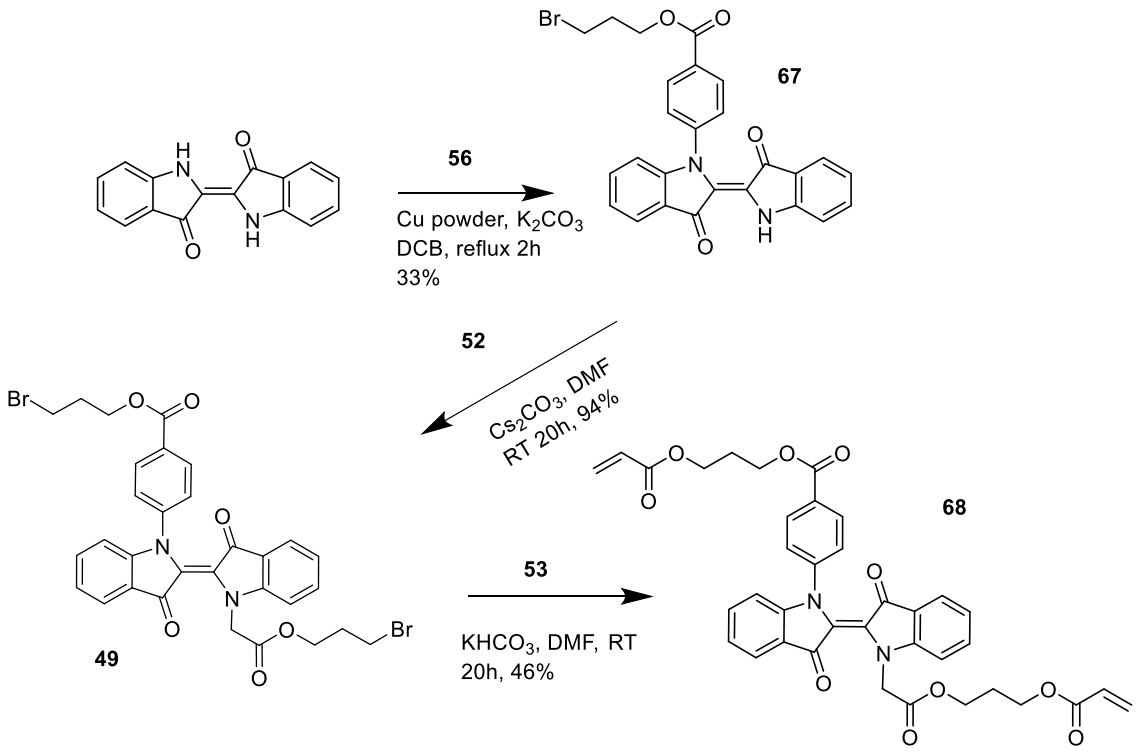

Scheme 18 *Synthetic route for asymmetric N,N'-disubstituted indigo.*

The synthesis of all *N,N'*-disubstituted indigos suffered from poor to moderate yields. Coupling reactions usually yielded a mixture of side products and purifying desired compounds was difficult. In addition, most of the compounds decompose on silica during column chromatography, so repeated purifications also lowered the total yield of reactions.

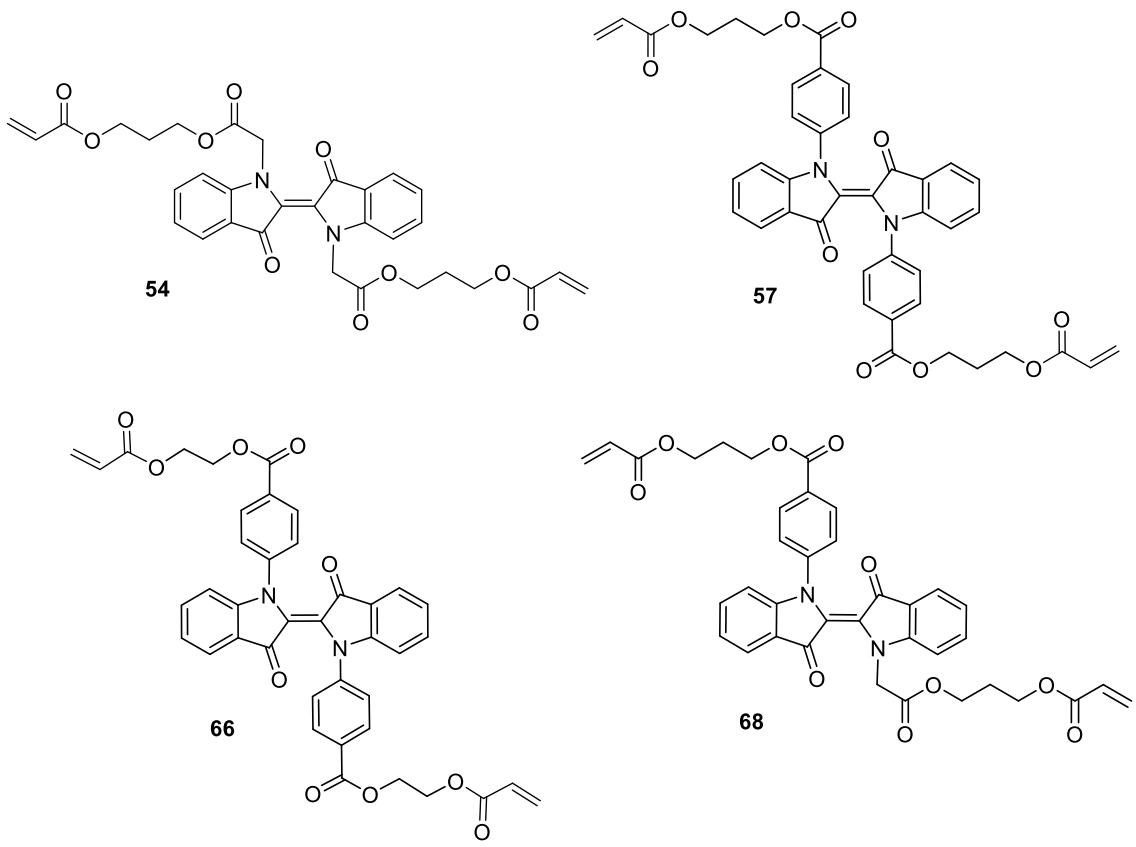

Figure 19 *Final products of synthetic work.*

The photochemical properties of the final products (Figure 19) were characterized in dilute MeCN solutions, as dopants in E7 liquid crystal mixtures and as dopants in poly-4-vinylpyridine (P4VP) films.

4.2 Photochemical characterization

Relevant photochemical theory and experimental methods for determining the key properties of the studied indigo compounds are presented in this chapter together with the results of the work. Representative figures are shown for each relevant experimental method, the rest can be found in experimental section (Chapter 6). Properties were studied in three environments, in a dilute acetonitrile solution, as dopant in an E7 liquid crystal mixture and as dopant in a poly-4-vinylpyridine (P4VP) film. Studied properties include molar extinction coefficients, thermal lifetime of the *Z* isomer, photostationary state (PSS) compositions and order parameter for the liquid crystal mixture.

4.2.1 Photoswitching in solution

Spectrophotometer measures intensity of light before the sample I_{in} and after the sample I_{out} at different wavelengths, and calculates the absorbance of the sample at different wavelengths as

$$\boldsymbol{A(\lambda) = log_{10}(\frac{I_{in}(\lambda)}{I_{out}(\lambda)})} \quad (1)$$

Molar extinction coefficient $\varepsilon(\lambda)$ can be calculated from Beer-Lambert law

$$\boldsymbol{A(\lambda) = \varepsilon(\lambda)cl} \quad (2)$$

when concentration of absorbing species, c, and length of light path, l, are known. c is usually given in mol dm^{-3} and l in cm, giving [ε] = l mol^{-1} cm^{-1} = M^{-1} cm^{-1}. After irradiating the *E* isomer with certain wavelength λ until the spectrum doesn't change anymore, a photostationary state (PSS$_\lambda$) is reached. In the case of the studied indigo photoswitches, the *Z* isomer doesn't absorb over 650nm and the absorbance beyond this wavelength is attributed solely to the *E* isomer [29]. Thus, the PSS composition can be calculated when plotting A_{pss}/A_E against wavelength and looking for a horizontal part around 650nm.

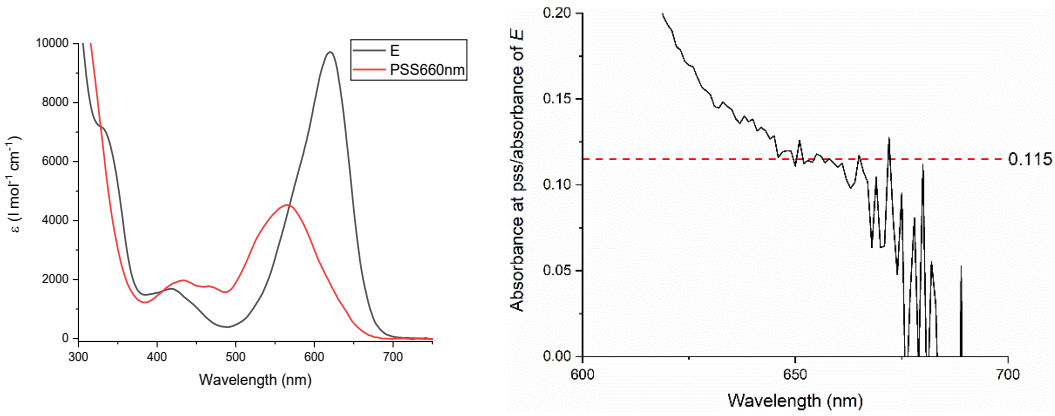

***Figure 20** Calculating PSS$_{660}$ composition for N,N'-dialkylindigo.*

This A_{pss}/A_E ratio represents the amount of *E* isomer in a given PSS. In Figure 20 the PSS$_{660}$ composition would be 11.5% *E* and 88.5% *Z*. As long as there is enough separation between the absorption spectra of the *E* and *Z* isomers, the negative photochromic nature of indigo allows us to calculate the pure *Z* spectrum from PSS and *E* spectra with

$$\boldsymbol{A_Z = \frac{A_{PSS} - E\% * A_E}{Z\%}} \quad (3)$$

For *N,N'*-diarylindigo however, the dark spectrum is not pure *E* isomer. Absorbance in dark can be written with absorbances of isomers and their ratios

$$\boldsymbol{A_{dark} = xA_E + (1-x)A_Z} \quad (4)$$

where *x* is the molar fraction of *E*. Respectively, absorbance at any photostationary state can be written

$$A_{PSS} = yA_E + (1 - y)A_Z \quad (5)$$

where *y* is ratio of *E* at this state. If the thermal isomerization of the indigo is slow enough, as in the case of aryl indigos, the ratio of *E* and *Z* isomers can be estimated from NMR data by comparing the integrals of the signals attributing to each isomer (Appendix 14), giving us values for *x* and *y*. Now we can calculate the spectrum for pure *E* isomer

$$A_E = \frac{A_{dark}(1-y) - A_{PSS}(1-x)}{x(1-y) - y(1-x)} \quad (6)$$

and use the PSS/*E* method to calculate *Z* spectra.

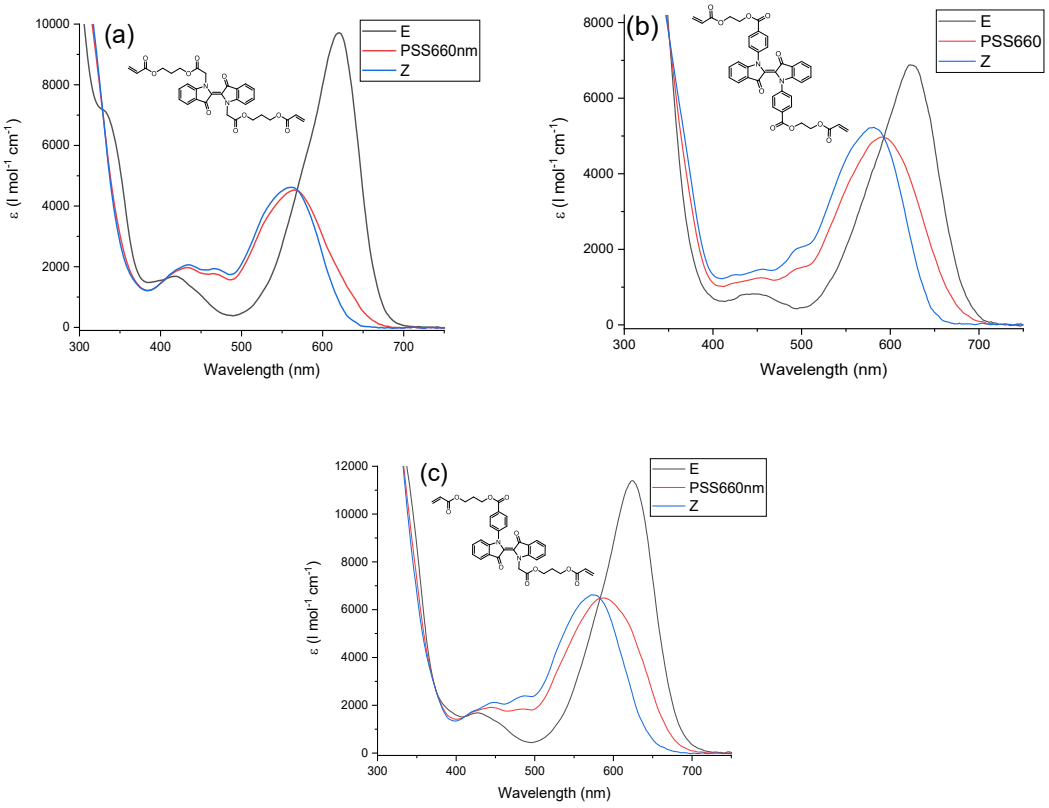

Figure 21 *PSS_{660}-, E- (for **54** & **68**), calculated E- (for **66**) and calculated Z spectra for dialkyl- (a), diaryl- (b) and asymmetric indigo (c).*

The measured and calculated spectra are presented in Figure 21. From these, absorption maxima were picked and molar extinction coefficients for these peaks were calculated, see **Error! Reference source not found.**.

Lifetime *τ* for *Z* isomer is defined as the time in which the amount of the *Z* isomer is reduced to 1/e of its initial amount (e ≈ 2.72). In this work the lifetime is calculated for the

thermal relaxation from PSS_{660} to the equilibrium in dark, even though this is not pure *E* isomer in all cases. An exponential decay function

$$A = A_0 e^{-\frac{t}{\tau}} \quad (7)$$

was fitted to absorbance against time data in Origin 2019b and lifetimes (t1 in Figure 22) were collected.

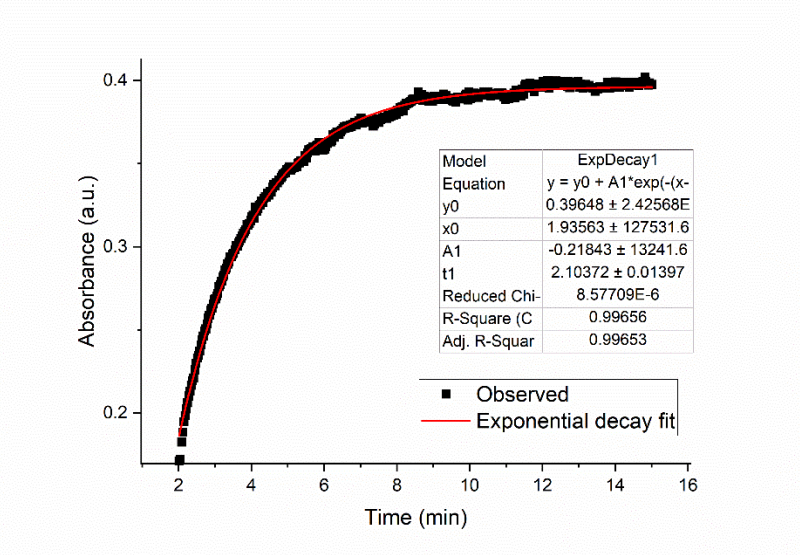

***Figure 22** Lifetime fit for **54**, absorbance measured at 620nm.*

Lifetimes for all studied compounds, as well as other presented properties are listed in **Error! Reference source not found.**.

***Table 2** Key properties of studied indigo compounds (E / Z isomers)*

Side-chain	λ_{max} (nm)	ε ($M^{-1}\,cm^{-1}$)	τ (min)	Z% at PSS_{660}
Alkyl	620 / 562	9700 / 4620	2.1 ± 0.02	88.5
Aryl	625 / 581	6880 / 5230	70 ± 1.10	63.5
Asym	624 / 573	11400 / 6620	5.6 ± 0.11	69

As seen from **Error! Reference source not found.**, all properties of the *N,N'*-disubstituted indigos in a MeCN solution follow the expectations from Ref. [29]. Lifetime for *N,N'*-dialkyl indigo is the shortest and the longest for *N,N'*-diaryl indigo. *N,N'*-dialkyl indigo has the most *Z*-isomer in PSS_{660}, while *N,N'*-diaryl indigo has the least, which is a bit unexpected as quite similar structures in Ref. [29] had 77% and 80-82% *Z*-isomer in PSS_{660}

for alkyl- and aryl side-chains. When there is an electron-withdrawing ester group in the alkyl chain attached to indigo nitrogens, the separation between *E* and *Z* absorption maxima is largest ($\Delta\lambda$=58 nm). Aryl group with electron-withdrawing group in para-position increases the lifetime of the *Z* isomer significantly, while still having a good $\Delta\lambda$ of 44 nm. For asymmetric substitution pattern the properties land between these two, being closer to *N,N'*-dialkyl indigo in lifetime. All compounds showed good fatigue resistance, only a tiny decrease in absorbance (0.9–2.1%) was observed after 1 h continuous irradiation with 660 nm LED at 520mW power.

4.2.2 Liquid crystal mixture

The synthesized indigo compounds were studied as dopants in an E7 liquid crystal. E7 and the studied compound (2 or 4 m-%) were mixed in DCM, and the solvent was evaporated under reduced pressure. 10 µm planar cells were filled with mixture and spectra were recorded with a spectrophotometer.

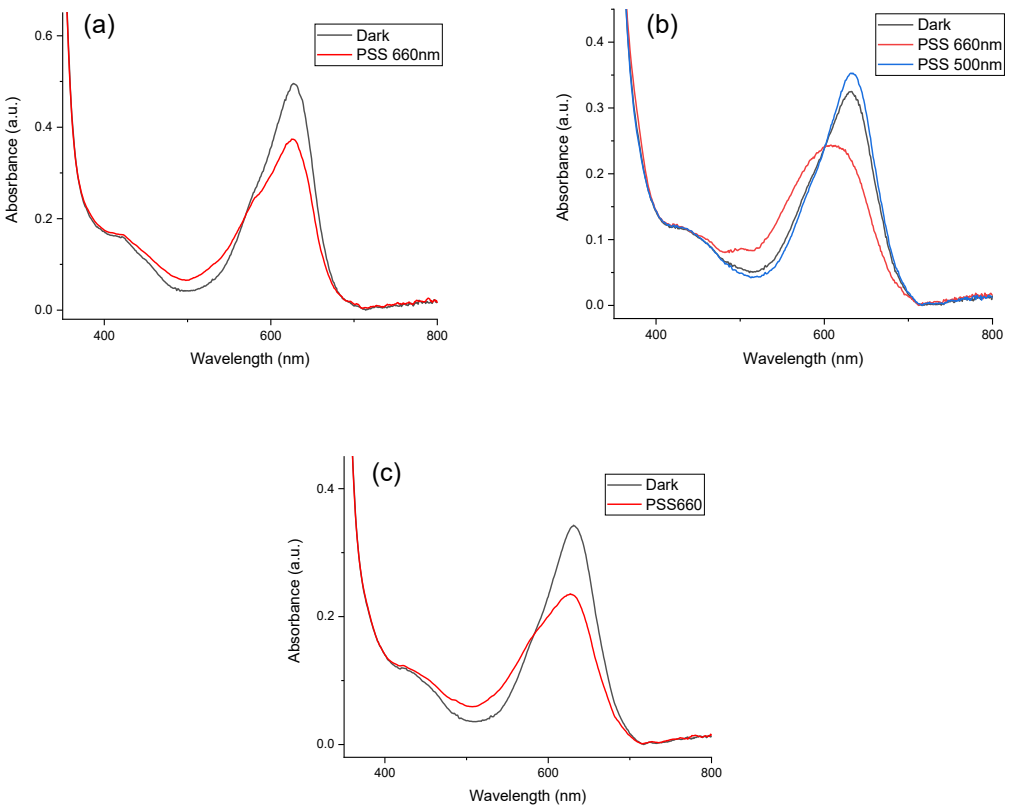

Figure 23 *Absorption spectra for dialkyl- (a), diaryl- (b) and asymmetric indigo (c) as a dopant in E7 liquid crystal.*

From recorded data the photostationary state composition was estimated with equation 3 and lifetime for the *Z* isomer was calculated. The order parameter *S* for a liquid crystal mixture can be calculated with

$$\boldsymbol{S = \frac{A_{\parallel} - A_{\perp}}{A_{\parallel} + 2A_{\perp}}} \qquad (8)$$

[117] by measuring the spectra with 2 different polarizations of light. $A_{\parallel}$ is absorbance with parallel polarization (0 in Figure 24) and $A_{\perp}$ perpendicular polarization (90 in Figure 24) of light with respect to the LC cell alignment.

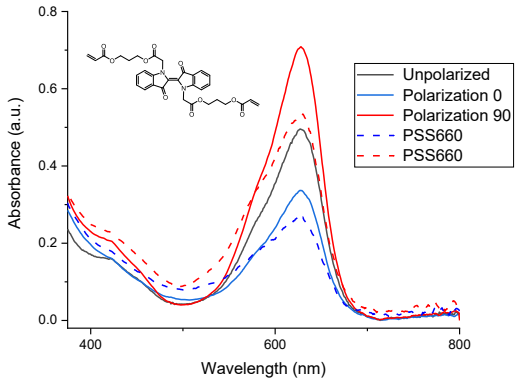

Figure 24 *Absorption spectra of* ***54*** *with different polarizations, PSS_{660} with respective polarization with dashed line.*

Now for **54**,

$$S_E = \frac{A_{\parallel} - A_{\perp}}{A_{\parallel} + 2A_{\perp}} = \frac{0.33 - 0.71}{0.33 + 2 * 0.71} = -0.22$$

$$S_{PSS_{660}} = \frac{A_{\parallel} - A_{\perp}}{A_{\parallel} + 2A_{\perp}} = \frac{0.26 - 0.52}{0.26 + 2 * 0.52} = -0.2$$

and change in molecular orientation during irradiation

$$\Delta S_{h\upsilon} = S_E - S_{PSS_{660}} = -0.02$$

During measurements photobleaching, or by definition fatigue [7], of indigo compound was observed. To estimate fatigue, 10 irradiation cycles (660 nm for 30 s, 30 s off) were made (Figure 25) and degree of degradation *x* was calculated from

$$\boldsymbol{y = (1 - x)^n} \qquad (9)$$

where n is the number of irradiation cycles and y is the non-degraded fraction after the n cycles. For **54** (Figure 25), after reducing the baseline from data, we get

$$x = 1 - \sqrt[9]{1 - \frac{A_1 - A_{10}}{A_1}} = 1 - \sqrt[9]{1 - \frac{0.26048 - 0.23743}{0.26048}} = 0.0102$$

which would mean it takes approximately 56 cycles for half of the **54** to be degraded (Z_{50} value in definition of fatigue [7]).

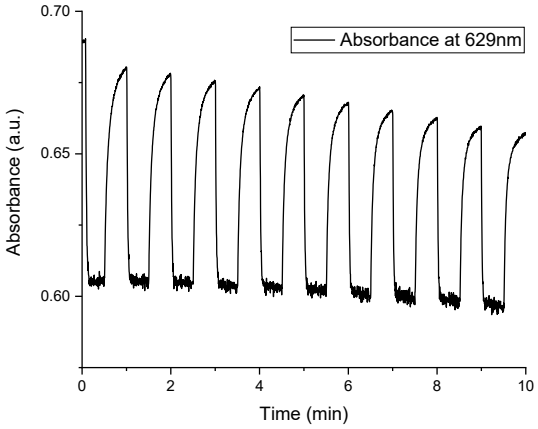

Figure 25 *Irradiation cycles for* ***54.***

Results of characterization as dopants in E7 LC for studied indigo photoswitches can be found from following table

Table 3 *Key properties for studied indigo compounds doped in E7 liquid crystal*

	τ	λ_{max} (*E*/PSS$_{660}$)	*Z* at PSS$_{660}$	S_E / S_{pss660}	ΔS_{hv}	x / Z_{50}
Alkyl	7.2 s	628 / 627	27 %	-0.22 / -0.2	-0.02	0.01 / 56
Aryl	29 ± 3 min	633* / 611	> 48%*	0.11* / 0.025	0.086	0.015 / 45**
Asym	4.2 s	631 / 629	35 %	-0.04 / -0.06	0.02	0.0095 / 76

* Aryl-indigo is not pure *E* in dark, PSS$_{500}$ was used as if it was *E* spectra for calculations
**Because of longer lifetime, cycles were made by cycling 660 nm and 500 nm LED instead of 660 nm and off, probably resulting in a smaller cyclability number

4.2.3 Polymer films

Indigo compounds were studied as dopants in poly (4-vinyl pyridine) (P4VP) thin films. First studies were made with 60kDa P4VP, and only minor photoswitching (~12% *Z* in PSS) was observed. After changing to 1.2kDa P4VP, which has lower glass transition temperature (t_g) of 61 °C [118] compared to 137–148 °C for 60kDa [119], [120], more isomerization was observed. This polymer was used for studies, also a sample from 8kDa P4VP (t_g = 132 °C from Ref. [121]) was made and similar photoswitching was observed. From the made films absorption spectra was recorded, seen in Figure 26.

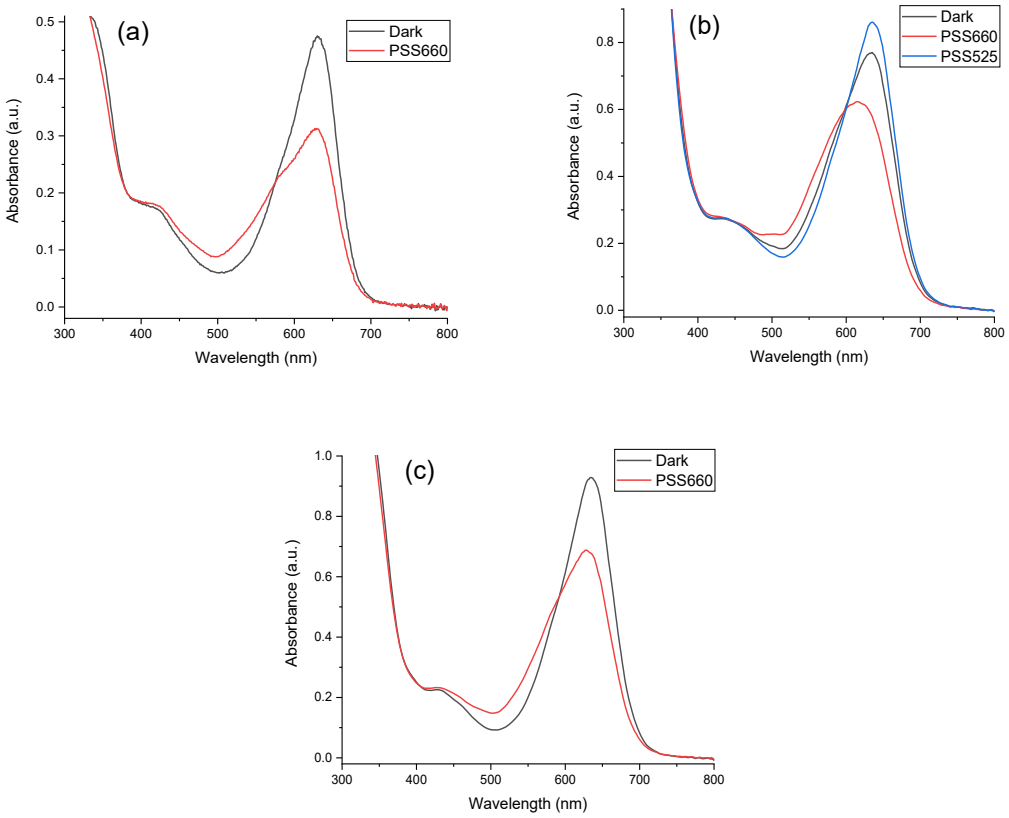

Figure 26 *Spectra dialkyl- (a), diaryl- (b) and asymmetric indigo (c) in 1,2kDa P4VP films*

The lifetime of the *Z* isomer was calculated the same way as before. It is notable that the absorbance of the indigo-doped films does not return back to the initial value, but remains lower, i.e, a part of the indigos remains in the *Z* state. Alkyl and asymmetric indigo relax quite close to the initial state, while the aryl indigo is left with more *Z*-isomer (Figure 27). However, it can be efficiently switched between PSS_{660} and PSS_{525}.

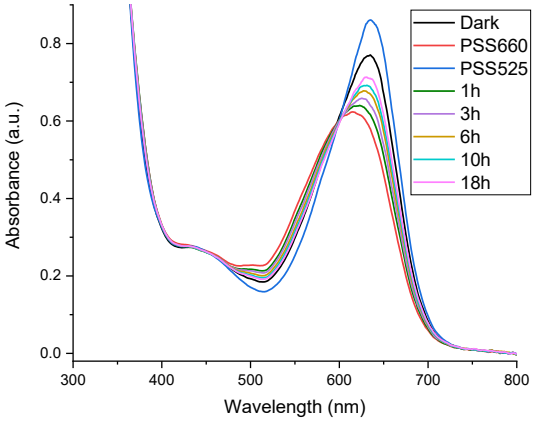

Figure 27 *Diaryl indigo spectra at different times after ceasing 660nm irradiation.*

For dialkyl and asymmetric indigo films, the dark spectrum was estimated to be pure *E* and the PSS composition was calculated the same way as in solution. For the aryl-compound the spectrum is presented for different photostationary states and the composition estimated as if PSS_{525} was pure *E*.

Table 4 *Key properties for indigo compounds as dopants in 1,2kDa P4VP films*

	λ_{max} (*E* / PSS_{660})	τ	*Z*% at PSS_{660}
Alkyl	630 / 629	6.4 ± 0.6 min	37
Aryl	635 / 615	8 ± 0.5 h	40*
Asym	635 / 628	30 ± 2.1 min	34

The thermal lifetime of different indigos follows same trend as in solution (**Error! Reference source not found.**), aryl substitution leads to longest lifetime and asymmetric substitution lies between alkyl and aryl. Estimations for *Z*% at PSS_{660} might be inaccurate because as seen from **Error! Reference source not found.**, λ_{max} for *E* and PSS_{660} are almost the same for alkyl and asymmetric indigo. Judging by the shape of the spectra (Figure 26) for studied compounds, the aryl indigo should have the highest *Z*% in PSS_{660} by a decent margin.

Photobleaching was observed when irradiating films for longer times (≥1 min), which can be seen from the moving of isosbestic point in absorption spectra and decrease of absorption peak around 630 nm without increasing of the shoulder around 600 nm. Because of light scattering on the thin film, the spectra had too much noise for continuous precise measurements during irradiation. Upon longer storage (over weekend) films started to crack, and for an 8 kDa P4VP polymer crystallized during solvent evaporation.

4.2.4 Summary of photochemical properties

Photochemical properties of the three studied indigo photoswitches were studied in dilute MeCN solutions, as dopants in an E7 liquid crystal environment and as dopants in P4VP polymer films. In all of the different environments the *N,N'*-dialkyl indigo had the shortest thermal *E* lifetime, and the *N,N'*-diaryl indigo had the longest thermal lifetime. Asymmetric indigo had lifetime between these two, being closer to the *N,N'*-dialkyl indigo. Between different environments, the lifetime was shortest in liquid crystal and longest in polymer. $E \rightarrow Z$ isomerization was more efficient in solution than in solid environment. This could stem from the rigidity of solid materials which might make rotation around the central double bond in indigo molecule physically hindered. Surprisingly, all three indigo molecules had similar *E* to *Z* conversion in polymer films, even though physical hindrance should lead to the indigo with big aryl sidechain being able to rotate less than a molecule with a smaller sidechain. The short lifetimes of the dialkyl and asymmetric indigos dominate the PSS in liquid crystal, making diaryl indigo the most efficient in *E* to *Z* conversion in this environment.

All studied componds had good fatigue resistance in solution, but photobleaching was observed in both liquid crystal mixture and polymer films.

5. CONCLUSIONS

In this work, carried out at Tampere University in Smart Photonic Materials group, three new indigo photoswitches were designed and successfully synthesized. Molecules with similar cores had been synthetized before and their photoswitching studied in solution. Hence, the aim of this study was to (i) further modify molecular structures to enable covalent linkage to polymers and (ii) to study their photochemical properties and isomerization dynamics in solution as well as polymeric and liquid crystalline environments.

The synthetic methods used consisted of elementary reactions and previously published routes. All synthetic steps had moderate yields, as reported in literature before. Some reactions suffered from a vast amount of side products or decomposition of designed product. Further studies are required for the optimization of the molecular designs and synthetic pathways. Nevertheless, in this work desired products were successfully synthetized, paving the way for characterizing the photochemical properties of indigo photoswitches in the solid state, and in longer term, utilizing them in, e.g., light-to-mechanical energy conversion.

Photochemical properties in dilute acetonitrile solution are similar to the previously reported qualities of molecules with similar cores. The *N,N'*-dialkyl indigo had an *E* lifetime of 2 minutes and 87% *Z*-isomer in PSS_{660}, compared to 2.8 min and 77% with quite similar alkyl chain in Ref. [29]. The *N,N'*-diaryl indigo had lifetime of 70 minutes and 63.5% *Z*-isomer in PSS_{660}, in comparison other quite similar *N,N'*-diaryl indigos have lifetime of 81–408 min and 80–83% *Z*-isomer in PSS_{660} in Ref. [29]. Asymmetric indigo had lifetime of 5.6 minutes and 69% *Z*-isomer in PSS_{660}, compared to 3.5 min and 56% with quite similar structures in Ref. [29]. Only minor photodegradation (0.9–2.1%) was seen after 1h of continuous irradiation at 660 nm. In an LC environment the lifetimes for studied molecules were surprisingly short, in the scale of seconds for the *N,N'*-dialkyl- and asymmetric indigos, for which the $E \rightarrow Z$ conversion was estimated to be only 35–27%. The *N,N'*-diarylindigo had a lifetime of 30 minutes and an estimated 50% conversion upon irradiation, which is a promising result. All compounds showed cyclability for over 50 cycles. Compared to solution measurements, lifetimes in polymer films were longer, ranging from 6 minutes to 8 hours. The $E \rightarrow Z$ conversion for all compounds was estimated to be around 40%, and the aryl-substituted indigo could be described as bistable in a polymer film.

In conclusion, all synthetized photoswitches were compatible with polymer films and could be incorporated into LCs as dopants. All photoswitches isomerize from *E* to *Z* with 660nm irradiation and from *Z* to *E* with 500nm or 525nm irradiation in all studied environments. In dilute MeCN solution only minor photodegradation was observed, and in LC and polymer films the photoswitches had decent stability towards fatigue. *N,N'*-diarylindigo is nearly bistable in polymer films, which makes it attractive for applications.

This work consisted mostly of synthesis of the indigo photoswitches, which had some problems due to molecular design and unoptimized reactions. For further studies molecular design should use hydroxy-groups instead of bromines in ends of sidechains to reduce the amount of side-products in reactions. Comparing photoswitching in solution and in polymer films, and between the few different polymers tried in this work, photoswitching might be more efficient in other polymers. From the three synthesized indigo photoswitches, the diaryl indigo is the most promising for solid state applications. Next steps in this line of research could be (i) the optimization of the synthetic routes, (ii) studying photoswitching efficiency in different polymers to find optimal conditions, and (iii) polymerizing indigo photoswitches to be covalently bond to LCEs and studying the photochemical effect in photoactuation.

6. EXPERIMENTAL

All the experimental work was carried out in Tampere University. General synthetic methods are described in Chapter 6.1, followed by synthetic routes for studied indigo compounds in Chapters 6.2–6.4. Photochemical studies are described in chapter 6.5.

6.1 General synthetic methods

All solvents and reagents used were commercial and purchased from Sigma Aldrich, TCI Europe, VWR or FluoroChem and used as received without further purifications. When used, dry solvents were acquired using Inert PureSolv solvent purification system. Reactions were monitored with thin-layer chromatography (TLC) and developed plates were visualized in room light, with UV irradiation (256nm) or with potassium permanganate and phosphomolybdic acid staining.

Nuclear magnetic resonance spectra (NMR) were measured with a 500 MHz JEOL ECZR 500 (125 MHz for ^{13}C) instrument. Chemical shifts are given in ppm and referenced to solvent signal ($CDCl_3$: δ = 7.26 ppm (^{1}H), 77.16 ppm (^{13}C)). Multiplicities are abbreviated as follows: singlet (s), doublet (d), doublet of doublets (dd), triplet of doublets (td), triplet (t), doublet of triplets (dt), quartet (q), pentet (p), and multiplet (m). Coupling constants (J) were analyzed with JEOL Delta v5.3.1. software and are given in Hz.

6.2 Symmetrical alkyl

6.2.1 3-bromopropyl 2-bromoacetate (52)

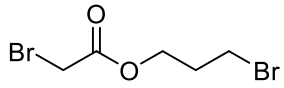

3-bromopropan-1-ol (10 g, 72 mmol, 1.0 eq.) and potassium carbonate (20 g, 145 mmol, 2.0 eq.) were dissolved in 250 ml of dry DCM under argon. Bromoacetyl bromide (14.5 g, 72 mmol, 1.0 eq.) was added dropwise to mixture at 0 °C, and mixture was stirred at room temperature overnight under argon. The reaction mixture was filtered, washed with H_2O, dried with magnesium sulfate and concentrated under reduced pressure to yield 7.59 g of desired product (yield 40.7%) as colourless oil. ^{1}H-NMR (500 MHz, $CDCl_3$) δ 4.31 (t, J = 6.0 Hz, 2H), 3.83 (s, 2H), 3.47 (t, J = 6.6 Hz, 2H), 2.23-2.18 (p, 2H). ^{13}C-NMR (126 MHz, $CDCl_3$) δ 167.2, 63.9, 31.4, 29.1, 25.7. Appendix 1.

6.2.2 bis(3-bromopropyl) 2,2'-(3,3'-dioxo-[2,2'-biindolinylidene]-1,1'-diyl)(E)-diacetate (47)

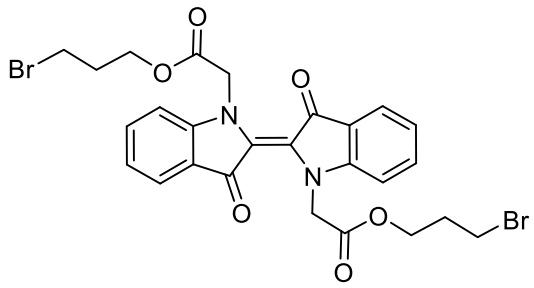

First attempt: Indigo (500 mg, 1.9 mmol, 1.0 eq.), **52** (2.0 g, 7.6 mmol, 4.0 eq.) and cesium carbonate (1.25 g, 3.8 mmol, 2.0 eq.) were stirred in DMF (10 ml) under argon at RT overnight. TLC showed disappearance of **52**. The reaction mixture was filtered through silica, washed with H_2O, dried with magnesium sulfate and concentrated under reduced pressure. The crude product was purified with column chromatography (Silica 60, 30% EtOAc / Hexane) to yield turquoise solid. The product showed characteristic peaks in NMR but wasn't pure. A new purification with column chromatography (Silica 60, 20% EtOAc / Hexane), same NMR. Combined with optimization reactions products.

Best attempt: Indigo (100 mg, 0.38 mmol, 1.0 eq.), **52** (400 mg, 1.54 mmol, 4.0 eq.) and cesium carbonate (249 mg, 0.76 mmol, 2.0 eq.) were stirred in dry DMF (3 ml) under argon at RT overnight. Diluted with EtOAc, filtered through a plug of silica, washed with brine and H_2O, dried with magnesium sulfate and concentrated under reduced pressure. Purified with column chromatography (Silica 60, 20% EtOAc / Hexane) to yield 57 mg of desired product (yield 24%) as turquoise solid. Product appears to spontaneously decompose, used as such on next reaction.

^{1}H-NMR (500 MHz, $CDCl_3$) δ 7.72 (d, J = 8.6 Hz, 2H), 7.54 (t, J = 7.7 Hz, 2H), 7.08 (t, J = 7.4 Hz, 2H), 7.02 (d, J = 8.6 Hz, 2H), 4.77 (s, 4H), 4.33 (t, J = 6.0 Hz, 4H), 3.40 (t, J = 6.3 Hz, 4H), 2.21-2.16 (p, 4H). Appendix 2, ^{13}C was not measured because of spontaneous decomposition.

6.2.3 (E)-((2,2'-(3,3'-dioxo-[2,2'-biindolinylidene]-1,1'-diyl)bis(acetyl))bis(oxy))bis(propane-3,1-diyl) diacrylate (54)

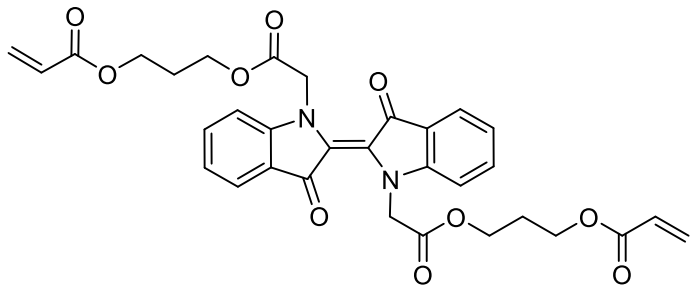

47 (62 mg, 0.10 mmol, 1.0 eq.), acrylic acid (23.8 µl, 0.35 mmol, 3.5 eq.) and potassium bicarbonate (25 mg, 0.25 mmol, 2.5 eq.) were stirred in DMF (1 ml) under argon at RT overnight. TLC showed starting materials, stirred the reaction mixture at 50 °C for 4 h. Diluted with EtOAc, washed with brine and H_2O, dried with magnesium sulfate and concentrated under reduced pressure. The crude product was purified with column chromatography (Silica 60, 20 → 40% EtOAC / Hexane) to yield 16,2 mg of product (yield 27%) as blue solid. ^{1}H-NMR (500 MHz, $CDCl_3$) δ 7.71 (d, J = 6.9 Hz, 2H), 7.53 (t, J = 7.7 Hz, 2H), 7.07 (t, J = 7.4 Hz, 2H), 7.02 (d, J = 8.0 Hz, 2H), 6.38 (d, J = 18.9 Hz, 2H), 6.08 (dd, J = 17.2, 10.3 Hz, 2H), 5.81 (d, J = 12.0 Hz, 2H), 4.76 (s, 4H), 4.29 (t, J = 6.3 Hz, 4H), 4.20 (t, J = 6.3 Hz, 4H), 2.05-2.01 (p, 4H). ^{13}C-NMR (126 MHz, $CDCl_3$) δ 186.2, 169.1, 166.1, 153.6, 135.9, 131.1, 128.3, 126.9, 124.5, 122.2, 121.9, 111.1, 62.1, 61.0, 51.3, 28.0. Appendix 3.

6.3 Symmetrical aryl

6.3.1 3-bromopropyl 4-iodobenzoate (56)

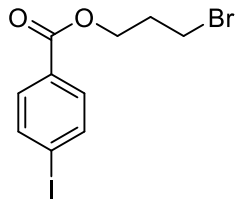

4-Iodobenzoyl chloride (4.21 g, 15.83 mmol, 1.1 eq.) and DMAP (0.175 g, 1.44 mmol, 0.1e q) and TEA (3.0 ml, 21.56 mmol, 1.5 eq.) were dissolved in dry DCM (100 ml). Added 3-bromopropan-1-ol (1.3 ml, 14.39 mmol, 1.0 eq.) dropwise at 0 °C, stirred for 1,5 h at 0 °C and 30min at RT. Washed with H_2O, dried with magnesium sulfate and concentrated under reduced pressure. The crude product was purified with column chromatography (Silica 60, DCM), but separation was bad. Recrystallized the crude product

from MeOH to yield 4,61 g (yield 86,9%) of product as white crystals. ^{1}H-NMR (500 MHz, $CDCl_3$) δ 7.79 (d, J = 8.6 Hz, 2H), 7.72 (d, J = 8.6 Hz, 2H), 4.45 (t, J = 6.0 Hz, 2H), 3.52 (t, J = 6.6 Hz, 2H), 2.33-2.28 (p, 2H). ^{13}C-NMR (126 MHz, $CDCl_3$) δ 166.0, 137.9, 131.1, 129.5, 101.1, 63.0, 31.8, 29.5. Appendix 4.

6.3.2 bis(3-bromopropyl) 4,4'-(3,3'-dioxo-[2,2'-biindolinylidene]-1,1'-diyl)(E)-dibenzoate (48)

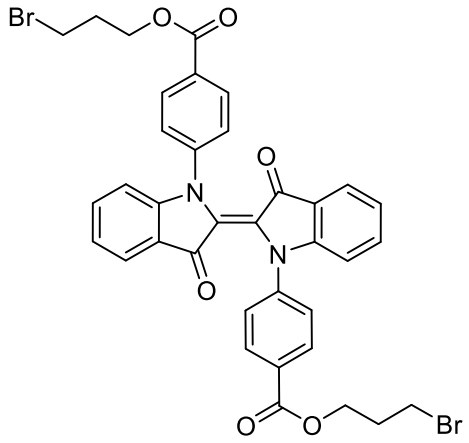

Attempt 1: DCB (10 ml) was bubbled with argon for 15 min. Added indigo (200 mg, 0.77 mmol, 1.0 eq.), **56** (713 mg, 1.93 mmol, 2.5 eq.) and potassium carbonate (315 mg, 2.3 mmol, 3 eq.) under argon. Catalytic amount of Cu powder was added the reaction mixture was refluxed for 5 h. The reaction mixture was filtered through a plug of silica and concentrated under reduced pressure. The crude product was purified with column chromatography (Silica 60, 1st DCM, 2nd 5 → 20% EtOAc / DCM, 3rd 2 → 5% MeOH / DCM) to yield 50 mg of turquoise solid. NMR showed still impurities, and product seems to decompose on silica, used as such on next reaction.

Attempt 2: DCB (5 ml) was bubbled with argon for 15min. Added mono-arylated indigo (100 mg, 0.2 mmol, 1.0 eq.), **56** (81 mg, 0.22 mmol, 1.1 eq.), potassium carbonate (41.4 mg, 0.3 mmol, 1.5 eq.) and Cu powder (catalytic amount) under argon. Refluxed for 10 h under argon, filtered through a plug of silica and concentrated under reduced pressure. The crude product was purified twice with column chromatography (Silica 60, 30% EtOAc / Hexane) to yield 18,6 mg of product (yield 12.5%) as turquoise solid. Product decomposes on silica while in column.

^{1}H-NMR (500 MHz, $CDCl_3$) δ 8.22 (d, J = 8.0 Hz, 3H), 7.62 (d, J = 8.6 Hz, 3H), 7.59-7.53 (m, 2H), 7.42 (t, J = 7.2 Hz, 1H), 7.09 (d, J = 8.6 Hz, 1H), 7.04 (t, J = 7.2 Hz, 1H), 4.49 (t, J = 6.0 Hz, 2H), 4.42 (t, J = 6.0 Hz, 2H), 3.57 (t, J = 6.6 Hz, 2H), 3.33 (t, J = 6.9 Hz,

2H), 2.34-2.29 (m, 4H). ^{13}C-NMR (126 MHz, $CDCl_3$) δ 184.3, 165.6, 152.5, 146.2, 138.5, 135.5, 131.2, 128.3, 126.1, 125.4, 124.6, 122.8, 121.8, 111.2, 64.8, 62.9, 32.6, 31.9, 29.5, 1.6. Appendix 5.

6.3.3 bis(3-(acryloyloxy)propyl) 4,4'-(3,3'-dioxo-[2,2'-biindolinylidene]-1,1'-diyl)(E)-dibenzoate (57)

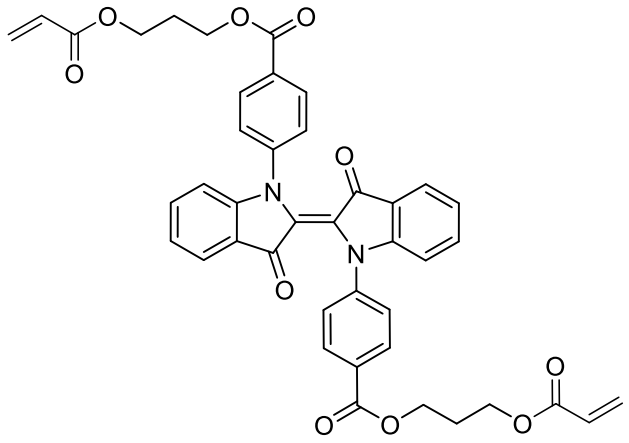

Attempt 1: **48** (impure from previous reaction, 50 mg, 0.067 mmol, 1.0 eq), acrylic acid (16.2 µl, 0.24 mmol, 3.5 eq.) and potassium bicarbonate (17 mg, 0.165 mmol, 2.5 eq.) were stirred in DMF (1 ml) overnight. Diluted with EtOAc, washed with brine and H_2O, dried with magnesium sulfate and concentrated under reduced pressure. The crude product was mixture of mono- and diacrylated product, used as such on next attempt.

Attempt 2: Product from previous attempt, acrylic acid (16.2 µl, 0.24 mmol, 3.5 eq.) and potassium bicarbonate (17 mg, 0.165 mmol, 2.5 eq.) were stirred in DMF (1 ml) overnight. Diluted with EtOAc, washed with brine and H_2O, dried with magnesium sulfate and concentrated under reduced pressure. The crude product was purified with colum chromatography (Silica 60, 1st 5 → 10% EtOAc / DCM, 2nd 50% EtOAc / Hexane) to yield 2 mg of product as turquoise solid.

6.3.4 2-hydroxyethyl 4-iodobenzoate (59)

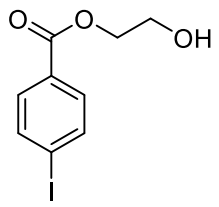

Ethylene glycol (21 ml, 376 mmol, 10 eq.), potassium carbonate (5.52 g, 40 mmol, 1.1 eq.) and DMAP (230 mg, 1.8 mmol, 0.05 eq.) were dissolved in dry DCM (200 ml) under

argon. 4-Iodobenzoyl chloride (10 g, 37.6 mmol, 1.0 eq.) was dissolved in dry DCM (40 ml) and added dropwise to reaction mixture at 0 °C. The reaction mixture was stirred for 10 min at 0 °C, washed with aqueous sodium bicarbonate solution, dried over magnesium sulfate and concentrated under reduced pressure. The crude product was purified with column chromatography (Silica 60, DCM) to yield 4.48 g of product (yield 41%) as white crystals. ^{1}H-NMR (500 MHz, $CDCl_3$ δ 7.79 (d, J = 8.6 Hz, 2H), 7.74 (d, J = 8.6 Hz, 2H), 4.45-4.43 (m, 2H), 3.94 (q, J = 5.0 Hz, 2H), 2.09 (t, J = 6.0 Hz, 1H). ^{13}C-NMR (126 MHz, $CDCl_3$) δ 166.6, 137.9, 131.2, 129.4, 101.2, 67.0, 61.4. Appendix 6

6.3.5 2-((tert-butyldimethylsilyl)oxy)ethyl 4-iodobenzoate (60)

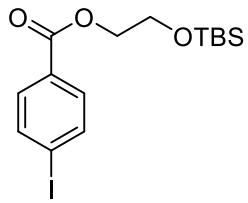

59 (4.48 g, 14.66 mmol, 1.0 eq.), TBS-chloride (5.5 g, 36.7 mmol, 2.5 eq.) and imidazole (2.5 g, 36.7 mmol, 2.5 eq.) were stirred in dry DCM (75 ml) at RT for 30 min. The reaction mixture was washed with aq. ammonium chloride, filtered through a plug of silica, dried with magnesium sulfate and concentrated under reduced pressure to yield 8.07 g of product as colourless oil. NMR showed unreacted TBS-chloride (δ 0.095 and 0.068) but used as such on next reaction. ^{1}H-NMR (500 MHz, $CDCl_3$) δ 7.78 (dd, J = 24.6, 8.6 Hz, 4H), 4.38 (t, J = 4.9 Hz, 2H), 3.94-3.92 (m, 2H), 0.91 (s, 3H), 0.89 (s, 9H). Appendix 7.

6.3.6 bis(2-((tert-butyldimethylsilyl)oxy)ethyl) 4,4'-(3,3'-dioxo-[2,2'-biindolinylidene]-1,1'-diyl)(E)-dibenzoate (61)

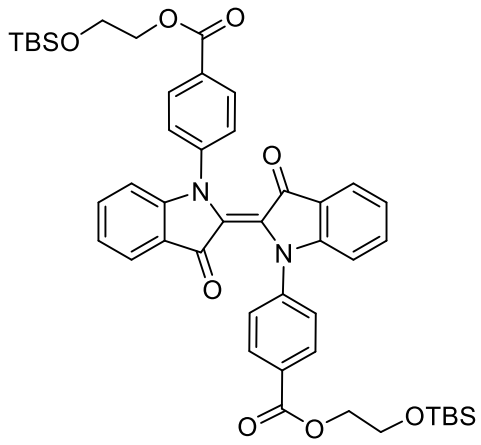

Indigo (1.45 g, 5.52 mmol, 1.0 eq.), **60** (7 g, 16.5 mmol, 3.0 eq) and potassium carbonate (2,3 g, 16.5 mmol, 3.0 eq.) were dissolved in DCB under argon. Added Cu powder (300 mg) and refluxed under argon for 4 h. Filtered through a plug of silica (0 → 20% EtOAc / DCM) and concentrated under reduced pressure. The crude product contains mixture of mono- and disubstituted indigo, on TLC monosubstituted product is between product-trans and product-cis isomers. Purified with twice with column chromatography (Silica 60, 20% EtOAc / Hexane) to yield 1,5 g of product as blue crystals. ^{1}H-NMR (500 MHz, $CDCl_3$) δ 8.25 (d, J = 8.6 Hz, 4H), 7.63 (d, J = 8.6 Hz, 4H), 7.58 (d, J = 7.4 Hz, 2H), 7.43 (t, J = 7.7 Hz, 2H), 7.10 (d, J = 8.6 Hz, 2H), 7.05-7.03 (m, 2H), 4.41 (t, J = 5.4 Hz, 4H), 3.97-3.95 (m, 4H), 0.92 (s, 18H), 0.11 (s, 12H). ^{13}C-NMR (126 MHz, $CDCl_3$) δ 184.3, 165.9, 165.6, 157.1, 152.6, 150.9, 146.0, 138.5, 137.0, 135.4, 131.4, 131.2, 130.3, 130.3, 128.6, 126.1, 126.0, 125.5, 125.3, 124.8, 124.5, 122.7, 121.8, 117.7, 111.4, 111.3, 66.7, 66.5, 61.4, 61.3, 26.0, 25.9, 18.4, 18.4, -2.9, -5.1. Appendix 8.

6.3.7 bis(2-hydroxyethyl) 4,4'-(3,3'-dioxo-[2,2'-biindolinylidene]-1,1'-diyl)(E)-dibenzoate (63)

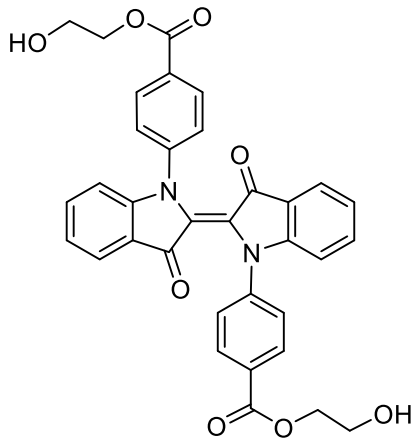

Failed attempt 1: **61** (426 mg, 0.52 mmol, 1.0 eq.) was dissolved to THF under argon. Added TBAF (1 mol/l, 1.56 ml, 3.0 eq.) at 0 °C and stirred for 5 min. TLC showed de-composition with very little product.

Failed attempt 2: **61** (366 mg, 0.45 mmol, 1.0 eq.) was dissolved to dry THF under argon. Added 3 Å molecular sieves, added TBAF (1 mol/l, 1.34 ml, 3.0 eq.) at 0 °C and stirred for 5 min. TLC showed decomposition very little product.

Failed attempt 3: **61** (48.6 mg, 59 µmol, 1.0e q.) was dissolved to dry THF under argon, added 3Å molecular sieves. TBAF (1 mol/l, 59 µl, 1.0 eq.) was added under argon at 0 °C. After 2 min and 5 min same TLC, **61** and little mono-deprotected product (**64**). Added

TBAF (1 mol/l, 59 µl, 1.0 eq.) after 10 min, 2 min after adding TLC showed little product, some **64**. Added TBAF (1 mol/l, 59 µl, 1.0 eq.) after 10 more minutes, 2 min after last addition decomposed with minor amount of product.

Failed attempt 4: **61** (51.6 mg, 63 µmol, 1.0 eq.) was dissolved to dry THF under argon, added 3 Å molecular sieves. TBAF (1 mol/l, 190 µl, 3.0 eq.) was added under argon and reaction was stirred 15 sec at 0 °C. Yielded mixture of **64**, **65** and decomposition products.

Attempt 5: **61** (51.7 mg, 63 µmol, 1.0 eq.) was dissolved to dry THF (1 ml) under argon, added 3 Å molecular sieves. Cooled down to -89 °C and added TBAF (1 mol/l, 190 µl, 3.0 eq.) under argon. The reaction mixture was stirred for 30 mins at -89 °C, TLC showed only **61**, let warm up. The reaction mixture was stirred for 30 min between -20 °C and -25 °C, quenched with aq. ammonium chloride, diluted with EtOAc, washed with brine and H_2O, dried with magnesium sulfate and concentrated under reduced pressure. The crude product was purified with column chromatography (Silica 60, 0 → 1% MeOH / EtOAc) to yield 6.3 mg (yield 17%) of product as turquoise solid. Recovered 6.5 mg of **61** (yield 12%) and 8.9 mg of **64** (yield 20%).

Attempt 6: **61** (210 mg, 256 µmol, 1.0 eq.) was dissolved to dry THF (4 ml) under argon, added 3 Å molecular sieves. TBAF (1 mol/l, 770 µl, 3.0 eq.) was added at -40 °C and the reaction mixture was stirred between -35 °C and -40 °C for 50 min. The reaction was quenched with aq. ammonium chloride, diluted with EtOAc, washed with brine and water, dried with magnesium sulfate and concentrated under reduced pressure. The crude product was purified with column chromatography (Silica 60, 0 → 2% MeOH / EtOAc) to yield 46.8 mg (yield 31%) of product as turquoise solid. Recovered 21.2 mg of **61** (yield 10%) and 40.4 mg of **64** (yield 22%).

Attempt 7: **64** (78.1 mg, 111 µmol, 1.0 eq.) was dissolved to dry THF (2 ml) under argon, added 3 Å molecular sieves. The reaction mixture was cooled to -30 °C, added TBAF (1 mol/l, 122 µl, 1.1 eq.) and stirred for 30 min between -25 °C and -30 °C. The reaction mixture was stirred 45 min further between -20 °C and -25 °C, quenched with aq. ammonium chloride, diluted with EtOAc, washed with brine and H_2O, dried over magnesium sulfate and concentrated under reduced pressure. The crude product was purified with column chromatography (Silica 60, 0 → 2% MeOH / EtOAc) to yield 26.6 mg (yield 40.6%) of product as turquoise solid. Recovered 38.3 mg **64** (yield 49.5%).

^{1}H-NMR (500 MHz, $CDCl_3$) δ 8.21 (d, J = 8.0 Hz, 3H), 7.57 (dd, J = 22.3, 8.0 Hz, 5H), 7.39 (t, J = 7.7 Hz, 2H), 7.12-7.00 (m, 4H), 4.47 (t, J = 4.6 Hz, 4H), 3.96 (t, J = 4.6 Hz,

4H). ^{13}C-NMR (126 MHz, $CDCl_3$) δ 184.3, 182.8, 166.1, 152.5, 151.0, 146.2, 141.8, 138.6, 135.5, 131.3, 130.4, 128.2, 127.6, 127.4, 126.1, 125.4, 124.6, 123.5, 122.8, 121.7, 111.2, 67.0, 61.5. Appendix 9.

6.3.8 bis(2-(acryloyloxy)ethyl) 4,4'-(3,3'-dioxo-[2,2'-biindolinylidene]-1,1'-diyl)(E)-dibenzoate (66)

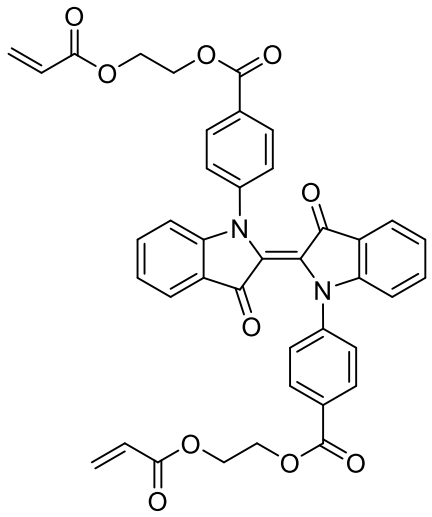

63 (46.8 mg, 84 µmol, 1.0 eq.), DMAP (a grain) and potassium carbonate (116 mg, 840 µmol, 10 eq.) were dissolved in dry DCM (5 ml) under argon. Added acryloyl chloride (68 µl, 840 µmol, 10 eq.) dropwise under argon. The reaction mixture was stirred at RT for 18 h, quenched with aq. sodium bicarbonate, diluted with DCM, washed with H_2O, dried with magnesium sulfate, filtered and concentrated under reduced pressure. The crude product was purified with column chromatography (Silica 60, 50% EtOAc / Hexane) to yield 26.2 mg (yield 44.6%) of product as turquoise solid.

1H-NMR (500 MHz, CHLOROFORM-D) δ 8.24 (d, J = 8.6 Hz, 4H), 7.84 (dd, J = 41.8, 7.4 Hz, 1H), 7.61 (dd, J = 25.5, 7.7 Hz, 5H), 7.42 (t, J = 7.7 Hz, 2H), 7.15-7.03 (m, 4H), 6.47 (dd, J = 17.2, 1.1 Hz, 2H), 6.18 (dd, J = 17.2, 10.3 Hz, 2H), 5.88 (dd, J = 10.6, 1.4 Hz, 2H), 4.60-4.58 (t, 4H), 4.52 (t, J = 4.3 Hz, 4H). ^{13}C-NMR (126 MHz, $CDCl_3$) δ 184.3, 166.1, 165.6, 152.5, 146.3, 142.1, 135.5, 131.7, 131.4, 130.4, 128.1, 128.1, 127.4, 126.1, 125.4, 124.6, 123.5, 122.8, 121.8, 111.2, 63.0, 62.4, 29.8. Appendix 9.

6.4 Asymmetric

6.4.1 3-bromopropyl (E)-4-(3,3'-dioxo-[2,2'-biindolinylidene]-1-yl)benzoate (67)

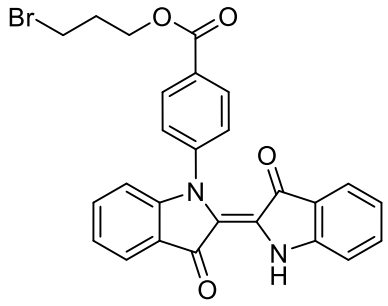

DCB (10 ml) was bubbled with argon for 20 min. Indigo (200 mg, 0.77 mmol, 1.0e q.), **56** (313 mg, 0.85 mmol, 1.1 eq.), potassium carbonate (159 mg, 1.15 mmol, 2.0 eq.) and Cu powder (catalytic amount) were added and the reaction mixture was refluxed for 2 h. The reaction mixture was filtered through a plug of silica and concentrated under reduced pressure. The crude product was purified with column chromatography (Silica 60, DCM) to yield 128 mg (yield 33%) as blue crystals. ^{1}H-NMR (500 MHz, $CDCl_3$) δ 10.49 (s, 1H), 8.18 (d, J = 8.0 Hz, 2H), 7.84 (d, J = 7.4 Hz, 1H), 7.50-7.43 (m, 5H), 7.11 (t, J = 7.4 Hz, 1H), 7.02 (t, J = 8.0 Hz, 2H), 6.91 (t, J = 7.4 Hz, 1H), 4.46 (dt, J = 34.0, 6.0 Hz, 2H), 3.58-3.34 (dt, J = 6.6 Hz, 2H), 2.37-2.32 (p, 2H). ^{13}C-NMR (126 MHz, $CDCl_3$) δ 189.4, 185.9, 165.8, 153.0, 151.5, 145.0, 137.8, 136.2, 135.8, 130.9, 128.6, 126.1, 124.9, 124.2, 122.1, 121.4, 121.2, 121.1, 120.0, 112.0, 111.6, 62.9, 31.9, 29.6. Appendix 11.

6.4.2 3-bromopropyl (E)-4-(1'-(2-(3-bromopropoxy)-2-oxoethyl)-3,3'-dioxo-[2,2'-biindolinylidene]-1-yl)benzoate (49)

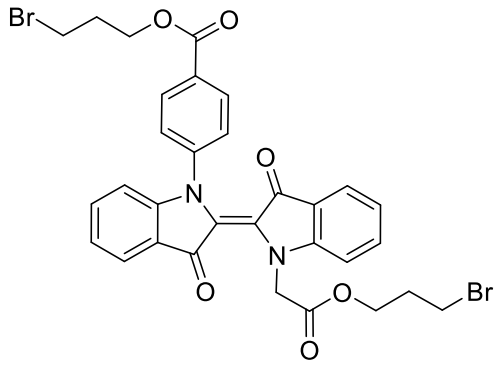

67 (73m g, 0.145 mmol, 1.0 eq.), **52** (101 mg, 0.388 mmol, 2.7 eq.) and cesium carbonate (71.7 mg, 0.22 mmol, 1.5 eq.) were dissolved to DMF (0.5 ml) under argon. The reaction mixture was stirred at RT for 18 h, diluted with EtOAc, washed with H_2O, dried with magnesium sulfate and concentrated under reduced pressure. The crude product was purified with column chromatography (Silica 60, 40% EtOAc / Hexane) to yield 92,8 mg (yield

94%) of product as turquoise solid. ^{1}H-NMR (500 MHz, $CDCl_3$) δ 8.15 (d, J = 8.6 Hz, 2H), 7.80 (d, J = 6.9 Hz, 1H), 7.58 (d, J = 8.6 Hz, 2H), 7.52 (d, J = 8.6 Hz, 2H), 7.50-7.46 (m, 1H), 7.19 (d, J = 8.0 Hz, 1H), 7.12 (t, J = 7.4 Hz, 1H), 7.02 (t, J = 8.0 Hz, 2H), 5.17 (s, 2H), 4.47 (t, J = 6.0 Hz, 2H), 4.36 (t, J = 6.0 Hz, 2H), 3.56 (t, J = 6.6 Hz, 2H), 3.39 (t, J = 6.6 Hz, 2H), 2.34-2.29 (p, 2H), 2.22-2.17 (p, 2H). ^{13}C-NMR (126 MHz, $CDCl_3$) δ 186.0, 184.4, 168.7, 165.7, 153.1, 152.4, 146.4, 135.8, 135.5, 131.1, 129.1, 127.8, 125.1, 124.7, 124.5, 124.1, 122.6, 122.5, 122.1, 121.8, 111.3, 110.6, 63.4, 62.8, 50.3, 31.9, 31.5, 29.6, 29.3. Appendix 12.

6.4.3 3-(acryloyloxy)propyl (E)-4-(1'-(2-(3-(acryloyloxy)propoxy)-2-oxoethyl)-3,3'-dioxo-[2,2'-biindolinylidene]-1-yl)benzoate (68)

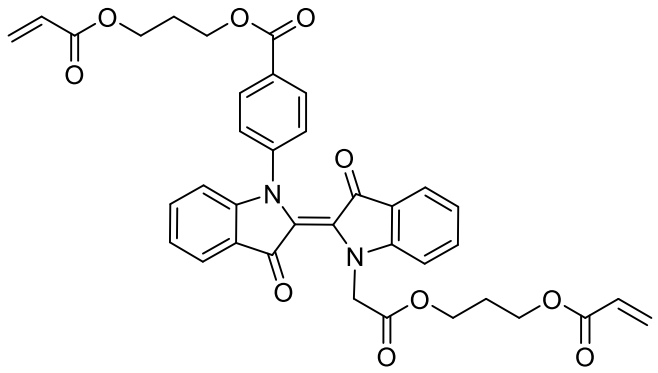

49 (69.8 mg, 0.102 mmol, 1.0 eq.), acrylic acid (23.8 µl, 0.35 mmol, 3.5 eq.) and potassium bicarbonate (25 mg, 0.25 mmol, 2.5 eq.) were stirred in dry DMF (1 ml) overnight at RT and 4 h at 50 °C. The reaction mixture was diluted with EtOAc, washed with brine and H_2O, dried with magnesium sulfate and concentrated under reduced pressure. The crude product was purified with column chromatography (Silica 60, 10% EtOAc / DCM) to yield 31.4 mg (yield 46%) as turquoise solid. ^{1}H-NMR (500 MHz, $CDCl_3$) δ 8.14 (d, J = 8.6 Hz, 2H), 7.80 (d, J = 6.9 Hz, 1H), 7.58 (d, J = 8.6 Hz, 2H), 7.52-7.45 (m, 3H), 7.19 (d, J = 8.0 Hz, 1H), 7.11 (t, J = 7.2 Hz, 1H), 7.02 (q, J = 8.2 Hz, 2H), 6.39 (td, J = 17.3, 1.3 Hz, 2H), 6.14-6.06 (dq, 2H), 5.84-5.80 (td, 2H), 5.17 (s, 2H), 4.42 (t, J = 6.3 Hz, 2H), 4.32 (dt, J = 16.6, 6.3 Hz, 4H), 4.22 (t, J = 6.3 Hz, 2H), 2.17-2.12 (p, 2H), 2.07-2.02 (p, 2H). ^{13}C-NMR (126 MHz, $CDCl_3$) δ 185.9, 184.4, 168.8, 166.2, 166.1, 165.8, 153.1, 152.4, 146.4, 135.8, 135.4, 131.2, 131.2, 131.1, 129.2, 128.3, 128.2, 127.8, 125.1, 124.7, 124.5, 124.1, 122.5, 122.5, 122.2, 121.8, 111.3, 110.6, 62.3, 61.7, 61.3, 60.9, 50.2, 28.2, 28.0, 1.1. Appendix 13.

6.5 Photochemical characterization

6.5.1 General methods

UV-Visible absorption spectra were recorded with an Agilent Cary 60 spectrophotometer with self-built setup (Figure 28). Photoexcitation was conducted using a Prior Lumen 1600 light source containing multiple narrow-band LEDs at different wavelengths without additional bandpass filters.

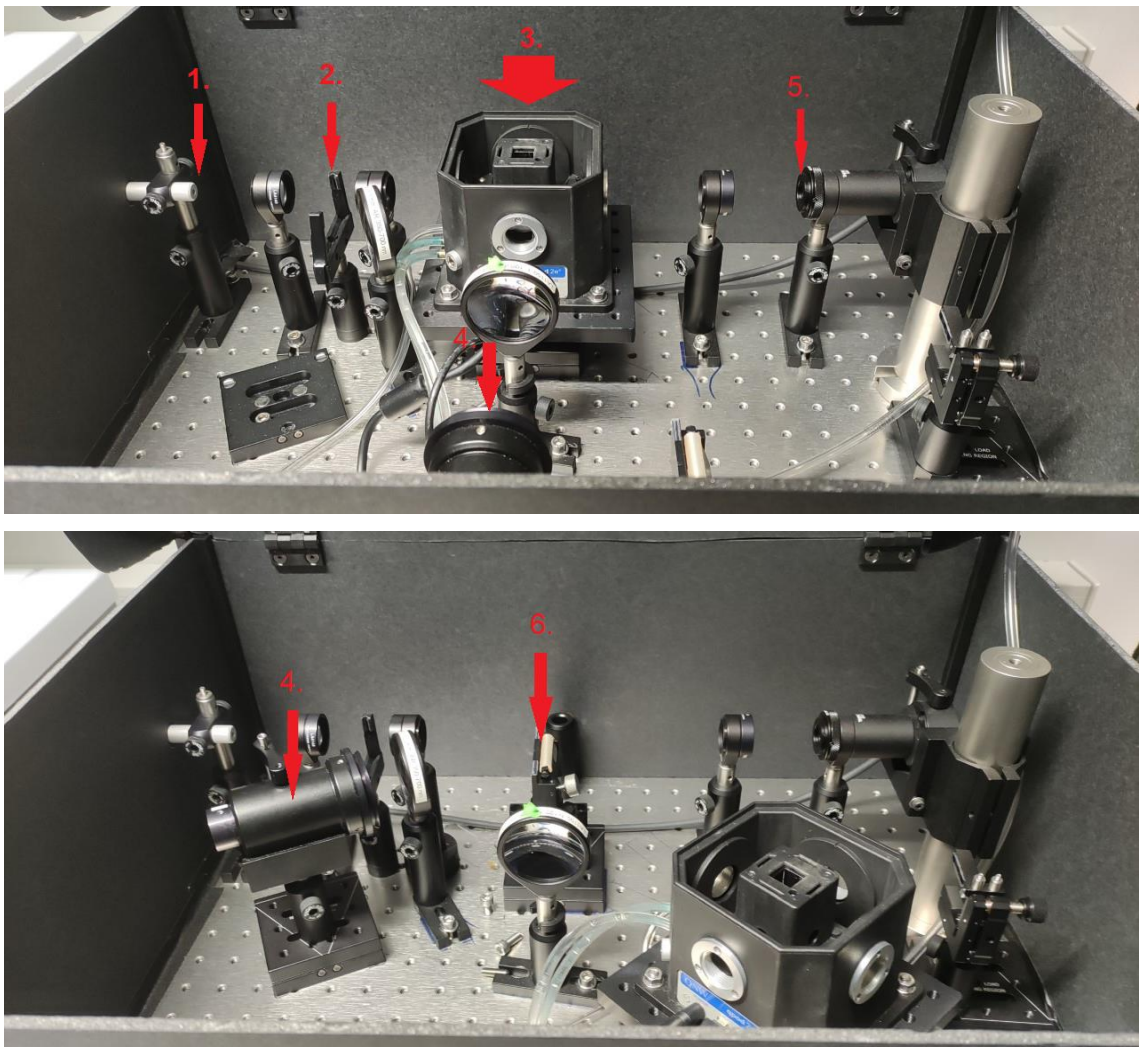

Figure 28 *Spectrometer setup built by Dr. Matti Virkki, above for solution measurements and below for solid samples. 1. spectrometer beam in to the setup, 2. holder for polarizer, 3. cuvette holder, 4. LED beam collimator, 5. spectrometer beam back to spectrometer, 6. sample holder.*

All measurements were carried out in dark so that room lights do not interfere.

6.5.2 Solution

All solution measurements were done in 75μM acetonitrile solutions at 25°C. Quartz absorption cuvettes with an optical path of 1.0 cm in an Ocean Optics Qpod 2e Peltier-thermostated cell holder with temperature accuracy is 0.1 °C were used. Photostationary states (PSSs) were reached by using 520 mW power of Prior LED with corresponding wavelengths.

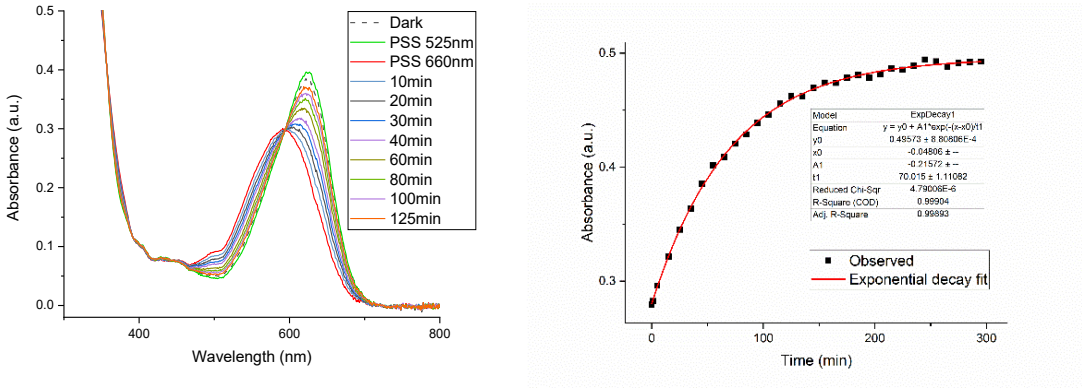

Figure 29 *PSSs and thermal relaxation (left), and lifetime fit (right) for diaryl indigo in 75μM MeCN solution.*

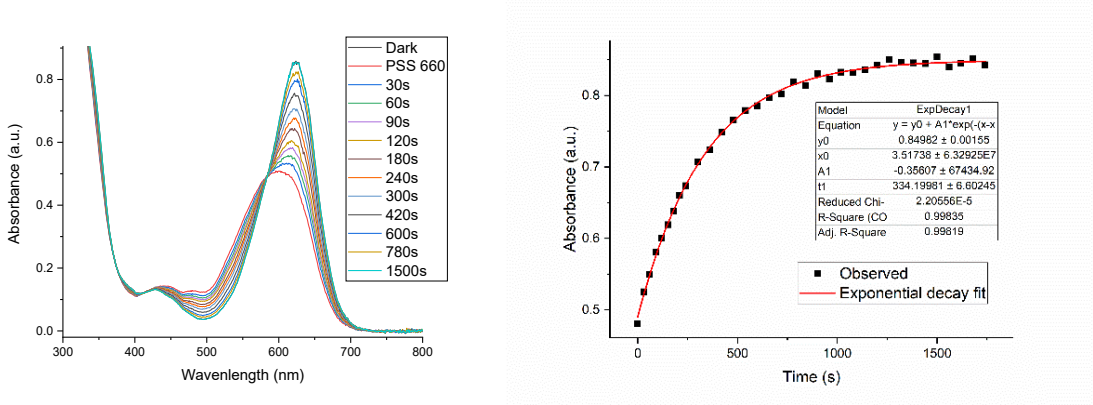

Figure 30 *Thermal relaxation (left) and lifetime fit (right) for asymmetric indigo in 75μM MeCN solution*

Thermal relaxation and lifetime fit for dialkyl indigo are already presented in results-section. As seen from Figure 29 diaryl indigo relaxes towards initial dark state, with lifetime of 70 minutes. Asymmetric indigo fully relaxes to initial dark state in 25 minutes, thermal lifetime being 5.6 minutes (Figure 30).

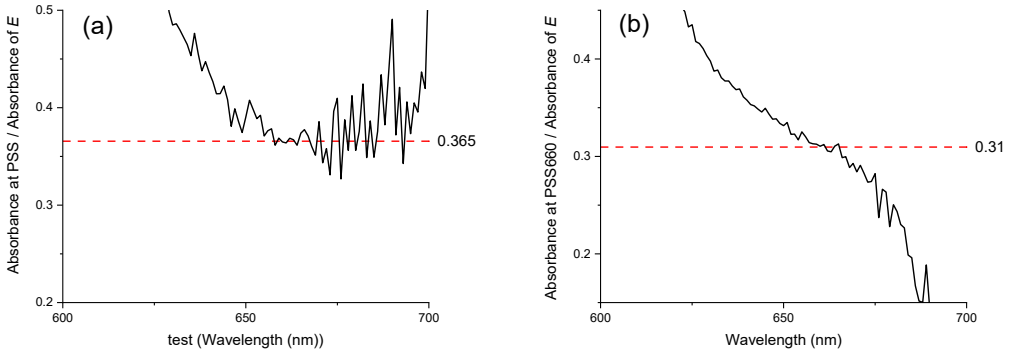

Figure 31 *PSS composition for diaryl- (a) and asymmetric indigo (b).*

To define PSS_{660} for diaryl indigo (Figure 31a), calculated *E* spectrum was used. Fatigue was estimated with 1h continuous irradiation with 660 nm LED at 520 mW power.

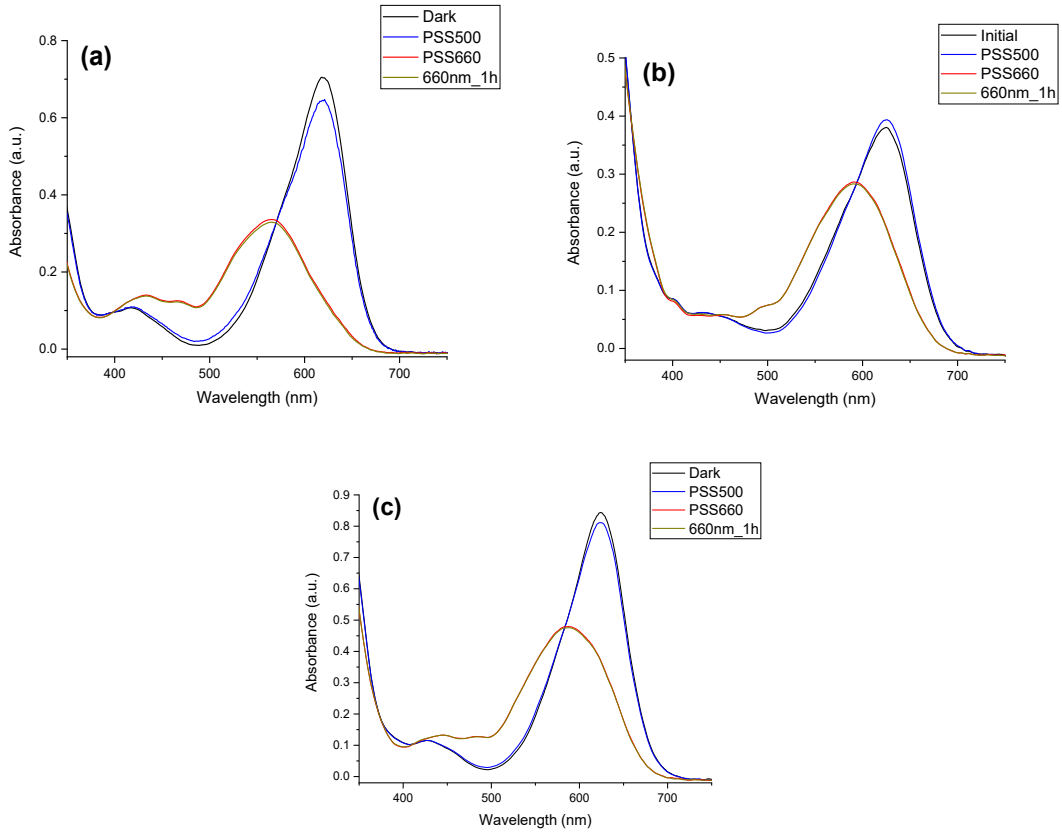

Figure 32 *Fatigue estimation in 75μM MeCN solution for dialkyl (a), diaryl (b) and asymmetric (c) indigo.*

Decrease in absorbance at PSS_{660} peak was calculated, for dialkyl indigo it decreased 2.1%, for diaryl 1.0% and for asymmetric indigo 0.9%. Also PSS_{500} spectra for all compounds in a 75 μM MeCN solution are found in Figure 32. PSS_{500} compositions for dialkyl indigo (91% *E*) and asymmetric indigo (95% *E*) show efficient two-way photoswitching with 660nm and 500nm LED.

6.5.3 Liquid crystals

Liquid crystal samples were made by mixing corresponding compound with E7 liquid crystal mixture in DCM, and evaporating solvent under reduced pressure. 10µm planar cells were filled with mixture by placing a drop of the mixture on open edge of the cell, and capillary force pulls the mixture in the cell. Absorbance measurements were done in spectrophotometer.

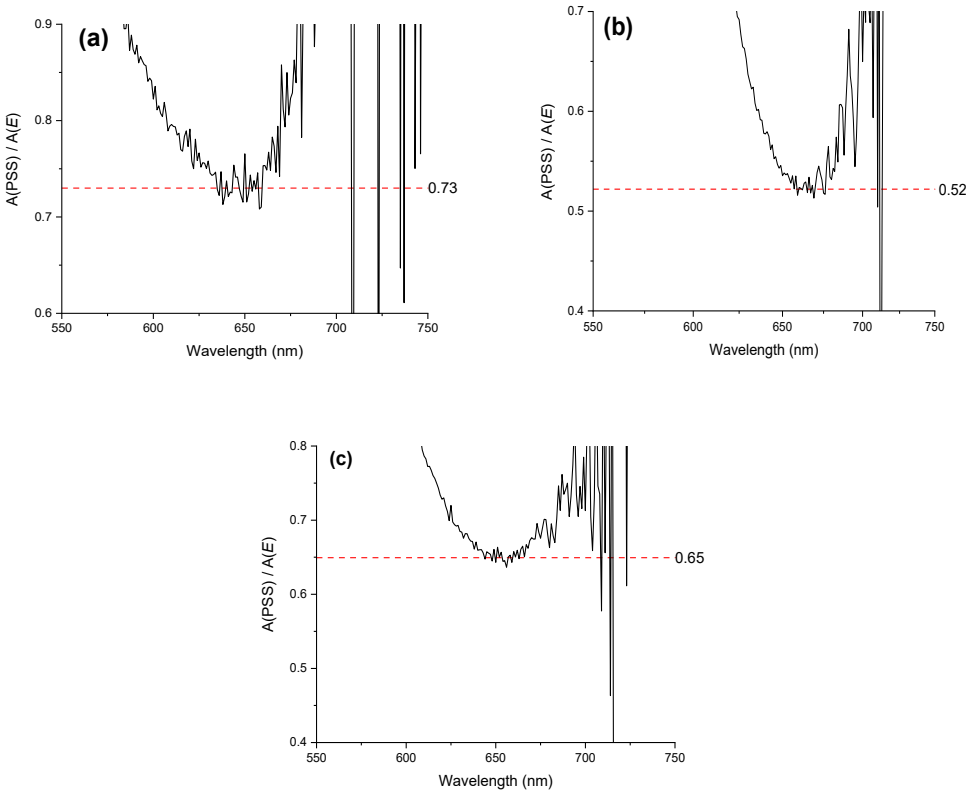

Figure 33 *PSS-compositions for dialkyl- (a), diaryl- (b) and asymmetric indigo as a dopant in E7 liquid crystal mixture.*

PSS-compositions were estimated the same way as in a solution. For diaryl indigo (Figure 33 b) PSS_{500} was used as *E* spectra, resulting in bigger amount of *E* in this estimation. Spectra were also measured with polarizer for order parameter calculations (Figure 34).

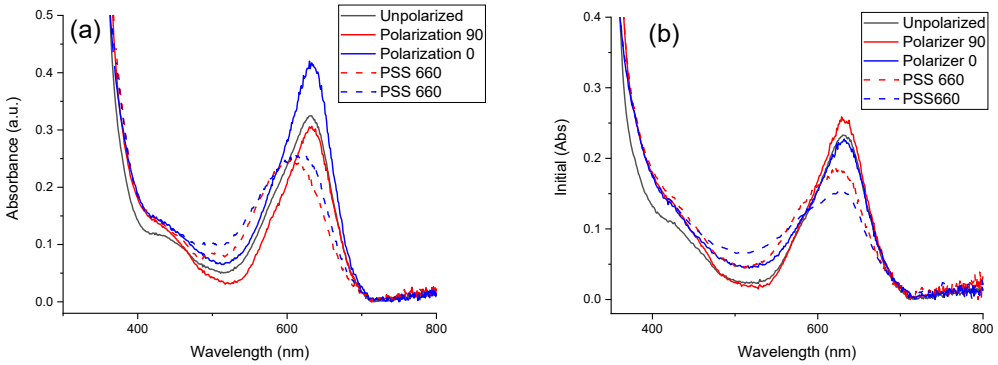

Figure 34 *Spectrum for diaryl (a) and asymmetric indigo (b) with polarizers for order parameter calculations.*

Baseline for each polarizer was reduced from the spectra before calculations. Fatigue resistance was estimated with 10 isomerization cycles.

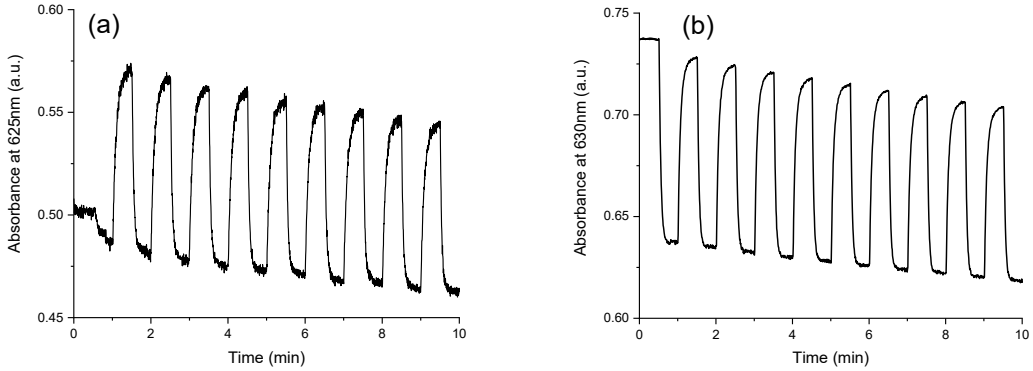

Figure 35 *Isomerization cycles for diaryl- (a) and asymmetric indigo (b).*

Due to longer lifetime of diaryl indigo, isomerization cycles were carried out by irradiating first with 660nm followed by 525nm instead of thermal relaxation as for dialkyl- and asymmetric indigo. Estimated fatigue resistance is therefore worse, because possible side reactions on both irradiations.

6.5.4 Polymer films

Indigo compounds were studied as dopants in P4VP thin films. Solution of P4VP with known concentration was made, indigo compound was added from stock solutions and mixed solution was filtered through 0,2 µm PTFE filter. Final films were made by drop-casting, 1/3rd of microscope slide was filled with 500-700 µl of 40 mg/ml P4VP solution with 2 m-% corresponding indigo compound in chloroform, solvent was let to slowly evaporate under cover for approximately 2 hours, and after seemingly dry film was heated to

60 °C for 10 minutes to remove any remaining solvent. Obtained films were not uniform and of unoptimal optical quality, but they had good areas from which measurements were done. Spincoating thin films on glass substrate with P4VP consentrations between 20 and 80 mg/ml and 1-3 m-% indigo compound was tried. Films were of good optical quality, but had too little absorbance for reliable measurements. Different molar masses of P4VP were tried, with M_{avg} of 60 kDa P4VP only minor photoswitching was seen. With P4VP with M of 1.2 kDa observed photoswitching was greater. 8 kDa P4VP was also tried, but it started to crystallize during solvent evaporation, from a small measurable part of the film, photoswitching close to a 1.2 kDa film was observed.

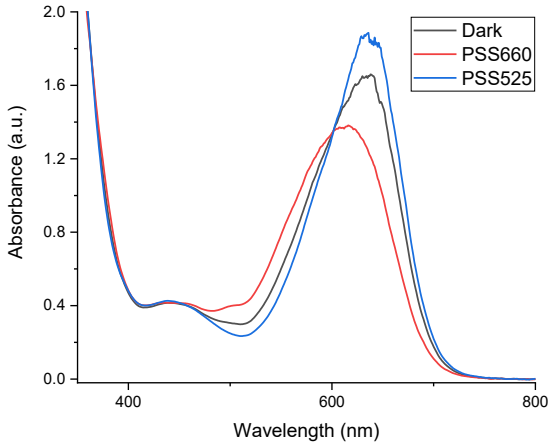

Figure 36 *PSSs and initial dark state for diaryl indigo* ***66*** *in a 8 kDa P4VP film, dark and* PSS_{660} *spectra are a bit flattened due to high absorbance.*

Estimating PSS_{660} composition with equation 3 (using PSS_{525} as *E*) leads to approximately 50% *Z* isomer. However spectra in Figure 36 are already smoothed and saturation can be seen even from the smoothed spectra, so accuracy of the given estimation is rather low.

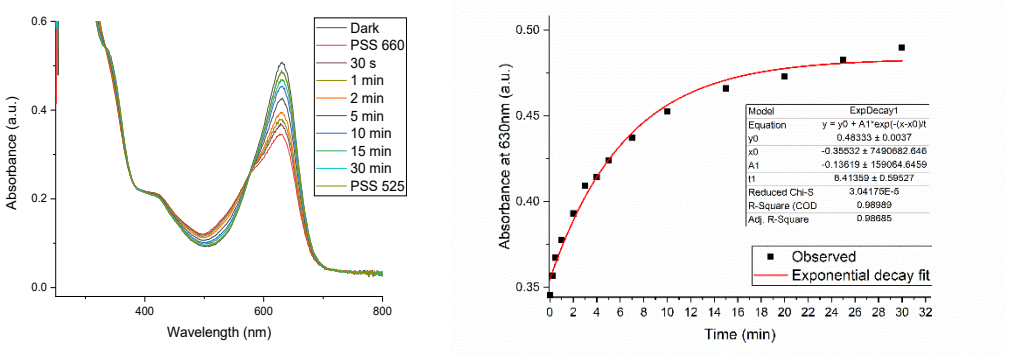

Figure 37 *Thermal relaxation (left) and respective lifetime fit (right) for dialkyl indigo as a dopant in a 1,2kDa P4VP film.*

Calculated lifetime for dialkyl indigo is 6.4 minutes, it relaxes almost back to initial dark state in 30 minutes. Efficient two-way switching can be achieved with 660nm and 525nm LED, PSS_{525} and 30 min thermal relaxation are on top of each other in Figure 37.

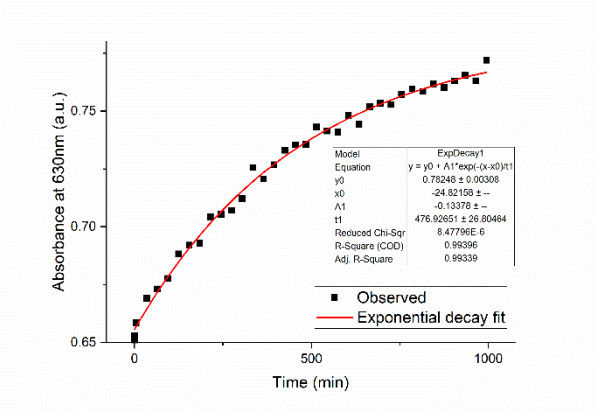

Figure 38 *Lifetime fit for diaryl indigo.*

As in Figure 27, diaryl indigo in a P4VP film does not return to original dark state, but relaxes slowly towards it. Fitting exponential decay function for this relaxation (Figure 38) gives time constant of 8h, which is used as a thermal lifetime even it does not return to original state.

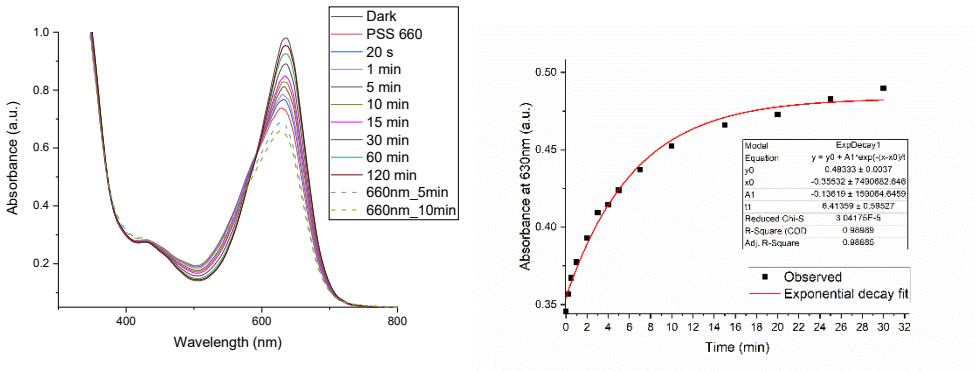

Figure 39 *Thermal relaxation (left) of asymmetric indigo in a P4VP film and respective lifetime fit (right).*

Asymmetric indigo relaxes thermally back to almost initial state with lifetime of 30 minutes. Fatigue was observed when irradiated for longer times (dashed lines in Figure 39).

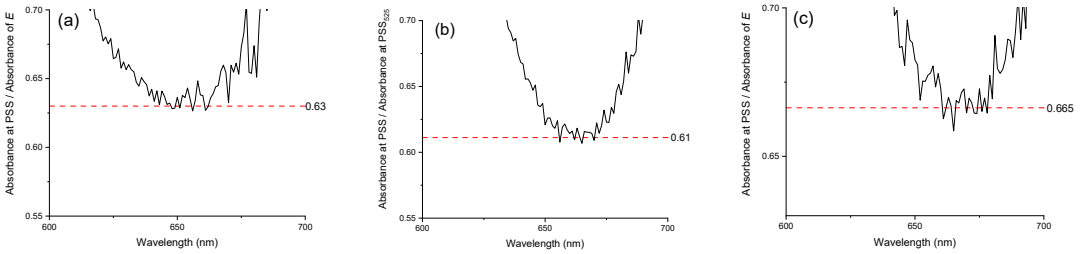

Figure 40 *Photostationary state estimations for dialkyl- (a), diaryl- (b) and asymmetric indigo (c).*

PSS compositions in the P4VP films were estimated with PSS/*E* method (Figure 40). Because diaryl indigo exists in a mixture of *E* and *Z* isomers in dark, PSS_{525} was used as a pure *E* spectrum leading to a minimum value.

REFERENCES

[1] R. Zhang, T. Belwal, L. Li, X. Lin, Y. Xu, and Z. Luo, “Nanomaterial-based biosensors for sensing key foodborne pathogens: Advances from recent decades,” *Compr. Rev. Food Sci. Food Saf.*, vol. 19, no. 4, pp. 1465–1487, Jul. 2020, doi: 10.1111/1541-4337.12576.

[2] A. G. Cuenca, H. Jiang, S. N. Hochwald, M. Delano, W. G. Cance, and S. R. Grobmyer, “Emerging implications of nanotechnology on cancer diagnostics and therapeutics,” *Cancer*, vol. 107, no. 3. John Wiley & Sons, Ltd, pp. 459–466, Aug. 01, 2006, doi: 10.1002/cncr.22035.

[3] D. Giakoumettis and S. Sgouros, “Nanotechnology in neurosurgery: a systematic review,” *Child’s Nervous System*, vol. 37, no. 4. Springer Science and Business Media Deutschland GmbH, pp. 1045–1054, Apr. 01, 2021, doi: 10.1007/s00381-020-05008-4.

[4] W. Seong Toh, C. Bindzus Foldager, M. Pei, and J. Hoi Po Hui, “Advances in Mesenchymal Stem Cell-based Strategies for Cartilage Repair and Regeneration,” doi: 10.1007/s12015-014-9526-z.

[5] H. B. Li, B. E. Tebikachew, C. Wiberg, K. Moth-Poulsen, and J. Hihath, “A Memristive Element Based on an Electrically Controlled Single-Molecule Reaction,” *Angew. Chemie - Int. Ed.*, vol. 59, no. 28, pp. 11641–11646, Jul. 2020, doi: 10.1002/anie.202002300.

[6] Y. Li *et al.*, “Pressure-Induced Conversion of a Paramagnetic FeCo Complex into a Molecular Magnetic Switch with Tuneable Hysteresis,” *Angew. Chemie - Int. Ed.*, vol. 59, no. 39, pp. 17272–17276, Sep. 2020, doi: 10.1002/anie.202008051.

[7] H. Bouas-Laurent and H. Dürr, “Organic photochromism,” *Pure Appl. Chem.*, vol. 73, no. 4, pp. 639–665, Apr. 2001, doi: 10.1351/pac200173040639.

[8] M.-M. Russew and S. Hecht, “Photoswitches: From Molecules to Materials,” *Adv. Mater.*, vol. 22, no. 31, pp. 3348–3360, Apr. 2010, doi: 10.1002/adma.200904102.

[9] Q. Tang, H. J. Quan, S. Liu, L. T. Liu, C. F. Chow, and C. Bin Gong, “An environmentally friendly, photocontrollable and highly recyclable catalyst for use

in a one-pot three-component Mannich reaction," *J. Mol. Catal. A Chem.*, vol. 421, pp. 37–44, Sep. 2016, doi: 10.1016/j.molcata.2016.05.006.

[10] B. M. Neilson and C. W. Bielawski, "Illuminating photoswitchable catalysis," *ACS Catal.*, vol. 3, no. 8, pp. 1874–1885, Aug. 2013, doi: 10.1021/cs4003673.

[11] I. V. Komarov, S. Afonin, O. Babii, T. Schober, and A. S. Ulrich, "Efficiently photocontrollable or not? Biological activity of photoisomerizable diarylethenes," *Chemistry - A European Journal*, vol. 24, no. 44. Wiley-VCH Verlag, pp. 11245–11254, Aug. 06, 2018, doi: 10.1002/chem.201801205.

[12] M. J. Fuchter, "On the Promise of Photopharmacology Using Photoswitches: A Medicinal Chemist's Perspective," *Journal of Medicinal Chemistry*, vol. 63, no. 20. American Chemical Society, pp. 11436–11447, Oct. 22, 2020, doi: 10.1021/acs.jmedchem.0c00629.

[13] A. J. Kirby and F. Hollfelder, "Biochemistry: Enzymes under the nanoscope," *Nature*, vol. 456, no. 7218. Nature Publishing Group, pp. 45–47, Nov. 06, 2008, doi: 10.1038/456045a.

[14] W. A. Velema, J. P. Van Der Berg, M. J. Hansen, W. Szymanski, A. J. M. Driessen, and B. L. Feringa, "Optical control of antibacterial activity," *Nat. Chem.*, vol. 5, no. 11, pp. 924–928, Nov. 2013, doi: 10.1038/nchem.1750.

[15] W. A. Velema, W. Szymanski, and B. L. Feringa, "Photopharmacology: Beyond proof of principle," *Journal of the American Chemical Society*, vol. 136, no. 6. American Chemical Society, pp. 2178–2191, Feb. 12, 2014, doi: 10.1021/ja413063e.

[16] A. Abdollahi, H. Roghani-Mamaqani, and B. Razavi, "Stimuli-chromism of photoswitches in smart polymers: Recent advances and applications as chemosensors," *Progress in Polymer Science*, vol. 98. Elsevier Ltd, p. 101149, Nov. 01, 2019, doi: 10.1016/j.progpolymsci.2019.101149.

[17] C. Ohm, M. Brehmer, and R. Zentel, "Liquid crystalline elastomers as actuators and sensors," *Advanced Materials*, vol. 22, no. 31. John Wiley & Sons, Ltd, pp. 3366–3387, Aug. 17, 2010, doi: 10.1002/adma.200904059.

[18] E. Vaselli, C. Fedele, S. Cavalli, and P. A. Netti, "'On-Off' RGD Signaling Using Azobenzene Photoswitch-Modified Surfaces," *Chempluschem*, vol. 80, no. 10, pp.

1547–1555, Oct. 2015, doi: 10.1002/cplu.201500179.

[19] M. Irie, “Diarylethenes for Memories and Switches,” *Chem. Rev.*, vol. 100, no. 5, pp. 1685–1716, 2000, doi: 10.1021/cr980069d.

[20] O. M. Wani, H. Zeng, and A. Priimagi, “A light-driven artificial flytrap,” *Nat. Commun.*, vol. 8, no. 1, pp. 1–7, May 2017, doi: 10.1038/ncomms15546.

[21] B. L. Feringa, “The Art of Building Small: From Molecular Switches to Motors (Nobel Lecture),” *Angewandte Chemie - International Edition*, vol. 56, no. 37. Wiley-VCH Verlag, pp. 11060–11078, Sep. 04, 2017, doi: 10.1002/anie.201702979.

[22] A. Fuhrmann, K. Broi, and S. Hecht, “Lowering the Healing Temperature of Photoswitchable Dynamic Covalent Polymer Networks,” *Macromol. Rapid Commun.*, vol. 39, no. 1, p. 1700376, Jan. 2018, doi: 10.1002/marc.201700376.

[23] A. Goulet-Hanssens, F. Eisenreich, and S. Hecht, “Enlightening Materials with Photoswitches,” *Advanced Materials*, vol. 32, no. 20. Wiley-VCH Verlag, p. 1905966, May 01, 2020, doi: 10.1002/adma.201905966.

[24] H. M. D. Bandara and S. C. Burdette, “Photoisomerization in different classes of azobenzene,” *Chem. Soc. Rev.*, vol. 41, no. 5, pp. 1809–1825, Feb. 2012, doi: 10.1039/c1cs15179g.

[25] M. Irie, T. Fukaminato, K. Matsuda, and S. Kobatake, “Photochromism of diarylethene molecules and crystals: Memories, switches, and actuators,” *Chemical Reviews*, vol. 114, no. 24. American Chemical Society, pp. 12174–12277, Dec. 24, 2014, doi: 10.1021/cr500249p.

[26] B. S. Lukyanov and M. B. Lukyanova, “SPIROPYRANS: SYNTHESIS, PROPERTIES, AND APPLICATION. (REVIEW)*,” 2005.

[27] M. Irimia-Vladu *et al.*, “Indigo - A natural pigment for high performance ambipolar organic field effect transistors and circuits,” *Adv. Mater.*, vol. 24, no. 3, pp. 375–380, Jan. 2012, doi: 10.1002/adma.201102619.

[28] E. D. Głowacki, G. Voss, L. Leonat, M. Irimia-Vladu, S. Bauer, and N. S. Sariciftci, “Indigo and Tyrian purple - From ancient natural dyes to modern organic semiconductors,” *Israel Journal of Chemistry*, vol. 52, no. 6. John Wiley & Sons,

Ltd, pp. 540–551, Jun. 01, 2012, doi: 10.1002/ijch.201100130.

[29] C. Y. Huang *et al.*, “N,N′-Disubstituted Indigos as Readily Available Red-Light Photoswitches with Tunable Thermal Half-Lives,” *J. Am. Chem. Soc.*, vol. 139, no. 42, pp. 15205–15211, Oct. 2017, doi: 10.1021/jacs.7b08726.

[30] M. J. Fuchter, “On the Promise of Photopharmacology Using Photoswitches: A Medicinal Chemist’s Perspective,” *Journal of Medicinal Chemistry*, vol. 63, no. 20. American Chemical Society, pp. 11436–11447, Oct. 22, 2020, doi: 10.1021/acs.jmedchem.0c00629.

[31] J. Boelke and S. Hecht, “Designing Molecular Photoswitches for Soft Materials Applications,” *Advanced Optical Materials*, vol. 7, no. 16. Wiley-VCH Verlag, p. 1900404, Aug. 01, 2019, doi: 10.1002/adom.201900404.

[32] R. S. Kularatne, H. Kim, J. M. Boothby, and T. H. Ware, “Liquid crystal elastomer actuators: Synthesis, alignment, and applications,” *Journal of Polymer Science, Part B: Polymer Physics*, vol. 55, no. 5. John Wiley and Sons Inc., pp. 395–411, Mar. 01, 2017, doi: 10.1002/polb.24287.

[33] J. Zhang, Q. Zou, and H. Tian, “Photochromic Materials: More Than Meets The Eye,” *Adv. Mater.*, vol. 25, no. 3, pp. 378–399, Jan. 2013, doi: 10.1002/adma.201201521.

[34] E. Merino, “Synthesis of azobenzenes: The coloured pieces of molecular materials,” *Chem. Soc. Rev.*, vol. 40, no. 7, pp. 3835–3853, Jun. 2011, doi: 10.1039/c0cs00183j.

[35] F. Hamon, F. Djedaini-Pilard, F. Barbot, and C. Len, “Azobenzenes-synthesis and carbohydrate applications,” *Tetrahedron*, vol. 65, no. 49. Elsevier Ltd, pp. 10105–10123, Dec. 05, 2009, doi: 10.1016/j.tet.2009.08.063.

[36] Z. Ahmed, A. Siiskonen, M. Virkki, and A. Priimagi, “Controlling azobenzene photoswitching through combined: Ortho -fluorination and -amination,” *Chem. Commun.*, vol. 53, no. 93, pp. 12520–12523, Nov. 2017, doi: 10.1039/c7cc07308a.

[37] Z. Mahimwalla, K. G. Yager, J. I. Mamiya, A. Shishido, A. Priimagi, and C. J. Barrett, “Azobenzene photomechanics: Prospects and potential applications,” *Polym. Bull.*, vol. 69, no. 8, pp. 967–1006, Nov. 2012, doi: 10.1007/s00289-012-

0792-0.

[38] J. Bahrenburg, K. Röttger, R. Siewertsen, F. Renth, and F. Temps, “Sequential photoisomerisation dynamics of the push-pull azobenzene Disperse Red 1,” *Photochem. Photobiol. Sci.*, vol. 11, no. 7, pp. 1210–1219, Jun. 2012, doi: 10.1039/c2pp05400k.

[39] C. Nançoz *et al.*, “Influence of the hydrogen-bond interactions on the excited-state dynamics of a push-pull azobenzene dye: The case of Methyl Orange,” *Phys. Chem. Chem. Phys.*, vol. 20, no. 10, pp. 7254–7264, Mar. 2018, doi: 10.1039/c7cp08390d.

[40] M. Dong, A. Babalhavaeji, S. Samanta, A. A. Beharry, and G. A. Woolley, “Red-Shifting Azobenzene Photoswitches for in Vivo Use,” *Acc. Chem. Res.*, vol. 48, no. 10, pp. 2662–2670, Oct. 2015, doi: 10.1021/acs.accounts.5b00270.

[41] O. Sadovski, A. A. Beharry, F. Zhang, and G. A. Woolley, “Spectral tuning of azobenzene photoswitches for biological applications,” *Angew. Chemie - Int. Ed.*, vol. 48, no. 8, pp. 1484–1486, Feb. 2009, doi: 10.1002/anie.200805013.

[42] M. Dong *et al.*, “Near-Infrared Photoswitching of Azobenzenes under Physiological Conditions,” *J. Am. Chem. Soc*, vol. 139, p. 56, 2017, doi: 10.1021/jacs.7b06471.

[43] C. Knie *et al.*, “Ortho-Fluoroazobenzenes: Visible Light Switches with Very Long-Lived Z Isomers,” *Chem. - A Eur. J.*, vol. 20, no. 50, pp. 16492–16501, Dec. 2014, doi: 10.1002/chem.201404649.

[44] H. Rau, “Azo Compounds,” in *Photochromism: Molecules and Systems*, Elsevier Inc., 2003, pp. 165–192.

[45] D. Pinheiro, A. M. Galvão, M. Pineiro, and J. S. S. de Melo, “Red-Purple Photochromic Indigos from Green Chemistry: Mono- *t* BOC or Di- *t* BOC *N* -Substituted Indigos Displaying Excited State Proton Transfer or Photoisomerization,” *J. Phys. Chem. B*, vol. 125, no. 16, pp. 4108–4119, Apr. 2021, doi: 10.1021/acs.jpcb.1c00120.

[46] D. Bléger and S. Hecht, “Visible-Light-Activated Molecular Switches,” *Angewandte Chemie - International Edition*, vol. 54, no. 39. Wiley-VCH Verlag, pp. 11338–11349, Sep. 01, 2015, doi: 10.1002/anie.201500628.

[47] J. Vapaavuori, C. G. Bazuin, and A. Priimagi, “Supramolecular design principles for efficient photoresponsive polymer-azobenzene complexes,” *Journal of Materials Chemistry C*, vol. 6, no. 9. Royal Society of Chemistry, pp. 2168–2188, Mar. 01, 2018, doi: 10.1039/c7tc05005d.

[48] D. Bléger, J. Schwarz, A. M. Brouwer, and S. Hecht, “O -fluoroazobenzenes as readily synthesized photoswitches offering nearly quantitative two-way isomerization with visible light,” *J. Am. Chem. Soc.*, vol. 134, no. 51, pp. 20597–20600, Dec. 2012, doi: 10.1021/ja310323y.

[49] F. Cicogna *et al.*, “Structural, thermal and photo-physical data of azo-aromatic TEMPO derivatives before and after their grafting to polyolefins,” *Data Br.*, vol. 6, pp. 562–570, Mar. 2016, doi: 10.1016/j.dib.2015.12.047.

[50] M. Irie and M. Mohri, “Thermally Irreversible Photochromic Systems. Reversible Photocyclization of Diarylethene Derivatives,” *J. Org. Chem.*, vol. 53, no. 4, pp. 803–808, Feb. 1988, doi: 10.1021/jo00239a022.

[51] S. Nakamura and M. Irie, “Thermally Irreversible Photochromic Systems. A Theoretical Study,” *J. Org. Chem.*, vol. 53, no. 26, pp. 6136–6138, Dec. 1988, doi: 10.1021/jo00261a035.

[52] R. M. Kellogg, M. B. Groen, and H. Wynberg, “Photochemically Induced Cyclization of Some Furyl-and Thienylethenes,” *J. Org. Chem.*, vol. 32, no. 10, pp. 3093–3100, 1967, doi: 10.1021/jo01285a035.

[53] G. Szalõki and J. L. Pozzo, “Synthesis of symmetrical and nonsymmetrical bisthienylcyclopentenes,” *Chemistry - A European Journal*, vol. 19, no. 34. John Wiley & Sons, Ltd, pp. 11124–11132, Aug. 19, 2013, doi: 10.1002/chem.201301645.

[54] S. Hiroto, K. Suzuki, H. Kamiya, and H. Shinokubo, “Synthetic protocol for diarylethenes through Suzuki-Miyaura coupling,” *Chem. Commun.*, vol. 47, no. 25, pp. 7149–7151, Jun. 2011, doi: 10.1039/c1cc12020d.

[55] M. Morimoto and M. Irie, “Photochromism of diarylethene single crystals: Crystal structures and photochromic performance,” *Chemical Communications*, no. 31. Royal Society of Chemistry, pp. 3895–3905, Aug. 21, 2005, doi: 10.1039/b505256d.

[56] H. Decker and T. v. Fellenberg, “Zur Begründung der Oxoniumtheorie,” *Justus Liebigs Ann. Chem.*, vol. 364, no. 1, pp. 1–44, 1909, doi: 10.1002/jlac.19093640102.

[57] W. Dilthey, C. Berres, E. Hölterhoff, and H. Wübken, “Beitrag Zur Kenntnis der Spiro-di-benzopyrane (Heteropolare Kohlenstoffverbindungen. IV),” *J. für Prakt. Chemie*, vol. 114, no. 1, pp. 179–198, Oct. 1926, doi: 10.1002/prac.19261140108.

[58] W. Dilthey and R. Wizinger, “Piperidin als Reagens auf Chinone und Farbstoffe,” *Berichte der Dtsch. Chem. Gesellschaft (A B Ser.*, vol. 59, no. 8, pp. 1856–1858, Sep. 1926, doi: 10.1002/cber.19260590830.

[59] Y. Hirshberg and E. Fischer, “Photochromism and reversible multiple internal transitions in some spiropyrans at low temperatures. Part I,” *J. Chem. Soc.*, no. 0, pp. 297–303, Jan. 1954, doi: 10.1039/JR9540000297.

[60] Y. Hirshberg and E. Fischer, “Low-temperature photochromism and its relation to thermochromism,” *J. Chem. Soc.*, no. 0, pp. 629–636, Jan. 1953, doi: 10.1039/jr9530000629.

[61] R. Klajn, “Spiropyran-based dynamic materials,” *Chemical Society Reviews*, vol. 43, no. 1. Royal Society of Chemistry, pp. 148–184, Jan. 07, 2014, doi: 10.1039/c3cs60181a.

[62] C. Brieke, F. Rohrbach, A. Gottschalk, G. Mayer, and A. Heckel, “Light-controlled tools,” *Angewandte Chemie - International Edition*, vol. 51, no. 34. pp. 8446–8476, Aug. 20, 2012, doi: 10.1002/anie.201202134.

[63] W. Szymański, J. M. Beierle, H. A. V. Kistemaker, W. A. Velema, and B. L. Feringa, “Reversible photocontrol of biological systems by the incorporation of molecular photoswitches,” *Chemical Reviews*, vol. 113, no. 8. American Chemical Society, pp. 6114–6178, Aug. 14, 2013, doi: 10.1021/cr300179f.

[64] T. Niazov, B. Shlyahovsky, and I. Willner, “Photoswitchable electrocatalysis and catalyzed chemiluminescence using photoisomerizable monolayer-functionalized surfaces and Pt nanoparticles,” *J. Am. Chem. Soc.*, vol. 129, no. 20, pp. 6374–6375, May 2007, doi: 10.1021/ja0707052.

[65] M. V. Peters, R. S. Stoll, A. Kühn, and S. Hecht, “Photoswitching of basicity,” *Angew. Chemie - Int. Ed.*, vol. 47, no. 32, pp. 5968–5972, Jul. 2008, doi:

10.1002/anie.200802050.

[66] T. Imahori, R. Yamaguchi, and S. Kurihara, “Azobenzene-tethered bis(trityl alcohol) as a photoswitchable cooperative acid catalyst for Morita-Baylis-Hillman reactions,” *Chem. - A Eur. J.*, vol. 18, no. 35, pp. 10802–10807, Aug. 2012, doi: 10.1002/chem.201201383.

[67] D. Wilson and N. R. Branda, “Turning ‘on’ and ‘off’ a pyridoxal 5’-phosphate mimic using light,” *Angew. Chemie - Int. Ed.*, vol. 51, no. 22, pp. 5431–5434, May 2012, doi: 10.1002/anie.201201447.

[68] M. M. Lerch, M. J. Hansen, G. M. van Dam, W. Szymanski, and B. L. Feringa, “Emerging Targets in Photopharmacology,” *Angewandte Chemie - International Edition*, vol. 55, no. 37. Wiley-VCH Verlag, pp. 10978–10999, Sep. 05, 2016, doi: 10.1002/anie.201601931.

[69] E. Bamberg, W. Gärtner, and D. Trauner, “Introduction: Optogenetics and Photopharmacology,” *Chemical Reviews*, vol. 118, no. 21. American Chemical Society, pp. 10627–10628, Nov. 14, 2018, doi: 10.1021/acs.chemrev.8b00483.

[70] J. Broichhagen, J. A. Frank, and D. Trauner, “A Roadmap to Success in Photopharmacology,” *Acc. Chem. Res.*, vol. 48, no. 7, pp. 1947–1960, Jul. 2015, doi: 10.1021/acs.accounts.5b00129.

[71] S. Stolik, J. A. Delgado, A. Pérez, and L. Anasagasti, “Measurement of the penetration depths of red and near infrared light in human ″ex vivo″ tissues,” *J. Photochem. Photobiol. B Biol.*, vol. 57, no. 2–3, pp. 90–93, Sep. 2000, doi: 10.1016/S1011-1344(00)00082-8.

[72] C. Ash, M. Dubec, K. Donne, and T. Bashford, “Effect of wavelength and beam width on penetration in light-tissue interaction using computational methods,” doi: 10.1007/s10103-017-2317-4.

[73] J. B. Trads *et al.*, “Sign Inversion in Photopharmacology: Incorporation of Cyclic Azobenzenes in Photoswitchable Potassium Channel Blockers and Openers,” *Angew. Chemie*, vol. 131, no. 43, pp. 15567–15574, Oct. 2019, doi: 10.1002/ange.201905790.

[74] M. Banghart, K. Borges, E. Isacoff, D. Trauner, and R. H. Kramer, “Light-activated ion channels for remote control of neuronal firing,” *Nat. Neurosci.*, vol. 7, no. 12,

pp. 1381–1386, Dec. 2004, doi: 10.1038/nn1356.

[75] J. Broichhagen *et al.*, “Optical control of insulin release using a photoswitchable sulfonylurea,” *Nat. Commun.*, vol. 5, no. 1, pp. 1–11, Oct. 2014, doi: 10.1038/ncomms6116.

[76] K. Gholamjani Moghaddam, G. Giudetti, W. Sipma, and S. Faraji, “Theoretical insights into the effect of size and substitution patterns of azobenzene derivatives on the DNA G-quadruplex,” *Phys. Chem. Chem. Phys.*, vol. 22, no. 46, pp. 26944–26954, Dec. 2020, doi: 10.1039/d0cp04392c.

[77] Z. L. Pianowski, “Recent Implementations of Molecular Photoswitches into Smart Materials and Biological Systems,” *Chemistry - A European Journal*, vol. 25, no. 20. Wiley-VCH Verlag, pp. 5128–5144, Apr. 05, 2019, doi: 10.1002/chem.201805814.

[78] “Researchers Submit Patent Application, "Light-Controlled Antibacterial Agent Composed Of Linear Cationic Oligopeptide And Multi-Arm B-Cyclodextrin", for Approval (USPTO 20210060165).,” *Med. Pat. Bus. Week*, pp. 10730–10730, Mar. 2021, Accessed: May 24, 2021. [Online]. Available: https://go.gale.com/ps/i.do?p=AONE&sw=w&issn=&v=2.1&it=r&id=GALE%7CA655759593&sid=googleScholar&linkaccess=fulltext.

[79] H. Yu, “Recent advances in photoresponsive liquid-crystalline polymers containing azobenzene chromophores,” *Journal of Materials Chemistry C*, vol. 2, no. 17. The Royal Society of Chemistry, pp. 3047–3054, May 07, 2014, doi: 10.1039/c3tc31991a.

[80] J. A. Rego, J. A. A. Harvey, A. L. MacKinnon, and E. Gatdula, “Asymmetric synthesis of a highly soluble ‘trimeric’ analogue of the chiral nematic liquid crystal twist agent Merck S1011,” *Liq. Cryst.*, vol. 37, no. 1, pp. 37–43, Jan. 2010, doi: 10.1080/02678290903359291.

[81] J. H. Porada, J. R.-M. Neudö, and D. Blunk, “Planar and distorted indigo as the core motif in novel chromophoric liquid crystals †,” *New J. Chem*, vol. 39, p. 8291, 2015, doi: 10.1039/c5nj01594d.

[82] J. Pina *et al.*, “Excited-State Proton Transfer in Indigo,” *J. Phys. Chem. B*, vol. 121, no. 10, pp. 2308–2318, Mar. 2017, doi: 10.1021/acs.jpcb.6b11020.

[83] A. Cully, J. Clune, D. Tarapore, and J. B. Mouret, “Robots that can adapt like animals,” *Nature*, vol. 521, no. 7553, pp. 503–507, May 2015, doi: 10.1038/nature14422.

[84] E. Morris, M. Chavez, and C. Tan, “Dynamic biomaterials: Toward engineering autonomous feedback,” *Current Opinion in Biotechnology*, vol. 39. Elsevier Ltd, pp. 97–104, Jun. 01, 2016, doi: 10.1016/j.copbio.2016.02.032.

[85] M. Scheiner, A. Sink, P. Spatz, E. Endres, and M. Decker, “Photopharmacology on Acetylcholinesterase: Novel Photoswitchable Inhibitors with Improved Pharmacological Profiles,” *ChemPhotoChem*, vol. 5, no. 2, pp. 149–159, Feb. 2021, doi: 10.1002/cptc.202000119.

[86] J. Konieczkowska, K. Bujak, and E. Schab-Balcerzak, “A short review of the photomechanical effect in azo-containing amorphous (Glassy) polymers,” *Express Polym. Lett.*, vol. 15, no. 5, pp. 459–472, 2021, doi: 10.3144/expresspolymlett.2021.39.

[87] M. Yamada *et al.*, “Photomobile polymer materials: Towards light-driven plastic motors,” *Angew. Chemie - Int. Ed.*, vol. 47, no. 27, pp. 4986–4988, Jun. 2008, doi: 10.1002/anie.200800760.

[88] A. H. Gelebart, G. Vantomme, E. W. Meijer, and D. J. Broer, “Mastering the Photothermal Effect in Liquid Crystal Networks: A General Approach for Self-Sustained Mechanical Oscillators,” *Adv. Mater.*, vol. 29, no. 18, p. 1606712, May 2017, doi: 10.1002/adma.201606712.

[89] J. A. Lv, Y. Liu, J. Wei, E. Chen, L. Qin, and Y. Yu, “Photocontrol of fluid slugs in liquid crystal polymer microactuators,” *Nature*, vol. 537, no. 7619, pp. 179–184, Sep. 2016, doi: 10.1038/nature19344.

[90] M. Lahikainen, H. Zeng, and A. Priimagi, “Reconfigurable photoactuator through synergistic use of photochemical and photothermal effects,” doi: 10.1038/s41467-018-06647-7.

[91] J. Patrakka, “AZOBENZENE PHOTOISOMERISATION IN HUMIDITY SENSING,” 2020.

[92] L. A. Huber, P. Mayer, and H. Dube, “Photoisomerization of Mono-Arylated Indigo and Water-Induced Acceleration of Thermal cis-to-trans Isomerization,”

ChemPhotoChem, vol. 2, no. 6, pp. 458–464, Jun. 2018, doi: 10.1002/cptc.201700228.

[93] Y. Zhuge, D. Xu, C. Zheng, and S. Pu, “An ionic liquid-modified diarylethene: Synthesis, properties and sensing cyanide ions,” *Anal. Chim. Acta*, vol. 1079, pp. 153–163, Nov. 2019, doi: 10.1016/j.aca.2019.06.039.

[94] F. Mollwo Perkin, “The present condition of the indigo industry,” *Nature*, vol. 63, no. 1618, pp. 7–9, 1900, doi: 10.1038/063007d0.

[95] G. Travasso, C. S. Santos, M. F. Oliveira-Campos, M. M. Raposo, and N. Prasitpan, “Indigo revisited,” 2003.

[96] G. M. Wyman and A. F. Zenhausern, “Spectroscopic Studies on Dyes. V. Derivatives of cis-Indigo,” *J. Org. Chem.*, vol. 30, no. 7, pp. 2348–2352, Jul. 1965, doi: 10.1021/jo01018a055.

[97] E. D. Głowacki, G. Voss, and N. S. Sariciftci, “25th anniversary article: Progress in chemistry and applications of functional indigos for organic electronics,” *Adv. Mater.*, vol. 25, no. 47, pp. 6783–6800, Dec. 2013, doi: 10.1002/adma.201302652.

[98] D. Franchi *et al.*, “Synthesis and characterization of new organic dyes containing the indigo core,” *Molecules*, vol. 25, no. 15, p. 3377, Aug. 2020, doi: 10.3390/molecules25153377.

[99] “The Nobel Prize in Chemistry 1905.” https://www.nobelprize.org/prizes/chemistry/1905/summary/ (accessed May 11, 2021).

[100] J. Mendoza-Avila, K. Chauhan, and R. Vazquez-Duhalt, “Enzymatic synthesis of indigo-derivative industrial dyes,” *Dye. Pigment.*, vol. 178, p. 108384, Jul. 2020, doi: 10.1016/j.dyepig.2020.108384.

[101] R. J. H. Clark, C. J. Cooksey, M. A. M. Daniels, and R. Withnall, “Indigo, woad, and Tyrian Purple: important vat dyes from antiquity to the present,” *Endeavour*, vol. 17, no. 4, pp. 191–199, Jan. 1993, doi: 10.1016/0160-9327(93)90062-8.

[102] J. Kühlborn, A. K. Danner, H. Frey, R. Iyer, A. J. Arduengo, and T. Opatz, “Examples of xylochemistry: Colorants and polymers,” *Green Chem.*, vol. 19, no. 16, pp. 3780–3786, Aug. 2017, doi: 10.1039/c7gc01244f.

[103] “Chemists go green to make better blue jeans,” *Nature*, vol. 553, no. 7687. Nature Research, p. 128, Jan. 11, 2018, doi: 10.1038/d41586-018-00103-8.

[104] T. M. Hsu *et al.*, “Employing a biochemical protecting group for a sustainable indigo dyeing strategy,” *Nat. Chem. Biol.*, vol. 14, no. 3, pp. 256–261, Mar. 2018, doi: 10.1038/nchembio.2552.

[105] D. C. Nobre *et al.*, “Photoresponsive N,N′-disubstituted indigo derivatives,” *Dye. Pigment.*, vol. 176, p. 108197, May 2020, doi: 10.1016/j.dyepig.2020.108197.

[106] S. Benkhaya, S. M’ rabet, and A. El Harfi, “A review on classifications, recent synthesis and applications of textile dyes,” *Inorganic Chemistry Communications*, vol. 115. Elsevier B.V., p. 107891, May 01, 2020, doi: 10.1016/j.inoche.2020.107891.

[107] F. Sánchez-Viesca and R. Gómez, “On the Baeyer-Emmerling Synthesis of Indigo Theoretical Advances in Aromatic Nitration View project Osazone Chemistry View project On the Baeyer-Emmerling Synthesis of Indigo,” *World J. Org. Chem.*, vol. 6, no. 1, pp. 6–12, 2018, doi: 10.12691/wjoc-6-1-2.

[108] A. Baeyer and V. Drewsen, “Darstellung von Indigblau aus Orthonitrobenzaldehyd,” *Berichte der Dtsch. Chem. Gesellschaft*, vol. 15, no. 2, pp. 2856–2864, Jul. 1882, doi: 10.1002/cber.188201502274.

[109] E. D. Głowacki *et al.*, “Air-stable organic semiconductors based on 6,6′-dithienylindigo and polymers thereof,” *J. Mater. Chem. C*, vol. 2, no. 38, pp. 8089–8097, Oct. 2014, doi: 10.1039/c4tc00651h.

[110] H. Schmidt, “Indigo-100 Jahre industrielle Synthese.”

[111] G. R. Chatwal and M. Arora, *Synthetic Dyes*. Mumbai, INDIA: Global Media, 2008.

[112] I. V. Klimovich *et al.*, “Novel functionalized indigo derivatives for organic electronics,” *Dye. Pigment.*, vol. 186, p. 108966, Feb. 2021, doi: 10.1016/j.dyepig.2020.108966.

[113] M. A. Manthrammel *et al.*, “Novel design and microelectronic analysis of highly stable Au/Indigo/n-Si photodiode for optoelectronic applications,” *Solid State Sci.*, vol. 93, pp. 7–12, Jul. 2019, doi: 10.1016/j.solidstatesciences.2019.04.007.

[114] J. Mei, K. R. Graham, R. Stalder, and J. R. Reynolds, “Synthesis of isoindigo-

based oligothiophenes for molecular bulk heterojunction solar cells," *Org. Lett.*, vol. 12, no. 4, pp. 660–663, Feb. 2010, doi: 10.1021/ol902512x.

[115] H. Tanaka and Y. Matsumoto, "A Simple Preparative Method of N-Arylindigos and Substitution Effect in UV/Visible Absorption," *Heterocycles*, vol. 60, p. 1805, Aug. 2003, doi: 10.3987/COM-03-9792.

[116] W. Lüttke, H. Hermann, and M. Klessinger, "Theoretically and Experimentally Determined Properties of the Fundamental Indigo Chromophore," *Angew. Chemie Int. Ed. English*, vol. 5, no. 6, pp. 598–599, Jun. 1966, doi: 10.1002/anie.196605982.

[117] M. T. Sims, "Dyes as guests in ordered systems: current understanding and future directions," *Liq. Cryst.*, vol. 43, no. 13–15, pp. 2363–2374, Dec. 2016, doi: 10.1080/02678292.2016.1189613.

[118] J. Vapaavuori, R. H. A. Ras, M. Kaivola, C. G. Bazuin, and A. Priimagi, "From partial to complete optical erasure of azobenzene-polymer gratings: Effect of molecular weight," *J. Mater. Chem. C*, vol. 3, no. 42, pp. 11011–11016, Oct. 2015, doi: 10.1039/c5tc01776a.

[119] P. Pandey, "Silver Particulate Films on Compatible Softened Polymer Composites," 2013.

[120] "Poly(4-vinylpyridine) average Mw ~60,000 | 25232-41-1." https://www.sigmaaldrich.com/FI/en/product/aldrich/472344 (accessed Jun. 28, 2021).

[121] Y. Yang, X. Zou, H. Ye, W. Zhu, H. Dong, and M. Bi, "Supporting Information A Modified Group Contribution Scheme to Predict Homopolymer Glass Transition Temperature through Limiting Property Dataset."

APPENDIX 1: ^{1}H AND ^{13}C NMR SPECTRA OF COMPOUND 52

^{1}H

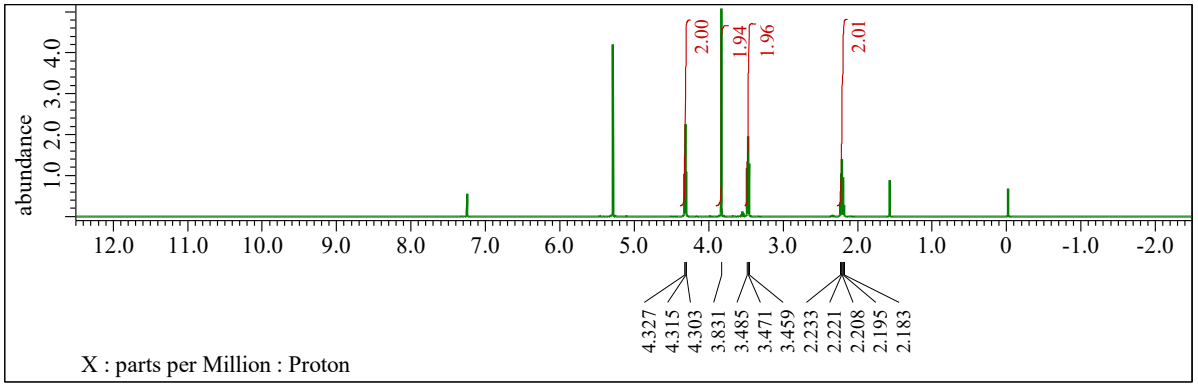

^{13}C

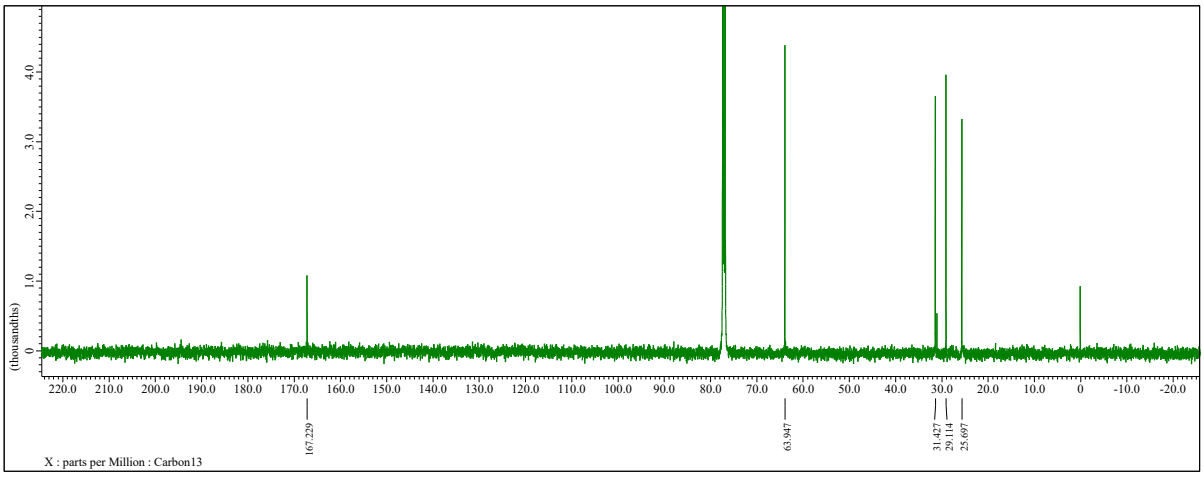

APPENDIX 2: ^{1}H NMR SPECTRUM OF COMPOUND 47

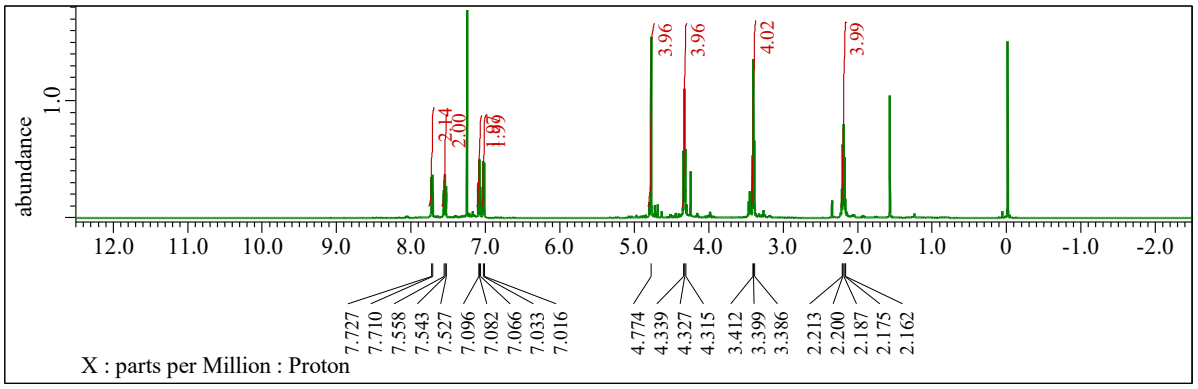

APPENDIX 3: ^{1}H AND ^{13}C NMR SPECTRA OF COMPOUND 54

^{1}H

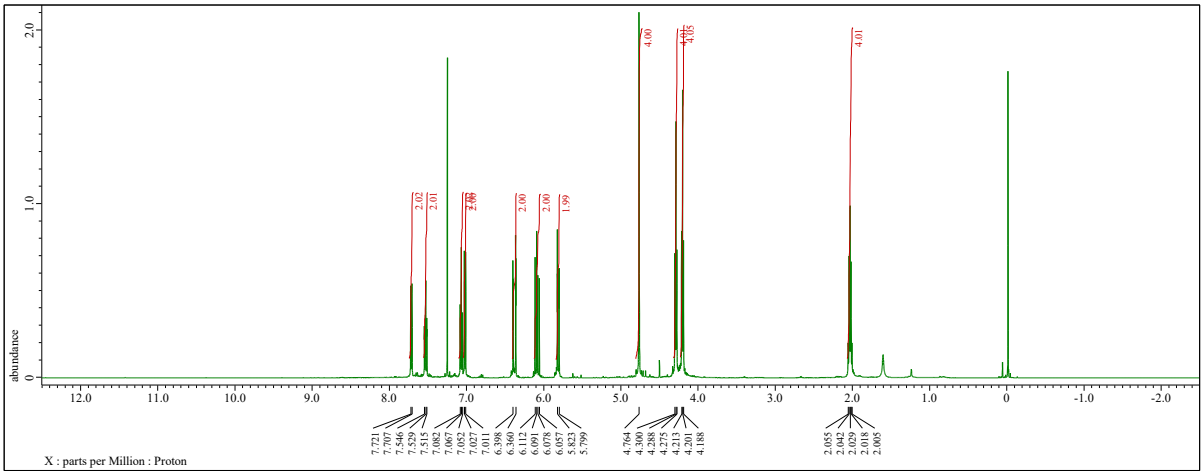

^{13}C

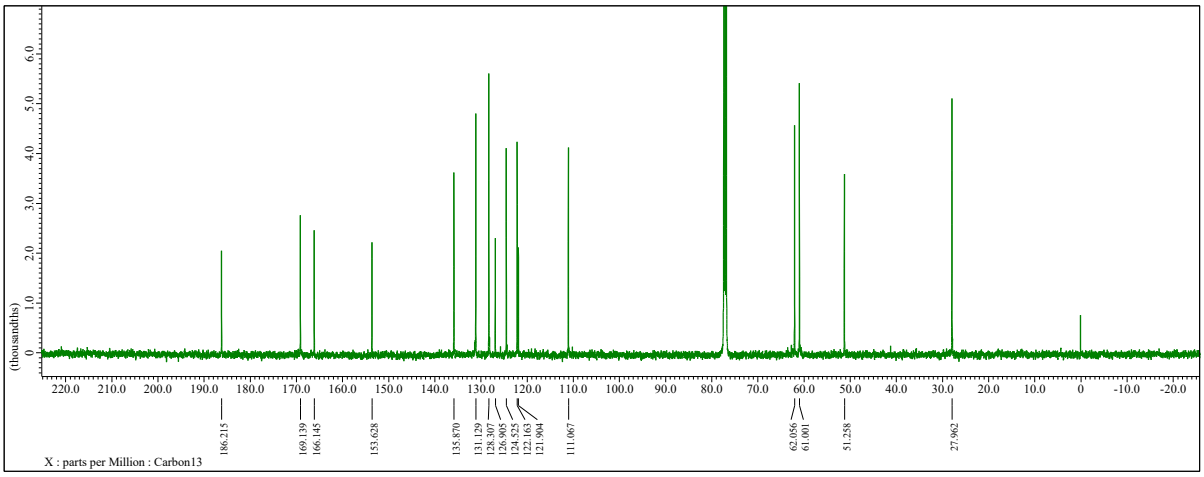

APPENDIX 4: ^{1}H AND ^{13}C NMR SPECTRA OF COMPOUND 56

^{1}H

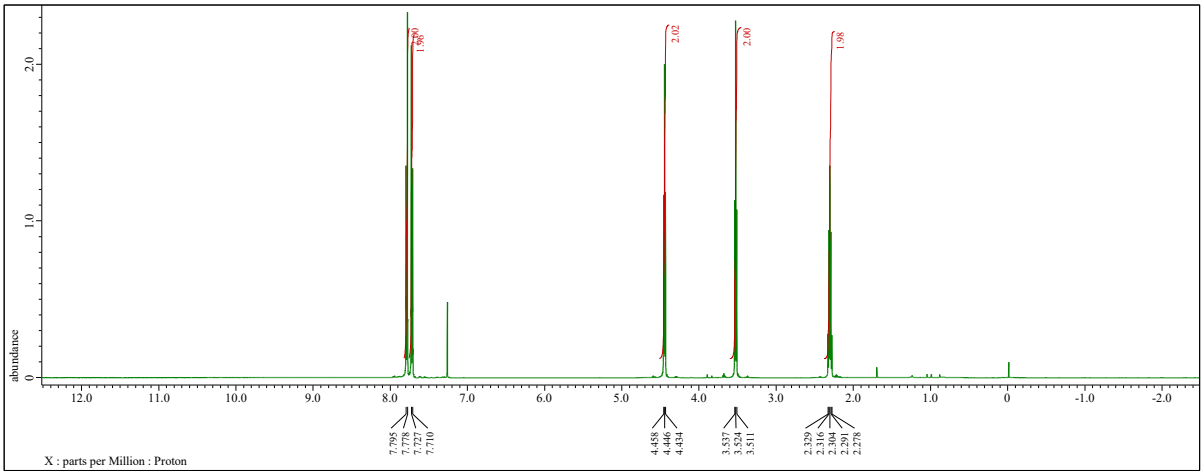

^{13}C

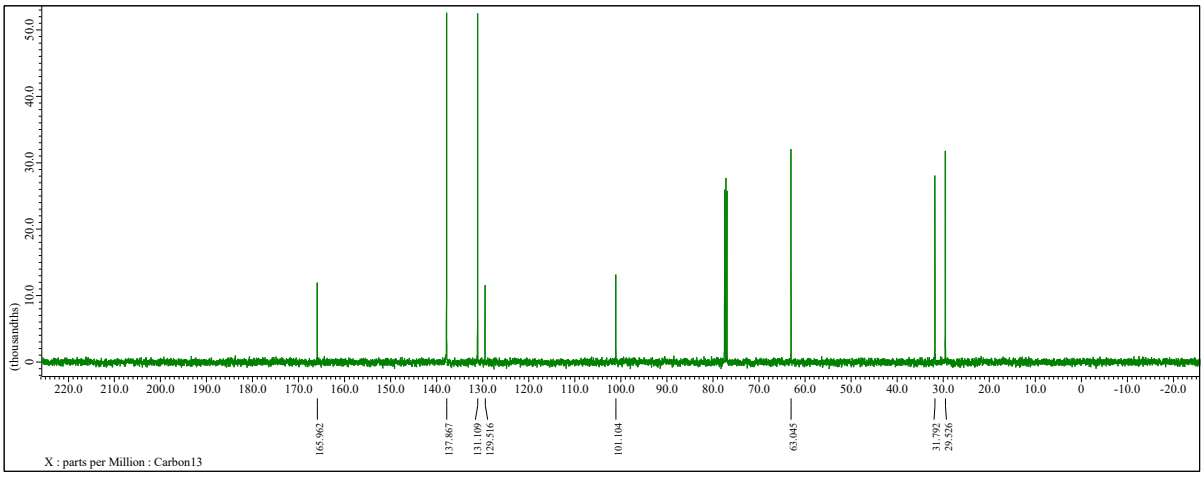

APPENDIX 5: ^{1}H AND ^{13}C NMR SPECTRA OF COMPOUND 48

^{1}H

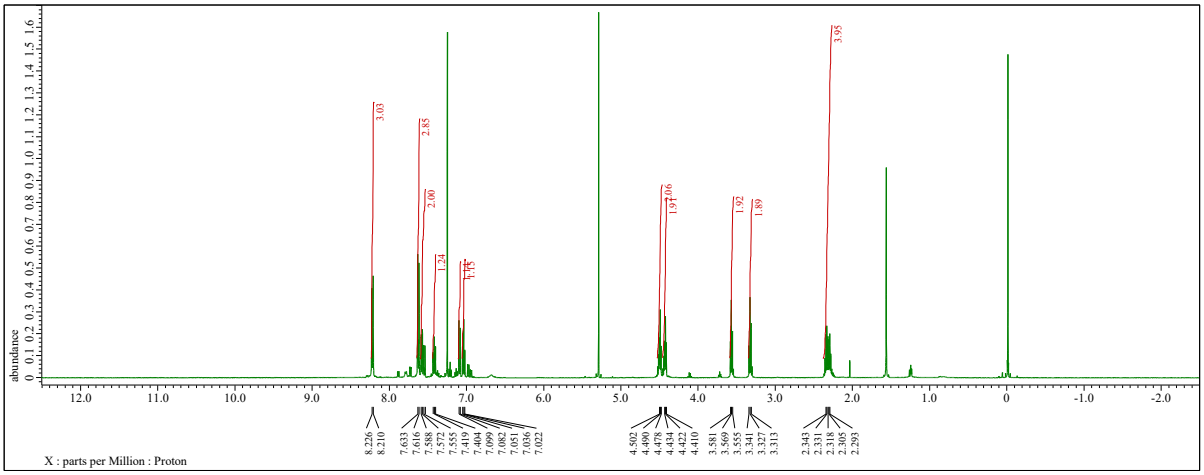

^{13}C

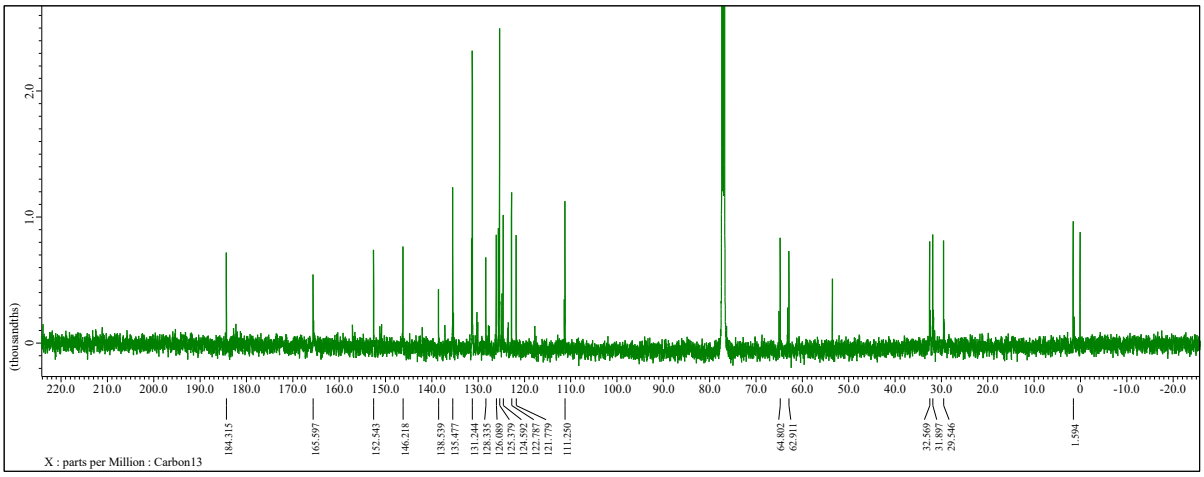

APPENDIX 6: ^{1}H AND ^{13}C NMR SPECTRA OF COMPOUND 59

^{1}H

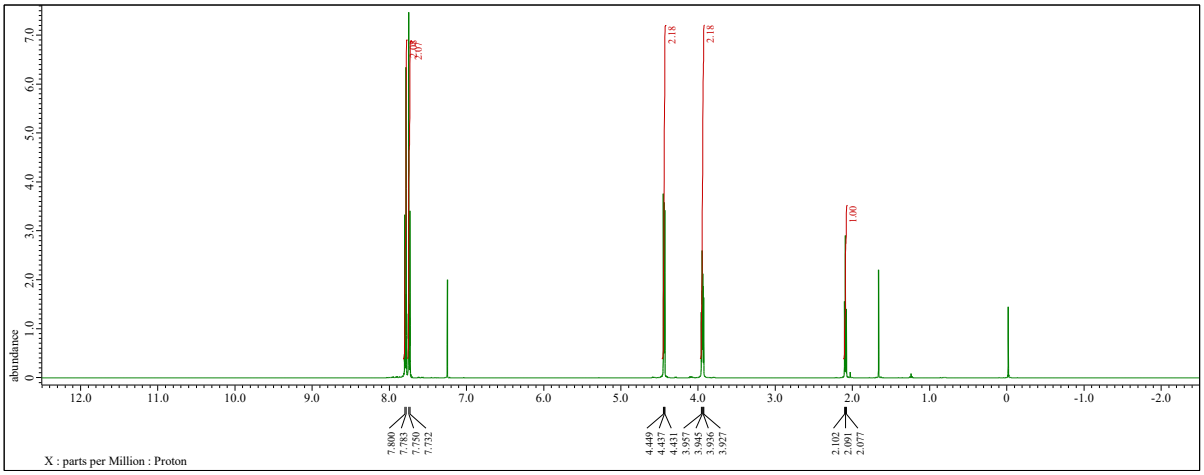

^{13}C

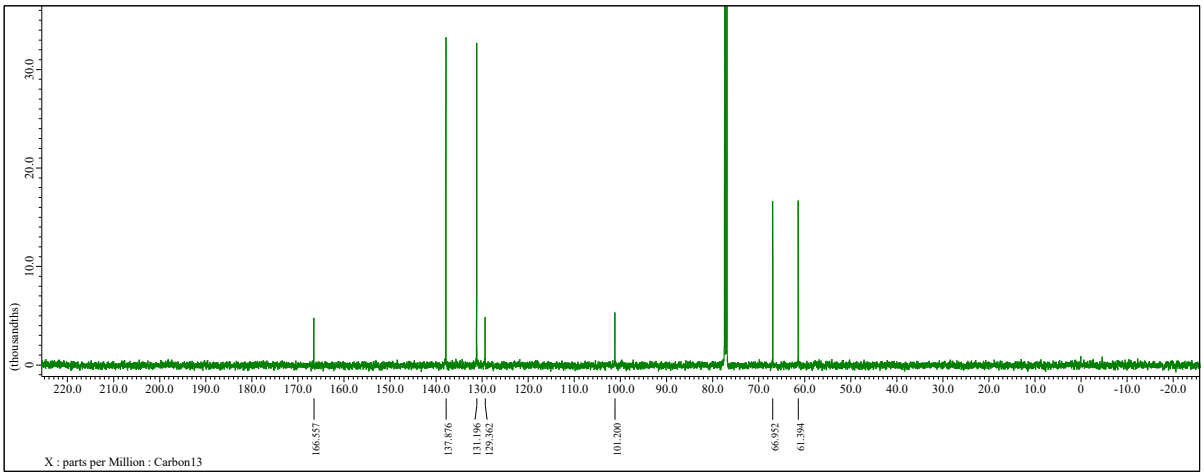

APPENDIX 7: ^{1}H NMR SPECTRUM OF COMPOUND 60

^{1}H

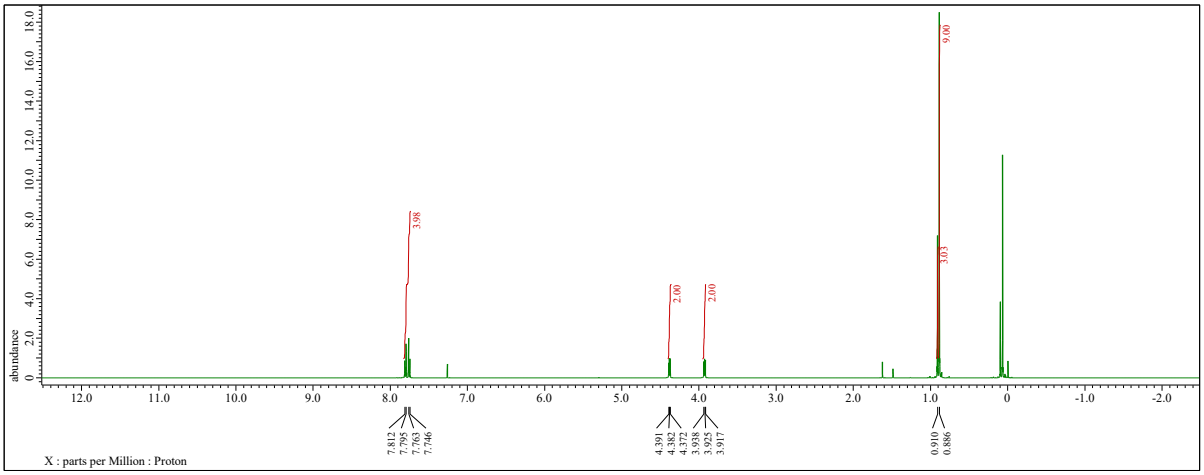

APPENDIX 8: ^{1}H AND ^{13}C NMR SPECTRA OF COMPOUND 61

^{1}H

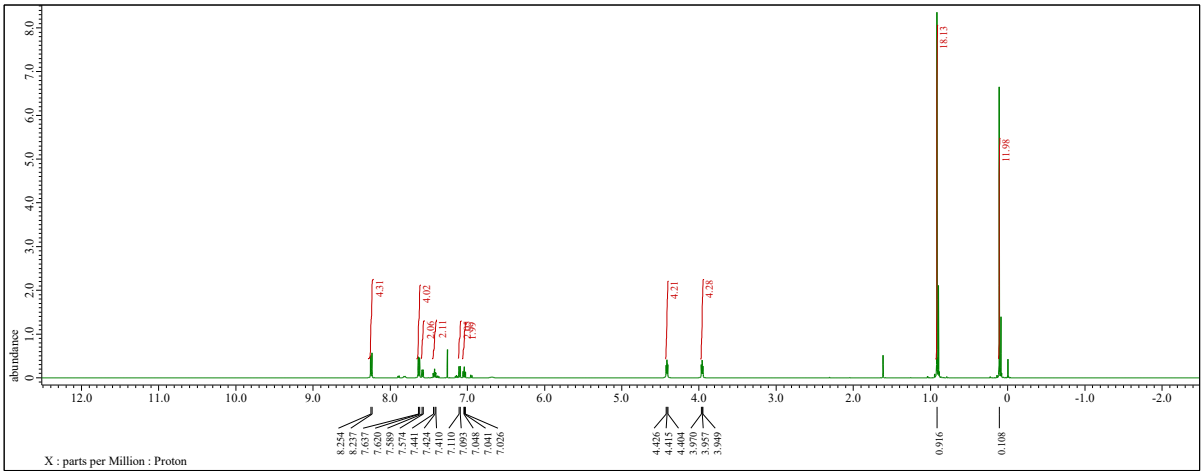

^{13}C

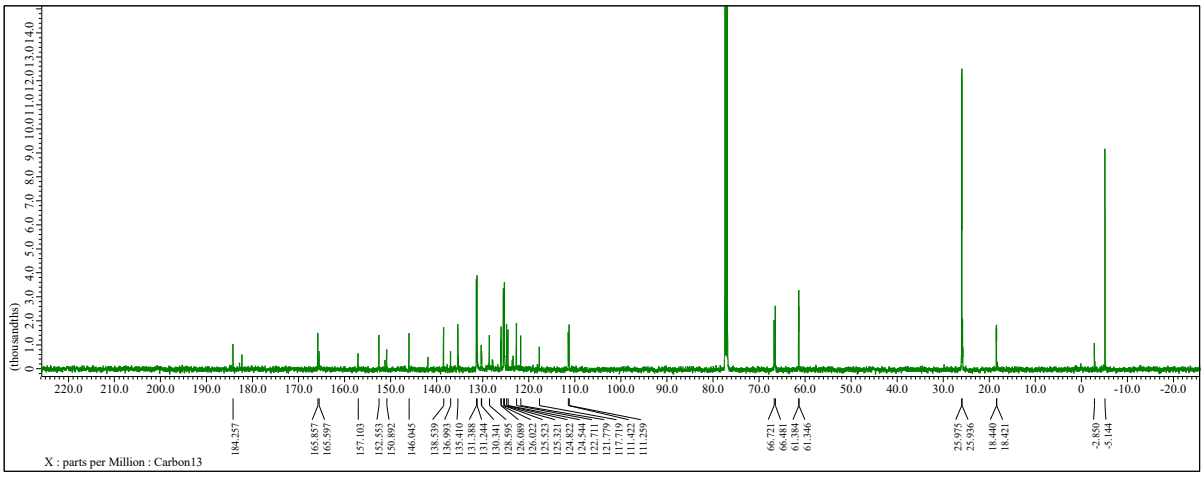

APPENDIX 9: ^{1}H AND ^{13}C NMR SPECTRA OF COMPOUND 63

^{1}H

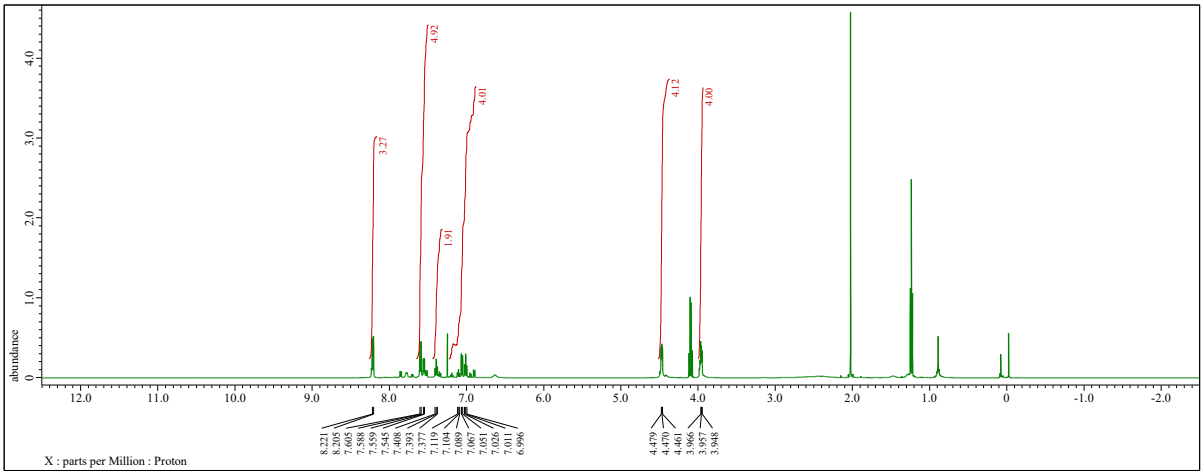

^{13}C

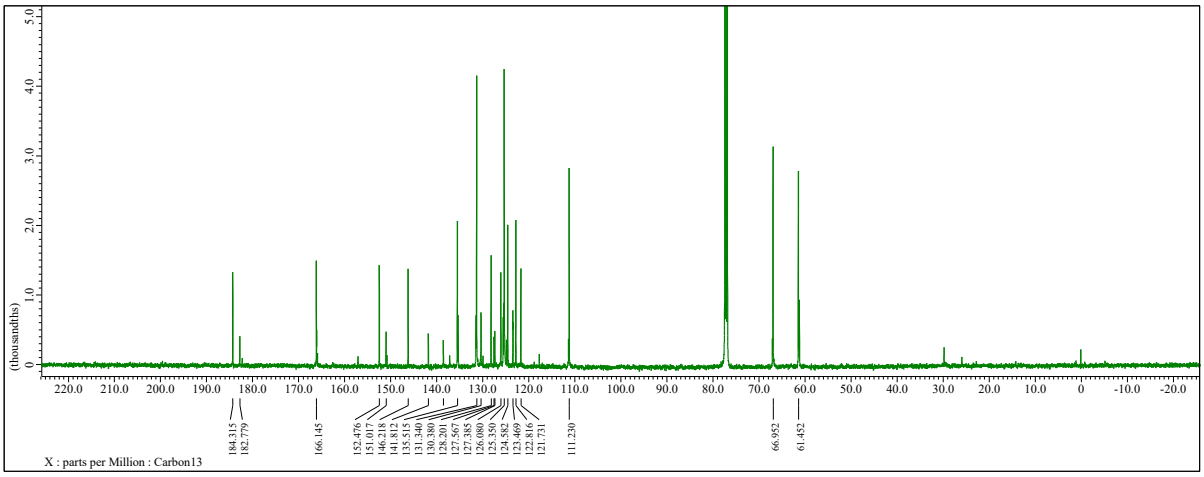

APPENDIX 10: ^{1}H AND ^{13}C NMR SPECTRA OF COMPOUND 66

^{1}H

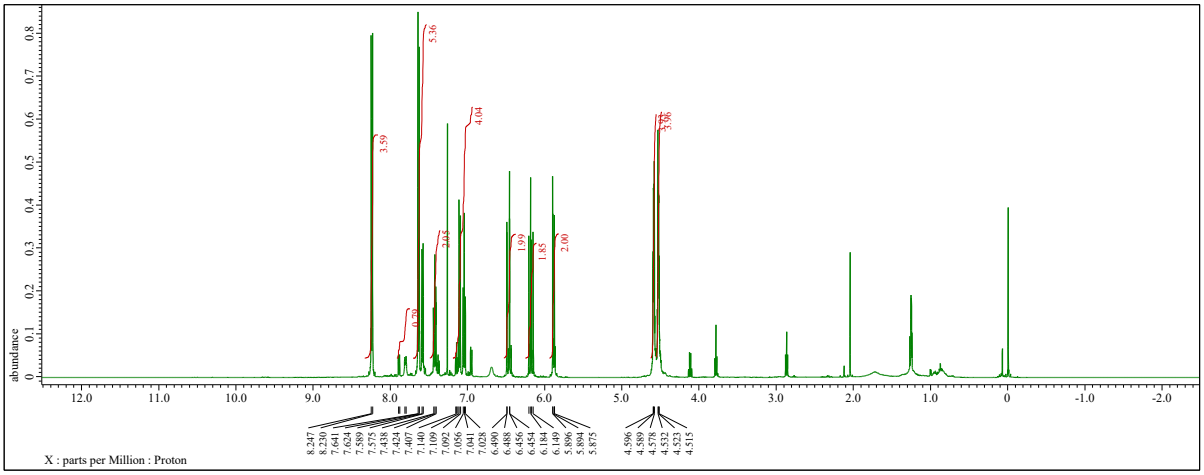

^{13}C

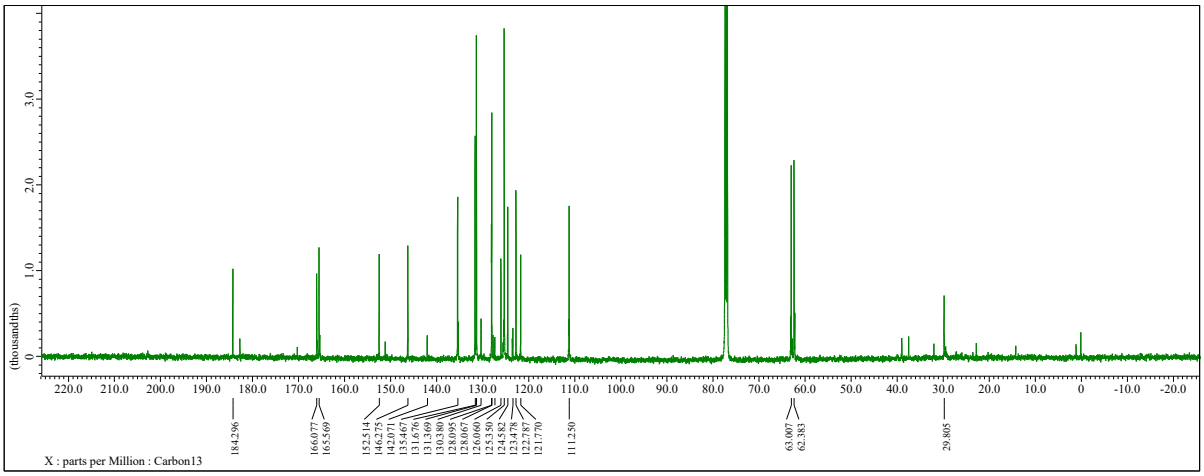

APPENDIX 11: ^{1}H AND ^{13}C NMR SPECTRA OF COMPOUND 67

^{1}H

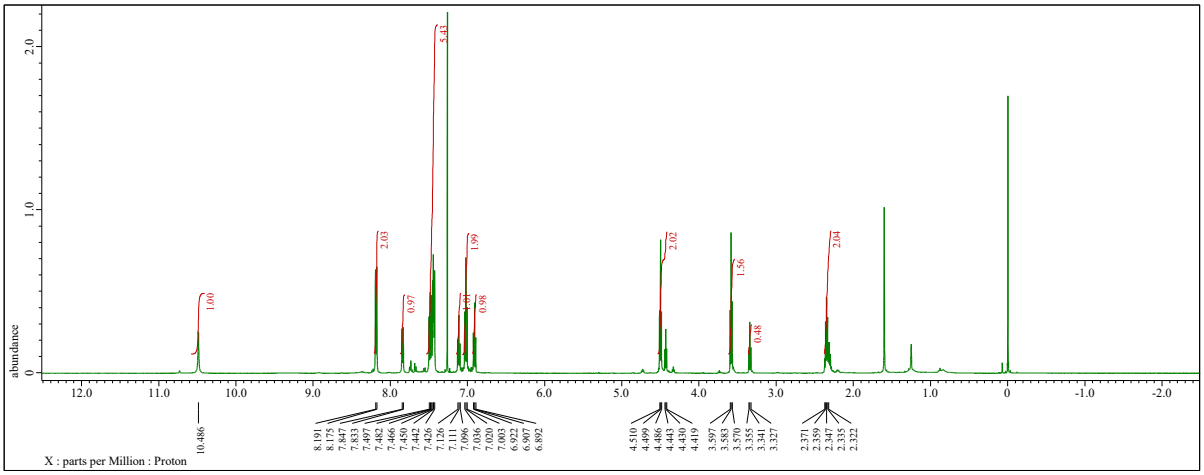

^{13}C

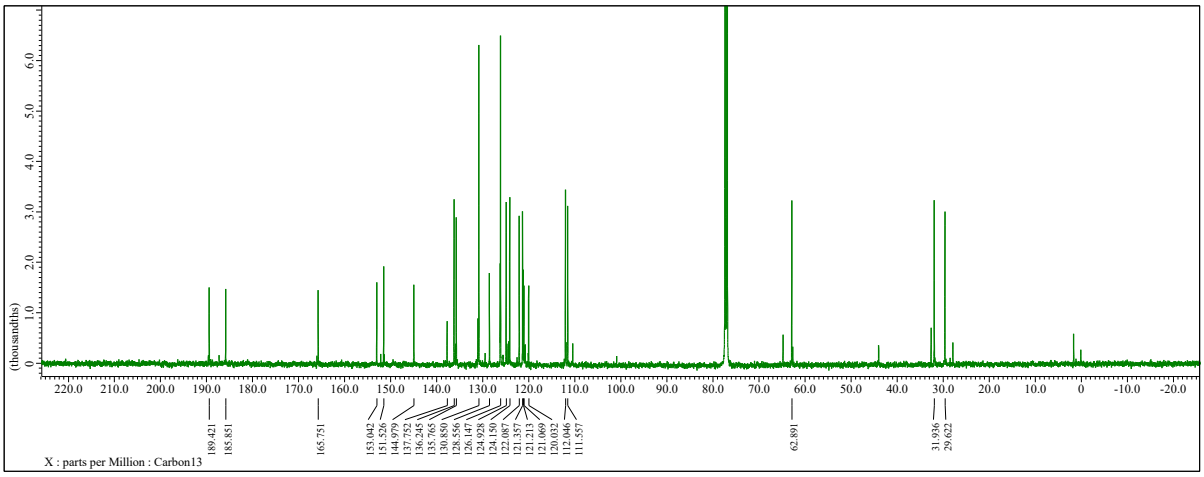

APPENDIX 12: ^{1}H AND ^{13}C NMR SPECTRA OF COMPOUND 49

^{1}H

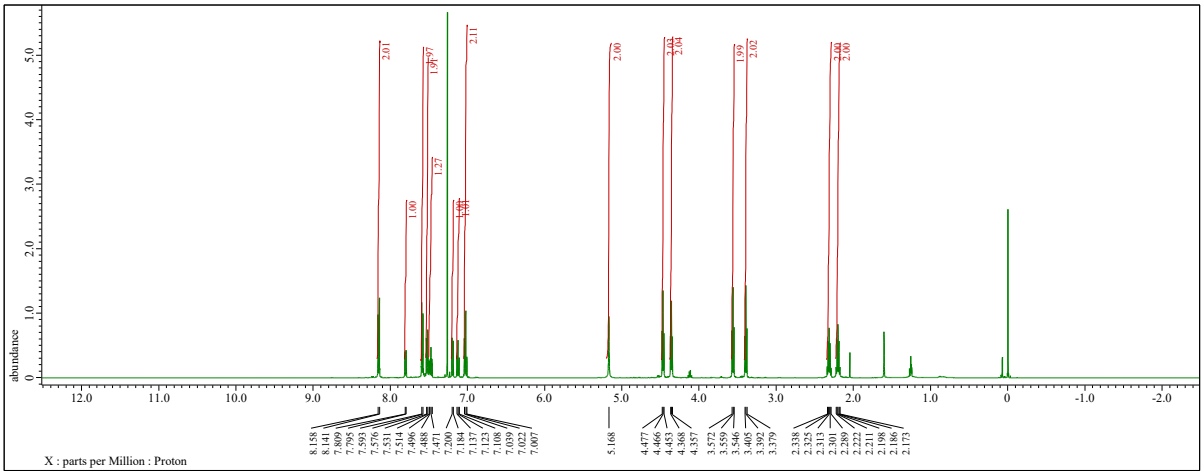

^{13}C

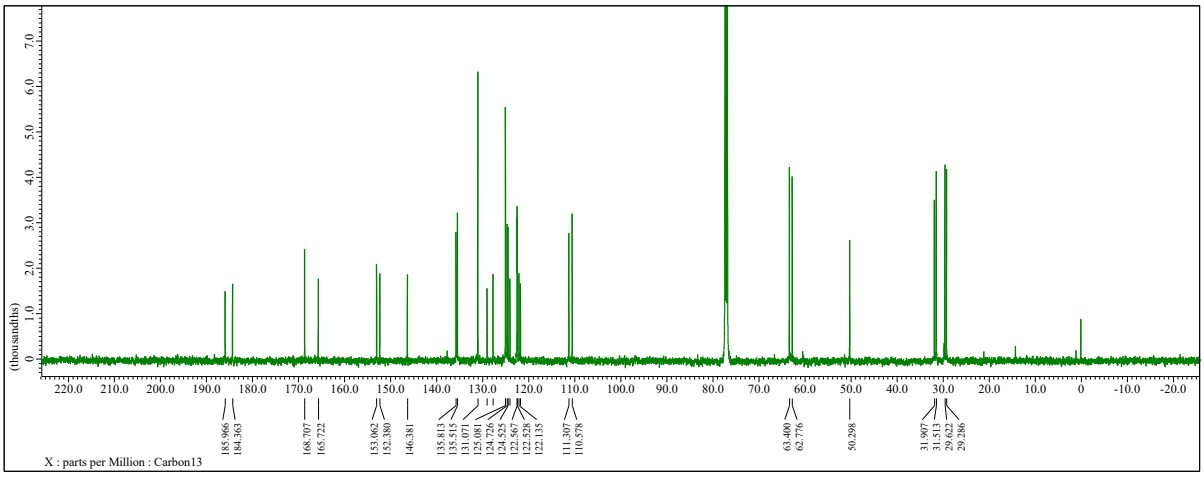

APPENDIX 13: ^{1}H AND ^{13}C NMR SPECTRA OF COMPOUND 68

^{1}H

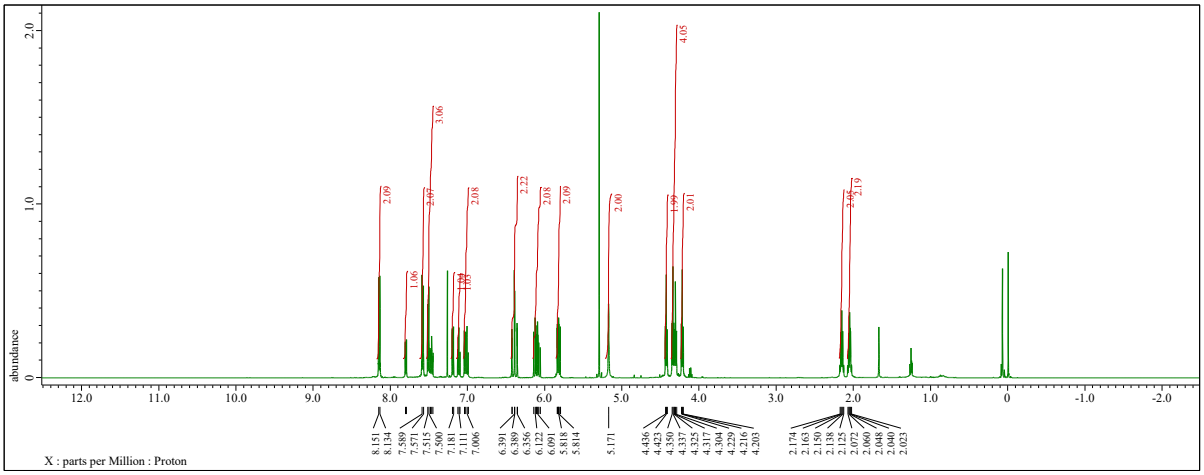

^{13}C

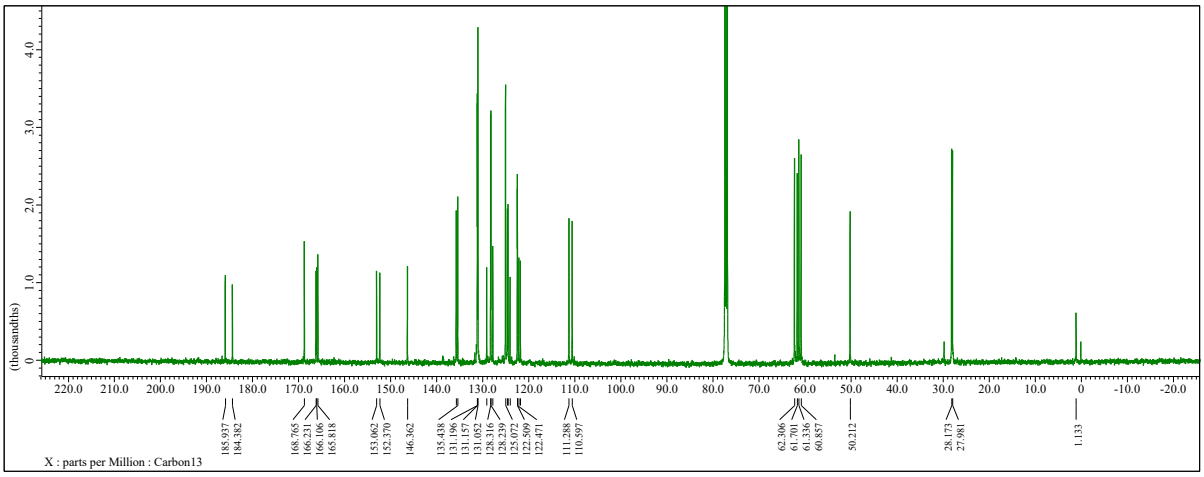

APPENDIX 14: PSS COMPOSITION OF DIARYL INDIGO FROM ^{1}H NMR SPECTRA OF COMPOUND 66

Spectrum in dark

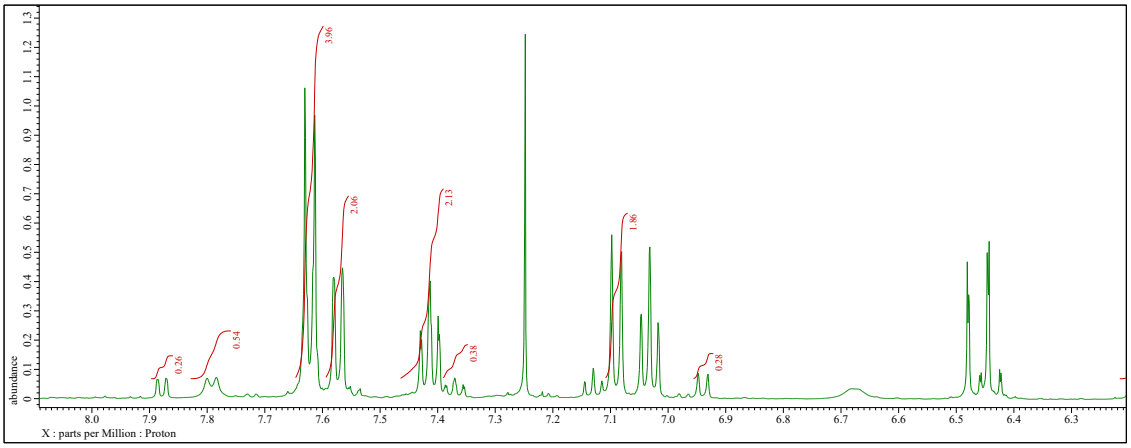

Spectrum after irradiation